STUDY OF

ELECTRICAL CONCENTRATION

OF

MINERALS

by

Roger G. Mora

Ingénieur de l'Ecole Nationale des Arts et Métiers
Lille, Paris 1952 - 1956

FRANCE

Submitted in Partial Fulfillment of the
Requirements for the Degree of

MASTER OF SCIENCE

from the

Massachusetts Institute of Technology

May 1958

Signature of Author
Department of Metallurgy
May 26, 1958

Signature of Professor
in Charge of Research

Signature of Chairman of
Department Committee on
Graduate Students

STUDY OF ELECTRICAL CONCENTRATION OF MINERALS

by

Roger G. Mora

Submitted to the Department of Metallurgy

On May 26, 1958

In Partial Fulfillment of the Requirements for the Degree of

MASTER OF SCIENCE

ABSTRACT

The main purpose of this thesis is to show how, from the basic principles of electricity, it is possible to understand the electrical concentration of minerals.

Rather than being a survey or collection of data on the subject from the literature, this thesis is an attempt to study the process from a fundamental viewpoint supported by experiments.

The Carpco machine was studied in some detail. For purposes of clarity this thesis has been divided into three main parts:

A. Theoretical Considerations

B. Technical Aspects of Electrical Concentration Processes

C. Experimental Study

However it should be remembered that this thesis represents a unified whole, rather than three distinct parts.

Theoretical equations have been derived to explain behaviours of minerals particles, and their discussion is a useful tool for an understanding of the processes.

Thesis Supervisor: A. M. Gaudin
Title: Richards Professor of Mineral Engineering

List Of Tables

List of Figures

ACKNOWLEDGEMENTS

The author wishes to express his gratitude and thanks to Professor A. M. Gaudin for his guidance and constructive criticism.

The research was made possible through the financial support provided by the Atomic Energy Commission and the French "Institut de Recherches de la Sidérurgie." The author is grateful for the financial assistance which has given him the opportunity of conducting this investigation and of furthering his education.

To all the members of the Richards Mineral Engineering Laboratory, the author wishes to express his thanks for the advice and help on many occasions and personal contacts which made the association such a pleasant one.

Notations and Symbols

a = Radius of the Electrical Equivalent Ellipsoid of Revolution

a_p = Acceleration, meter/second^2

A = Area, square meter

A_{eff} = Area of Contact, square meter

b = Characteristic Clearance Between the Drum and the Equivalent Ellipsoid

$B = \sqrt{\left(1+\frac{\mathcal{F}}{\mathcal{P}}\right)^2-1}$. Ionic Charging Constant

c = Length of the Electrical Equivalent Ellipsoid of Revolution

C = Capacity of a Condenser, Farads

C' = Capacity of a Particle Far From Any Other Body = $4\pi f a \epsilon_o$, Farads

C_p = Capacity of the Particle p on the Drum $C_p = mC'$, Farads

d = Distance of a Point Charge to a Wall, meter

D = Distance Between the Two Electrodes of the Carpco Machine, meter

e = Charge of the Electron

$\vec{E}$ = Field Strength, or gradient, volt/meter.

$\vec{E}_x$ = Field Strength Component in the x Direction, volt/meter

$\vec{E}_b$ = Air Breakdown Field Strength, volt/meter

$\vec{E}_i$ = Internal Field Strength, volt/meter

$\vec{E}_o$ = Field Strength of the Ionic Field, volt/meter

$\vec{E}_s$ = Field Strength of the Static Field, volt/meter

f = Capacity Shape Factor

$\vec{F}_p$ = Force on a Particle, newton

$\vec{F}_1$ = Attraction force on an ion due to the outside field

$\vec{F}_2$ = Attraction force on an ion due to the total dipole moment $\vec{P}$

$\vec{F}_3$ = Attraction force on an ion due to the net charge φ

$\vec{F}_{el}$ = Force of electrical nature, newton

$\mathcal{F} = \frac{E_o}{i'}$ = Ionic field characteristic

g = Gravity Acceleration = 9.81 meter/second^2

i = Intensity of the Ionic Field, ampere per unit length (meter)

i' = Density of Current of the Ionic field, ampere per square meter

k = Charging Shape Factor

k' = Ion mobility, square meter/Volt second

K_o = Relative Dielectric constant of free space = 1

K = Relative dielectric constant $K = \frac{\epsilon}{\epsilon_o}$

K_1 = Relative dielectric constant of medium 1; $K_1 = \frac{\epsilon_1}{\epsilon_o}$

K_2 = Relative dielectric constant of medium 2; $K_2 = \frac{\epsilon_2}{\epsilon_o}$

m = Clearance Correction for the individual capacity of a particle

m_p = Mass of a particle in kilograms

$M = 1 + \frac{\mathcal{F}}{\mathcal{P}}$ = ionic charging constant

$\vec{n}$ = Vector normal to a Given wall

N = Depolarization Factor

$\vec{P}$ = Total dipole moment, coulomb-meter

$\vec{P}_i$ = Specific dipole moment, coulomb per square meter

$\mathcal{P}$ = Leakage particle constant, ohm-meter

$\mathcal{P}'$ = Selectivity Factor in conductive induction charging

q_i = Charge, coulomb

q_v = Volumic charge density, coulomb per cubic meter

Q = Total charge, coulomb

Q_o = Initial charge, coulomb

Q_c = Charge due to contact, coulomb

Q_m = Maximum charge obtained by ion bombardment, coulomb

Q_s = Steady State Charge, coulombs

Q_x = Charge Acquired by Conductive Induction, coulomb.

r = Any given radius, meter

R = Outside Radius of a Corona Field, meter

R_1 = Radius of the Drum, meter

R_2 = Radius of the Electrode K, meter

R_b = Bulk resistance of a particle, ohm

R_p = Resistance of a particle, ohm

R_s = Surface Resistance of a particle, ohm

$\mathcal{R}$ = Critical reversing time, second

s = Any distance, meter

S = Total clearance between a plate condenser, meters

t = Time, second

$t^{\circ}c$ = Temperature , degree Centigrade

T = $\frac{Q}{Qm}$ ratio of actual charge over maximum ionic charge

$T^{\circ}K$ = Temperature, degree Kelvin

T_i = Any given T

T_f = $\frac{Q_s}{Qm}$ Final T

U = Steady state time constant characteristic.

V = Potential Difference, volt

W = Steady state time constant function

X = Intermediate Variable = M-T

Y = Intermediate Variable = $\frac{M-T}{B}$

γ = Conductivity, ohm^{-1} meter^{-1}

δ = Characteristic Static Field Angle, Radian

ϵ_o = Permitivity of free space, Farad per meter

ϵ = Permitivity of any medium, Farad per meter

ϵ_1 = Permitivity of medium 1, Farad per meter

ϵ_2 = Permitivity of medium 2, Farad per meter

θ = Any variable angle, radian

θ_o = Escaping angle, radian

θ_1 = Repulsive angle on a sphere, radian

ν = Clearance of the equivalent condenser of contact

σ = Charge density, coulomb per square meter

σ_c = Charge density due to contact charging, coulomb per square meter

σ_m = Maximum charge density, coulomb per square meter

Σ = Characteristic ionic angle

τ_i = Any given fixed time

τ_c = Leakage time constant

φ_1 = Image force function

φ_o = $\cos\theta_1$ particle repulsion variable

Φ = Force flux, newton per square meter

Ψ = Two cylinders capacity constant

φ = T/T_f = actual fraction of the steady state charge

$\bar{\omega}$ = Specific gravity, kilograms per cubic meter

ω = Angular velocity, radian per second

$\nabla \vec{E}$ = divergence $\vec{E} = \frac{\partial \vec{E}}{\partial x} + \frac{\partial \vec{E}}{\partial y} + \frac{\partial \vec{E}}{\partial z}$

$\nabla^2 V$ = Laplacian $V = \frac{\partial^2 V}{\partial x^2} + \frac{\partial^2 V}{\partial y^2} + \frac{\partial^2 V}{\partial z^2}$

$\frac{d\varphi^-}{dt}$ = Rate of Leakage, coulomb per second

$\frac{d\varphi^+}{dt}$ = Rate of Charging by ion bombardment, coulomb per second

Log x = Natural Logarithm of x

Table of Contents

A. THEORETICAL CONSIDERATIONS

I. Introduction

The process called "electrostatic separation" was known well before the beginning of this century. However very few applications of it are found in industry.

The lack of reproducibility of this process is frequently mentioned in the literature. Sometimes, "electrostatic separation" is called "electro-flotation."(1) No name, in fact, defines the process clearly. Since charges on the mineral particles are not static, it would be better to speak more generally of electrical concentration of minerals, this term bringing no limitation at all.

II. Generalities

Any solid solid separation process is based on the fact that solids have different physical or chemical, bulk or surface properties; gravity concentration utilizes differences in specific gravity and flotation, differences in surface physico-chemical properties. The greater the differences of related properties, the greater is the selectivity in concentration.

In electrical concentration, differences of electrical properties are utilized, namely, conductivity (γ) and dielectric constant ($\epsilon = K\epsilon_0$). All previously mentioned processes dealt with a potential field and with a medium. Electrical concentration operates with an electric field and a gaseous dielectric medium.

A separation is obtained when paths of two different particles are different and the greater the difference, the better the selectivity. A path of a particle is defined by the path of its center of gravity and governed by the following fundamental equation of rational mechanics:

$$\sum \vec{F}_p = m_p \vec{a}_p \qquad (1)$$

where indices p refer to the particle p.

The mass of a given particle is easily determined. When all of the forces acting on a given particle are known it is possible to compute its path and also to predict whether two particles of a given size will have paths of sufficient difference to allow a practical separation. The basic problem is the determination of the forces acting on a mineral particle.

III. Forces Applied To A Given Particle

Two types of forces are involved in electrical concentration, that is electrical and mechanical in nature.

(1) Forces of Mechanical Nature

This general term includes force of gravity, resistance of the medium during the motion, friction on a surface, and inertial forces due to prior motion, e.g., centrifugal force when the particle is placed on a rotating roll.

(2) Forces of Electrical Nature

These forces are due to the electrical field acting on a charged particle.

Purely mechanical forces require no special analysis since their intensities are well known; however forces of electrical nature require

detailed analysis.

IV. Study Of The Electric Field

Forces of Electrical nature are the result of the action of a field gradient on electrical charges distributed on a particle.

(A) Fields Independent Of Time

(1) Uniform Field

The sirplest example of a uniform field is the interior of a large condenser, which consists of two parallel conducting plates enclosing a medium e.g., vacuum the permittivity of which is equal to ϵ_o.

This is illustrated in Figure 1.

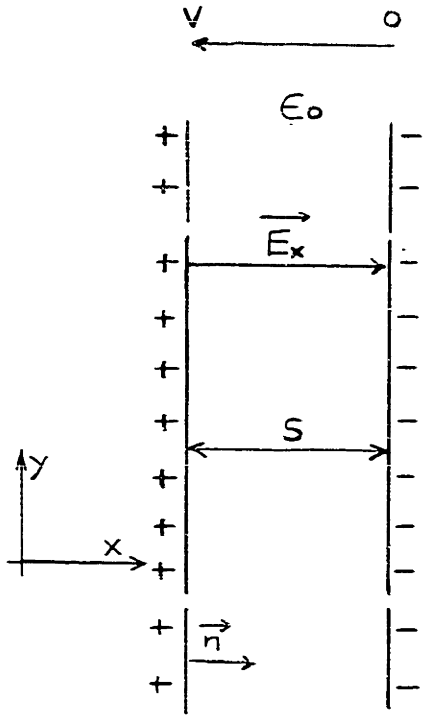

Figure 1. Plane condenser

The following relationships have been derived from the principles of electricity:

(1) $\vec{E}_x = -\frac{\partial V}{\partial S} = -\frac{V}{S}$ (2)

(2) $\vec{E}_x = \frac{\sigma}{\epsilon_o} \cdot \vec{n}$ (3)

(3) $\sigma A = Q$ and since

$$\frac{Q}{V} = C$$

$$\epsilon_o \vec{E}_x = \sigma = \epsilon_o \frac{V}{S}$$

$$\frac{Q}{V} = C = \frac{A\epsilon_o}{S} \quad (4)$$

In such a field the equipotential lines are parallel to the plates, and the lines of force are normal to the plates.

(2) Non-Uniform Field

Uniform fields are found very rarely in nature. The field between the two electrodes of most electrical separators is not uniform. In the investigation of non-uniform fields the following laws of electricity should be used:

$$(1) \qquad V = \frac{1}{4\pi\epsilon_o} \sum_{i=1}^{i=n} \frac{q_i}{r_i} \qquad \text{(Coulomb's Law)} \qquad (6)$$

$$(2) \int_{(A)} \vec{E} \cdot \vec{n} \cdot dA = \frac{1}{\epsilon_o} \sum_{i=1}^{i=n} q_i \qquad \text{(Gauss' Law)} \qquad (7)$$

where $\vec{E} = -$ gradient V

$$(3) \int_{(A)} \vec{E} \cdot \vec{n} \cdot dA = \int_{(V)} \nabla \cdot \vec{E} \cdot dV \quad , \quad \text{where} \qquad (8)$$

$\nabla \cdot \vec{E} =$ divergence $\vec{E} = \frac{\partial \vec{E}}{\partial x} - \frac{\partial \vec{E}}{\partial y} - \frac{\partial \vec{E}}{\partial z} = \frac{q_v}{\epsilon_o}$ i.e.,

$$\nabla^2 V = -\frac{q_v}{\epsilon_o} \qquad (9)$$

Consequently, a very good conductor, such as a metal, does not carry net charge inside its volume; thus $\int_{(A)} \vec{E} \cdot \vec{n} \cdot dA = 0$, then $\vec{E} = 0$ and V is a constant. Every metallic surface is an equi-potential surface and then, surfaces of force leave the surface at right angles.

The field map of the "Carpco" machine is shown in Figure 2.

The field gradient $\vec{E}$ will have the ~~maximum~~ greatest arithmetical values along BC; along CD, its value will be very small. Movement of electrode K enables changing the position of zone BCbc where the arithmetical value of the field ~~is greater~~ gradient.

The capacity between two cylinders is given by the formula:(2)

$$C = 2\pi\epsilon_0 \ell \Big/ \cosh^{-1}\left(\frac{D^2 - R_1^2 - R_2^2}{2R_1R_2}\right) \qquad (10)$$

$$C = 2\pi\epsilon_0 \ell \ \psi \qquad (11)$$

The significance of every letter is given in Figure 3. (ℓ stands for the length)

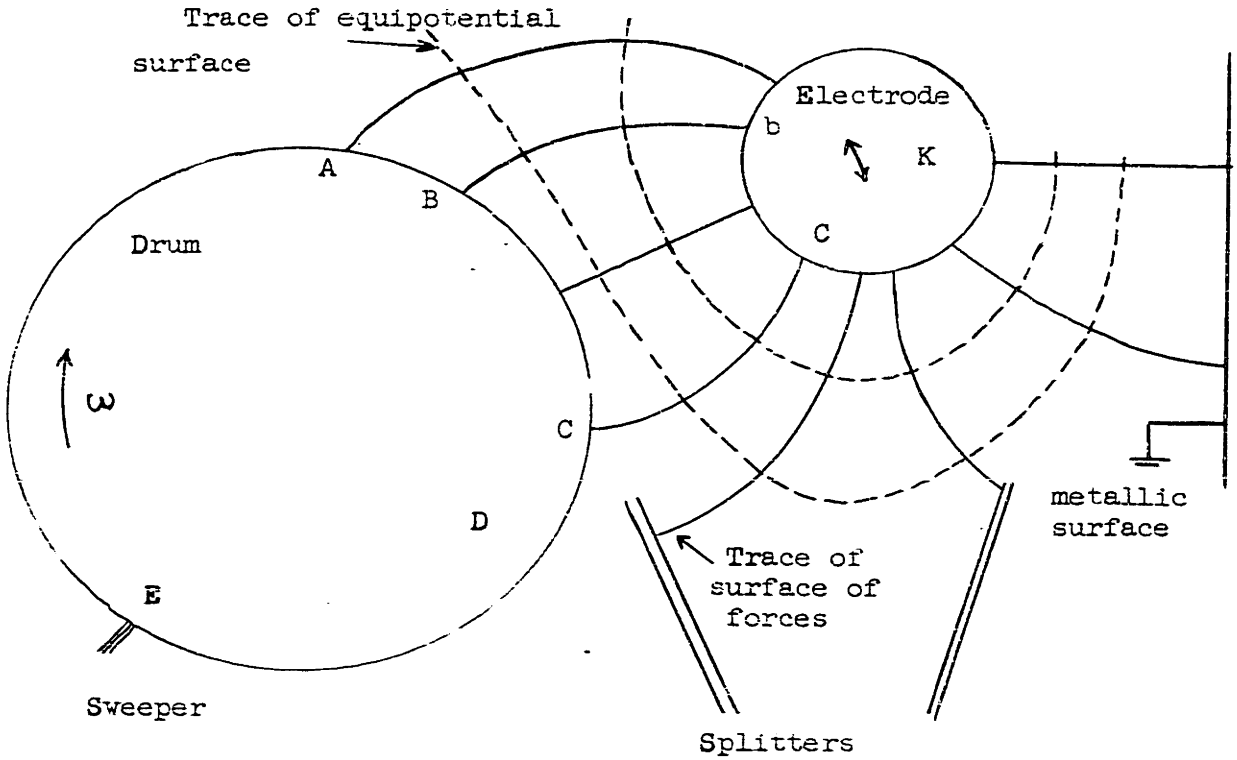

Figure 2. Schematic field map of the Carpco machine (A complete description of the machine is shown on Figure 39)

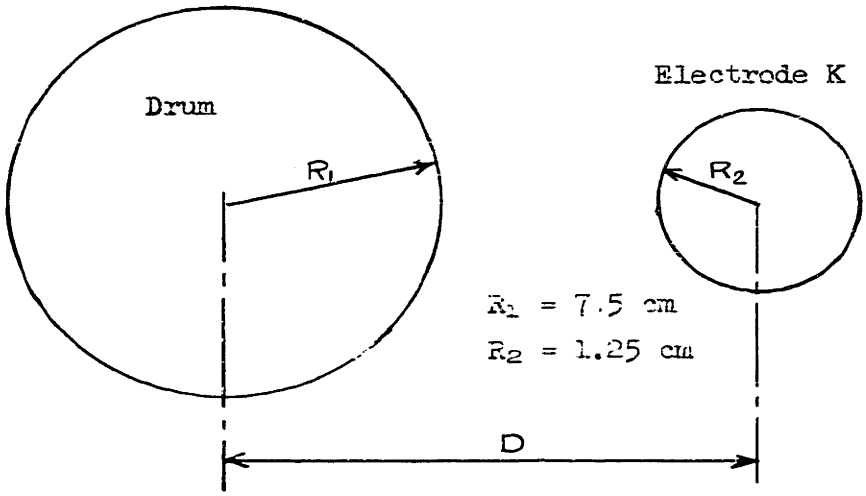

Figure 3: Bi-cylindrical condenser.

Table I gives the values of ψ (equation 11) for given distances D. Figure 4 is the illustration of Table I.

(3) Special Types of Non-Uniform Fields

(a) Corona Field

If we decrease the diameter of electrode K, represented on Figure 3, the electric field will become more and more concentrated, and the charge density on electrode K will become so large that emission of audible noises starts. This is known as the corona effect. If we increase the potential further, sparks are generated (brush discharge).

These succesive phenomena are explained by the formation of ions in the gas.

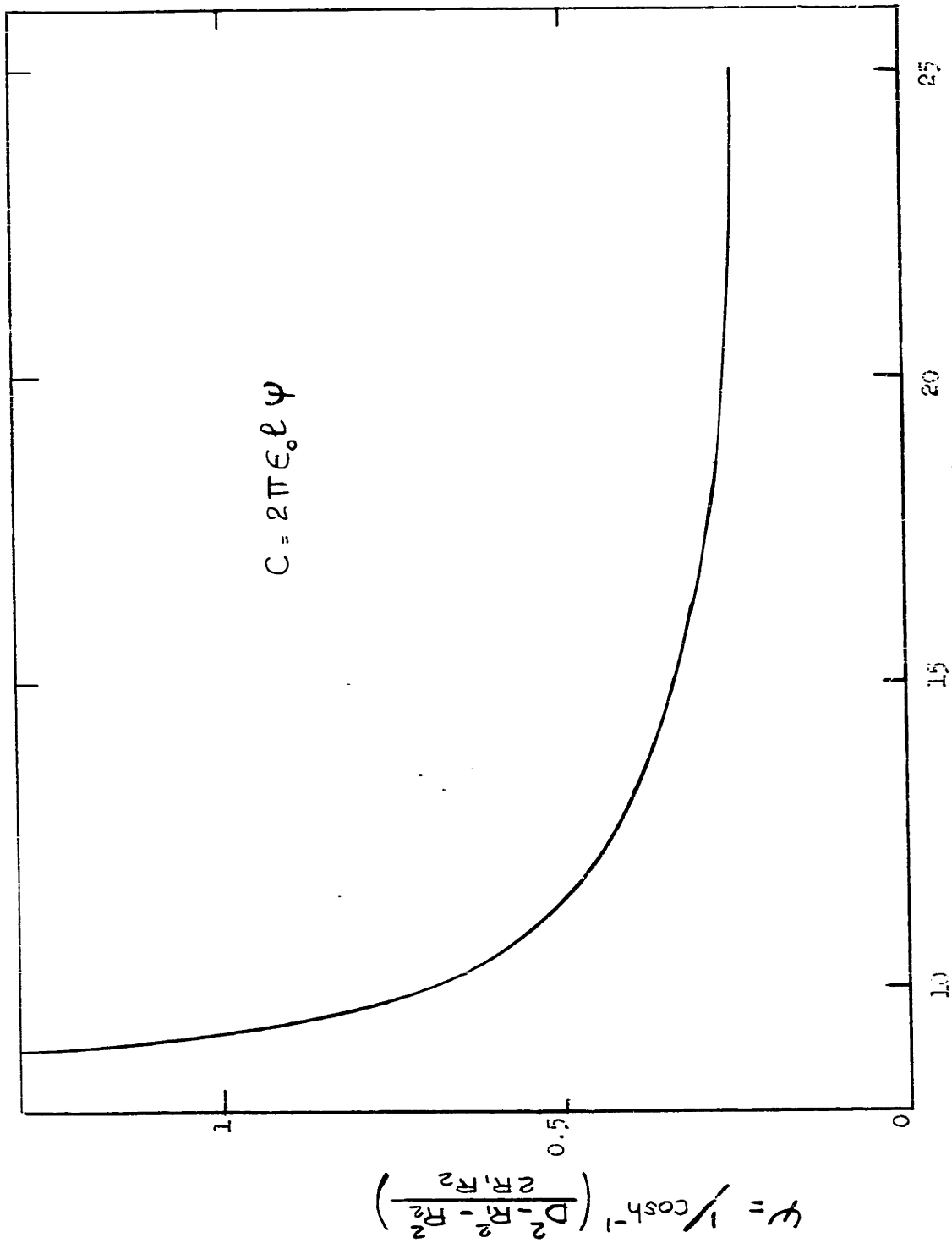

Figure 4: Variation of the capacity function of a bi-cylindrical condenser with the distance D between the two axes.

On the Carpco machine, such a field exists between the drum and the thin tungsten wire which is usually placed above the electrode K. (figure 39).

For an understanding of such a field, a simple study of a corona field will be useful.

Figure 5 represents such a field.

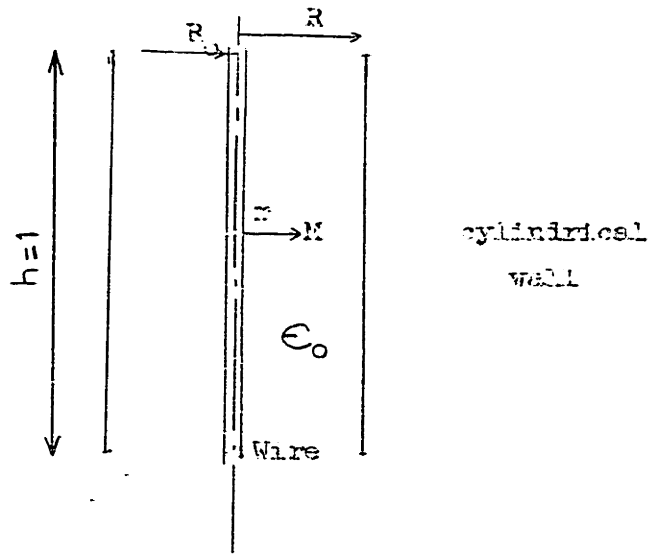

Figure 5: Corona field

At any point M in the field, we can write the Poisson equation, which in cylindrical coordinates is

$$\frac{\partial^2 V}{\partial r^2} + \frac{1}{r}\frac{\partial V}{\partial r} = -\frac{q_v}{\epsilon_o} \qquad (12)$$

Then, for time dt, $q_v = \frac{i\,dt}{2\pi r\,dr}$ (i being the intensity of the current flow)

$$q_v = \frac{i\,dt}{2\pi r\,dr} = \frac{i}{2\pi r}\left(\frac{dr}{dt}\right)^{-1}$$

The velocity of ions, $\frac{dr}{dt}$, is given by $k'\vec{E}_r = -k'\frac{\partial V}{\partial r}$

Equation (12) might be rewritten as:

$$r\frac{\partial^2 V}{\partial r^2} + \frac{\partial V}{\partial r} + \frac{i}{2\pi\epsilon_0}\frac{1}{k' E_r} = 0$$

or
$$r\left(\frac{\partial V}{\partial r}\right)\left(\frac{\partial^2 V}{\partial r^2}\right) + \left(\frac{\partial V}{\partial r}\right)^2 - \frac{i}{2\pi\epsilon_0 k'} = 0 \qquad (13)$$

Since $-\frac{\partial V}{\partial r} = E_r$

$$r\,E_r' \cdot E_r + E_r^2 - \frac{i}{2\pi\epsilon_0 k'} = 0$$

$$\frac{r}{2}\cdot\frac{d(E_r^2)}{dr} = \frac{i}{2\pi\epsilon_0 k'} - E_r^2$$

$$\frac{d(E_r^2)}{\left(i/2\pi\epsilon_0 k' - E_r^2\right)} = \frac{2}{r}\,dr$$

After integration

$$\text{Log}\left(\frac{i}{2\pi\epsilon_0 k'} - E_r^2\right) = \text{Log}\,\frac{C_1}{r^2}$$

and
$$\frac{C_1}{r^2} = \frac{i}{2\pi\epsilon_0 k'} - E_r^2$$

When $i = 0$, $E_r^2 = -\frac{C_1}{r^2}$, and $E_r = \pm \frac{1}{r}\sqrt{-C_1}$;

But the capacity of the condenser is $\frac{2\pi\epsilon_0}{\text{Log } r/R_0}$, and

$$Q = \frac{2\pi\epsilon_0 V}{\text{Log } r/R_0} \quad \text{since} \quad E_r = -\frac{Q}{2\pi\epsilon_0 r}$$

Therefore, $$E_r = -\frac{2\pi\epsilon_0 V}{2\pi\epsilon_0 r} \cdot \frac{1}{\text{Log } r/R_0} = \frac{V}{r} \cdot \frac{1}{\text{Log } r/R_0}$$

By substitution, $\sqrt{-C_1} = \frac{V}{\text{Log } r/R_0}$, and if we

let $-C_1 = A^2$ we have $A = \frac{V}{\text{Log } r/R_0}$

Then the equation is $$E_r = -\sqrt{\frac{i}{2\pi\epsilon_0 k'} + \frac{V^2}{\text{Log } r/R_0}} \qquad (14)$$

Pauthenier[3] gives a graph which is reproduced in Figure 6. From the graph, we see that E_r is essentially equal to : $-\sqrt{\frac{i}{2\pi\epsilon_0 k'}}$ especially for the voltage difference commonly used (usually very high).

(b) Field Due To A Discrete Charge

Another very important field to consider is that of a charged particle placed in front of a conducting grounded plate.

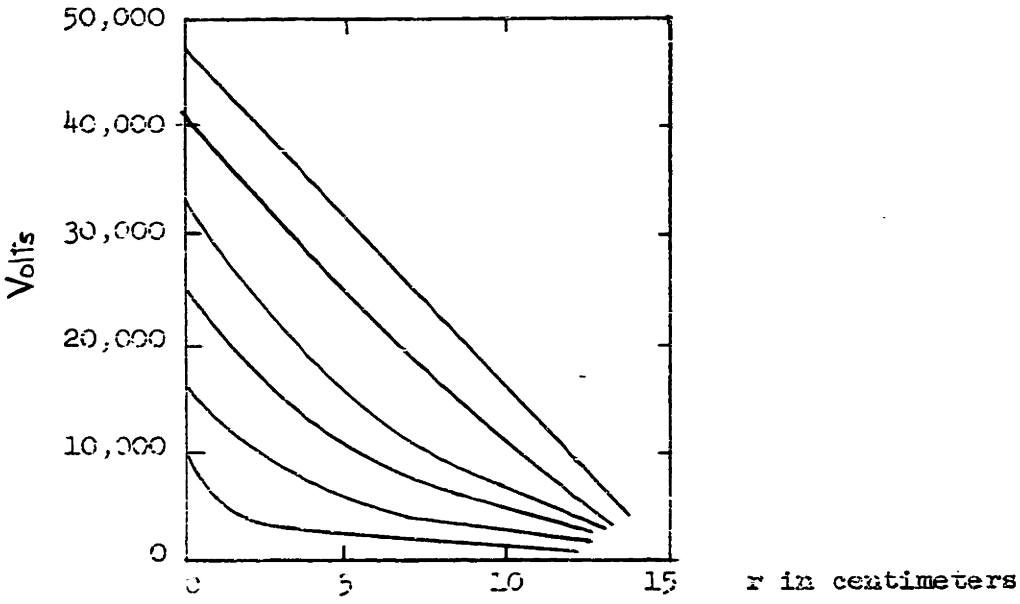

Figure 6: Potential distribution in a Corona Field for Various Potentials of the Central Wire

Such a field is represented in Figure 7. This case can be treated by the method of images, considering the fact that the present field is half the field which will exist between two particles of opposite charge, placed at a distance 2d from one another. The median axis is an equipotential line where V = 0 (Figure 8).

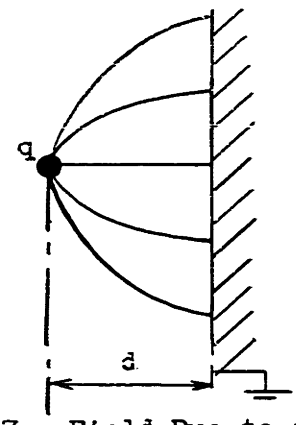

Figure 7: Field Due to a Discrete Charge in Front of a Grounded Plane Wall.

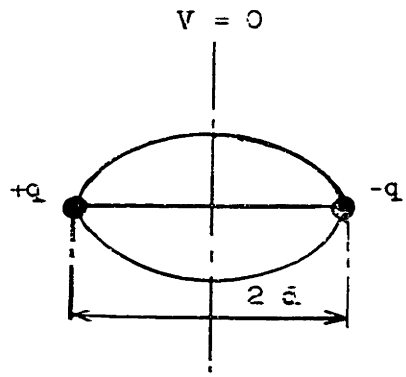

Figure 8: Image Force Principle

For this type of case, the expression for the force will be

$$F = -\frac{q^2}{16\pi\epsilon_0 d^2} \tag{15}$$

On the Carpco machine, (figure 39) we are not concerned with this simple case, but rather one such as that shown in Figure 9.

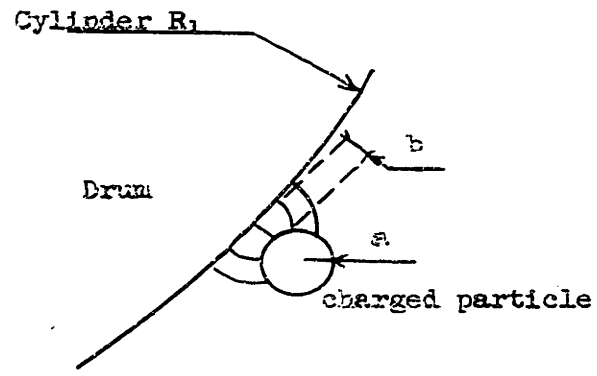

Figure 9: Field due to a Charged Particle in Front of a Grounded Cylinder

If we assume the charge of the particle to be concentrated at its center of gravity, the expression of the force will then be

$$F = -\frac{(-R_1 + b + a)\, R_1\, q^2}{4\pi\epsilon_0 \left[(R_1 + b + a)^2 - R_1^2\right]^2} = -\varphi_1 \cdot q^2 \tag{16}$$

Attention should be focused on the fact that, for the Carpco machine, the image force is holding the particle between points D and E because no more field is present here due to the presence of the splitters. (Figure 10)

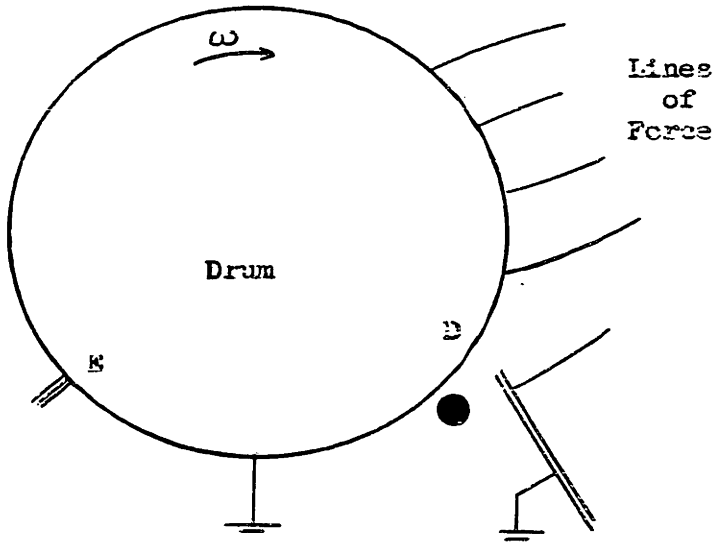

Figure 10: No-field Region in the Carpco Machine

(B) Time-Varying Fields

The previous discussion pertained to non-time-varying fields, even though in industrial separators, the fields are time-varying because the current used is half or full wave rectified. However, since the polarity is not reversed, one can use RMS values for voltage and fields.

There is, however, an interesting case with alternating fields. With such fields it is experimentally possible to perform separations of non-conductive particles. This is due to the fact that there is a phase angle between the vector $\vec{E}$ and the polarization vector $\vec{P}$ in a

dielectric, which angle varies with the frequency. However, this case will not be examined, by itself, since it would require a complete treatment.

V. Classification Of Minerals From The Electrical Viewpoint

It is habitual for electrical engineers to classify solids into three classes: conductors semi-conductors, and insulators. From the viewpoint of the solid state physics, it is possible to relate the ability to conduct electrons with the structure of a given material. Gaudin[4] made a useful classification of minerals for flotation purposes. It seems useful to extend it to problems encountered in electrical concentration. The classification presented in Figure 11 has been constructed from the general scheme given by Gaudin[4] and additional information from Pauling[5], Evans[6], Seitz[7], and Kittel[8].

The basis of this classification is the nature of the bonding between atoms of the crystal. Solids having:

(1) van der Waals bonds do not conduct electrons (good insulators),

(2) covalent bonds do not conduct electrons (good insulators),

(3) metallic bonds conduct electrons perfectly (good conductors),

(4) ionic bonds conduct electricity by means of ion transport (moderate insulators).

Specific combination of these different types of bonds gives a series of crystals whose electrical properties can be specifically predicted. (See figure 11).

Van der Waals 1 dim	2 dim	3 dim	Ionic	Metallic	Covalent	Ion Structures Have	Kinds of Crystal	Electrical Definition	Examples
		x					atomic	Insulator	He
		x			x		molecular	Insulator	S_2, I_2
	x				x		filament	Insulator	S_8
x				Δ	x		sheet	Insulator *	C graphite MoS_2
			Δ		x		diamantine	Insulator **	C diamond ZnS
			x		o		Simple ionic	Moderate Insulator***	NaCl PbS
			x		o	finite size	Complex ionic	Moderate Insulator+	SO_4Ca, CO_3Ca
			x		o	infinite length	Fiber	Moderate Insulator⊗	Silicates
			x		o	infinite area	Layer	Moderate Insulator □	Silicates
			x		o	infinite volume	Framework	Moderate Insulator ▽	Silicates
			Δ	Δ	Δ		Semi Conductors	Semi Conductors	Sulfides, Oxides Arsenides
				x			metallic	Conductor	Cu

* Insulator between sheets but conductor along the sheets either by resonance (graphite or by metallic bonding (MoS_2).

**Insulator but may become semi conductor by defect in the lattice (ZnS)

***Insulator but may become semi conductor by impurities or by defect.

+⊗□▽ Insulator but may become semi conductor (to a small extent)

x main bonding
o bonding within ions only
Δ possible bonding within ions only.

Figure 11. Classification of Minerals

Atomic, molecular, and filament crystals are obviously insulators because there is no way by which electrons or ions can be transferred.

Sheet structures should be insulating normal to the sheets. Along the sheets, however, since the bonding is not entirely covalent, electrons can be carried by so-called "quantum mechanical resonance" as in the case of graphite, or by partially metallic bonding as in the case of molybdenite.

Diamantine crystals are, strictly speaking, insulators. Diamond is a good example. However, in the case of sphalerite, impurities or defects in the lattice allow ions to be carried, and this is the origin of a semi-conduction phenomenon.

Simple ionic crystals like NaCl, KCl are moderate insulators; their conductivity is of the ionic type and at high enough temperature, they follow the law:

$$\gamma = D\, e^{-\alpha/T^{\circ}K}$$

where D and α are constants. (See Figure 12)

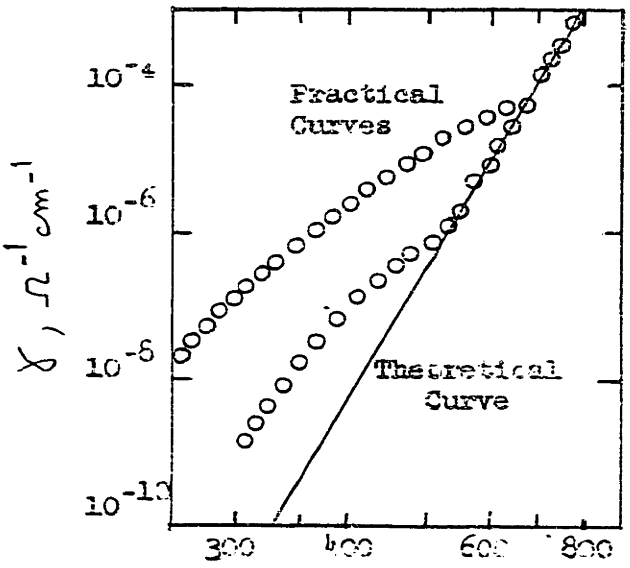

Figure 12: Dependence of the Conductivity of NaCl Upon the Temperature. (Ref. 7, Page 55).

At low temperatures the deviation arises from the impurities in the natural crystals.

However, if a crystal like PbS which otherwise resembles ionic crystals, in fact exhibits defects in its lattice, it becomes a semi-conductor, and in the electrical concentration process, its behavior will be analogous to that of a metallic conductor.

Complex ionic crystals are mainly moderate insulators; however, impurities may cause anomalous good conductivity.

Fiber, layer, and framework crystals are essentially insulators; however, to a lesser extent, conduction may take place due to the same causes as for ionic crystals.

The semi-conductor group is certainly the least clearly defined; and as it has been seen, simple ionic crystals may exhibit semi-conduction. Their special electrical behaviour comes from the fact that no exact kind of bonding is defined. Many factors influence their electrical conductivity such as for instance the amount of impurity and the partial pressure of the gas giving the cation.

For the case of cuprous oxide, Wagner and Dunwald[7] give the curves shown on Figure 13.

For the case of cadmium oxide, Wagner and Baumach[7] give the curve shown in Figure 14.

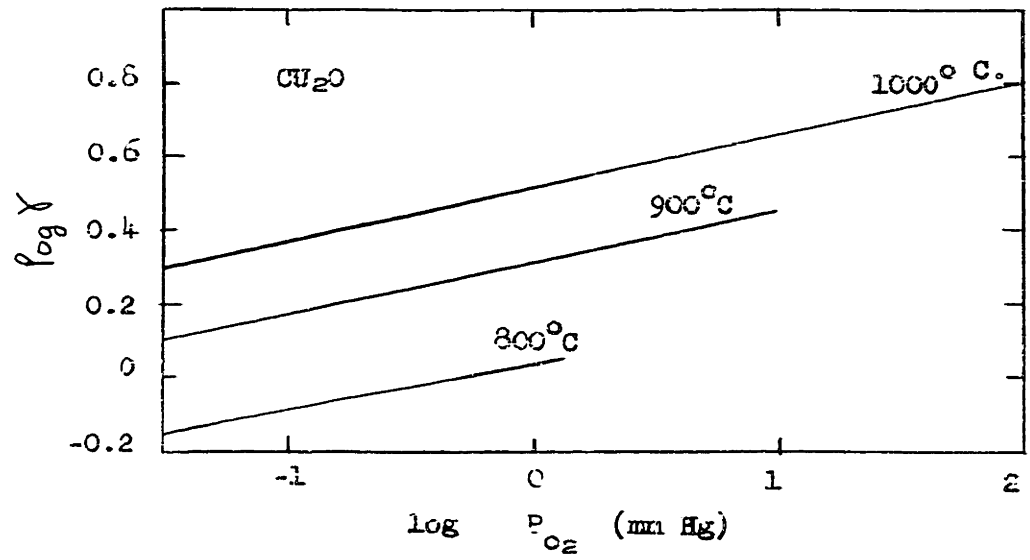

Figure 13: Dependence of the Conductivity of Cuprous Oxide Upon Oxygen Pressure (Ref. 7, page 71)

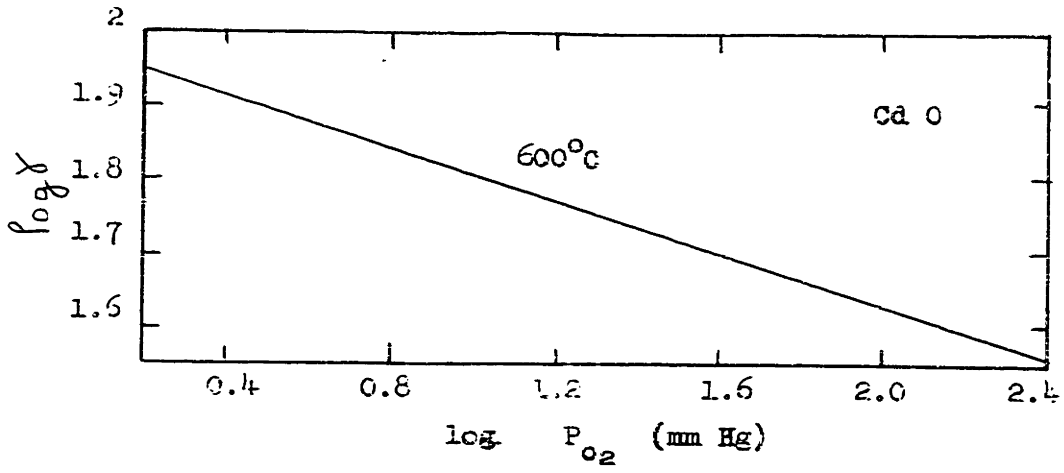

Figure 14: Dependence of the Conductivity of Cadmium Oxide Upon Oxygen Pressure (Ref. 7, page 71)

According to Seitz[7] there are two kinds of semi-conductors: those which contain impurities and those which do not.

The pure semi-conductors may be subdivided into those which conduct by free electrons and those which conduct by holes.

The following figures illustrate the different cases, using the band theory of solids.

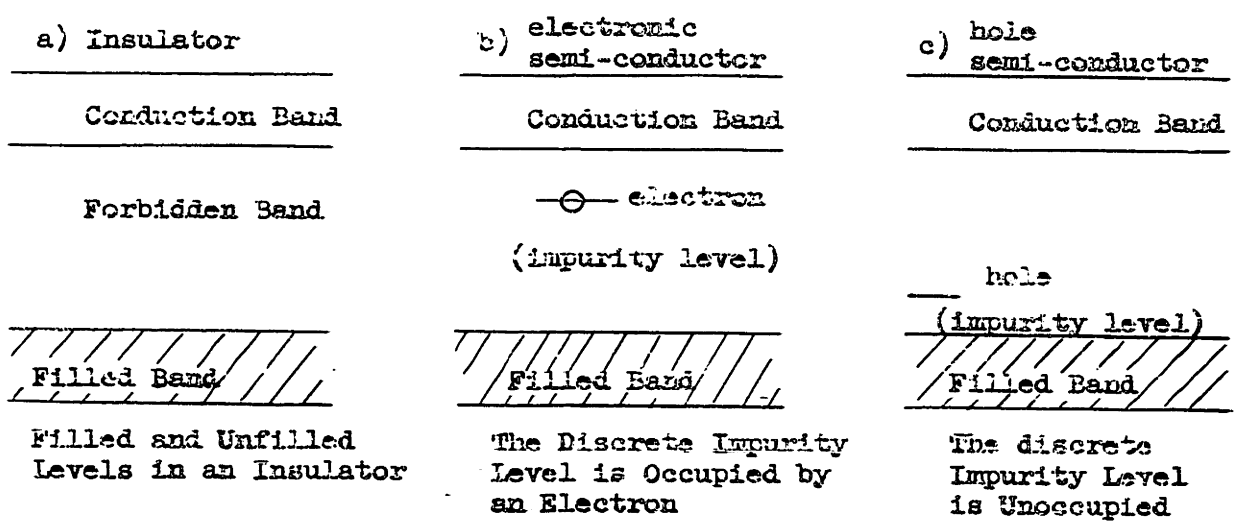

Figure 15: Insulator and Semi-conductors According to the Band Scheme

Then, for the case of cadmium oxide, heating produces an evaporation of oxygen and consequently gives an excess of cadmium ions. For the case of Cu_2O, conduction is performed by Cu^+ ion vacancies.

Semi-conductors like CdO are called excess semi-conductors, and those like Cu_2O are called deficit semi-conductors.

The effect of impurities is analogous to the effect of stoichiometric deficiencies.

Metallic crystals have free electrons and are conductors of electricity. However, metallic crystals are rarely found in nature, other than copper and gold.

This classification and this short review, have shown that electrical properties of minerals are related to their crystal structures. However, from the viewpoint of electrical concentration, there are some additional considerations. Even if liberation is assumed to be complete it is evident that the surface properties of a mineral might be quite different from those of the bulk; and during the process of separation, the surface properties might become so important that those of the bulk are insignificant. For instance, porous minerals and weathered minerals can exhibit quite surprising behaviour in their electrical separation. This is useful information because it shows that if we can modify the surface of a mineral particle, we can change its behaviour for this given separation. It will be seen later that for contact charging the particle shape is very important. For instance, from Figure 11 it can be seen that the layer crystal can be separated from the diamantine crystal by depending only on their shape difference. In one case, the contact areas will be very large, and in the other case it will be practically nil. For ionic bombardment

charging method it will be seen later that the shape is significant too, and that the behaviour of fiber crystals and layer crystals is somewhat different.

As a conclusion it may be stated that even if the classification is somewhat imperfect, nevertheless, its use provides a very helpful way to interpret the observed facts.

VI. Simple Charging Processes

For the purpose of computing forces, a knowledge of the charges is very essential. There are several ways to charge particles. Among them the most important are:

(1) conductive induction,

(2) contact electrification,

(3) ion bombardment.

One may conceive of a machine using only one of these charging processes; however, in the industrial machines, all the processes are used at the same time. Figures 16, 17, and 18 show the main features of such machines.

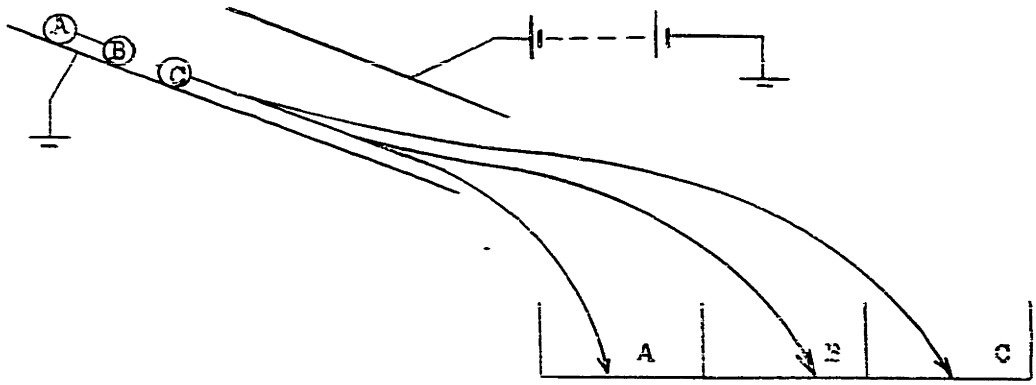

Figure 16: Electrical Concentration Using the Conductive Induction Charging

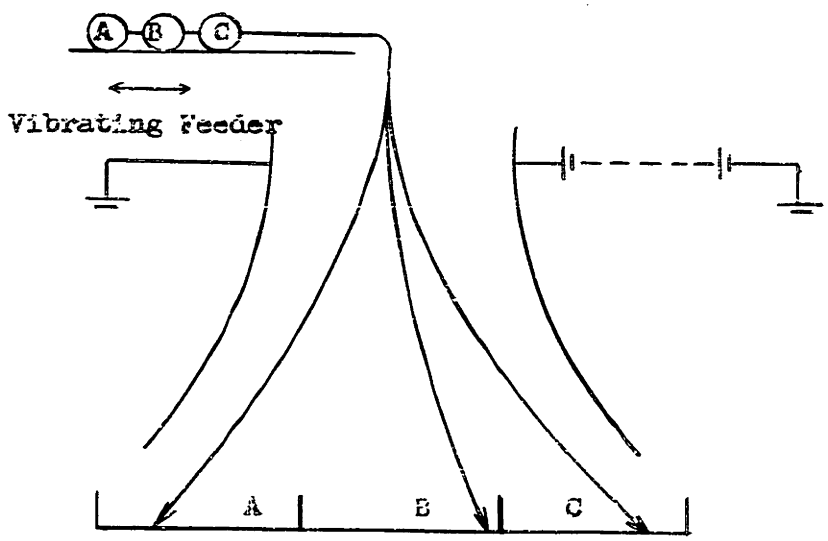

Figure 17: Electrical Concentration Using The Contact Potential Charging.

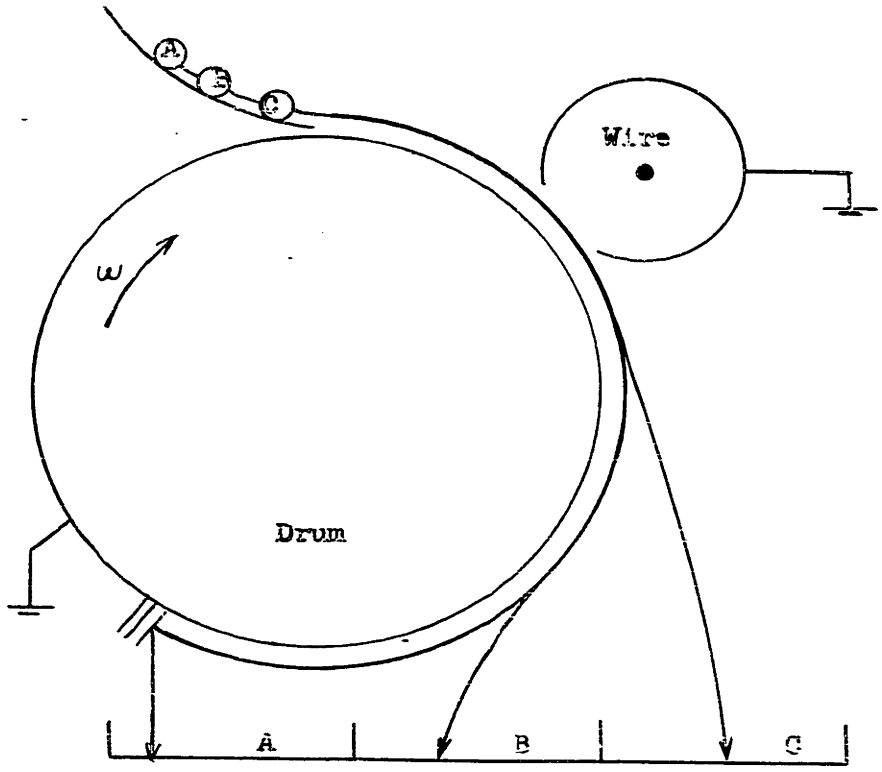

Figure 18: Electrical Concentration Using Ion Bombardment Charging

Before making an analytical study of each process, let us compare the possible selectivity of the three machines.

The machine represented by Figure 16 makes a separation due to the fact that (A) does not get charged, (B) gets a slight charge and (C) a considerable charge. The selectivity comes from the magnitude of charges of the same sign.

The machine represented by Figure 17 makes a separation due to the fact that (A) is positively charged, and (C) is more negatively charged than (B). Selectivity comes from the magnitude and sign of charges.

The machine represented by Figure 18 makes a separation due to the fact that (A) is much more negatively charged than (B) and (C). The selectivity comes from the magnitude of charges of the same sign.

However, for the machines in all three figures, the charges can be generated by contact also.

One reaches the conclusion that contact electrification gives a very selective process, but the two others give poor selectivity. This is why in the Carpco machine which we will study later, conductive induction and ion bombardment are used in competition, as to allow the maximum selectivity.

(1) Conductive Induction

Let us consider two particles of mineral, lying on the lower plate of our horizontal condenser, (Figure 19), where (1) is assumed to be a conductor and (2) is assumed a non-conductor.

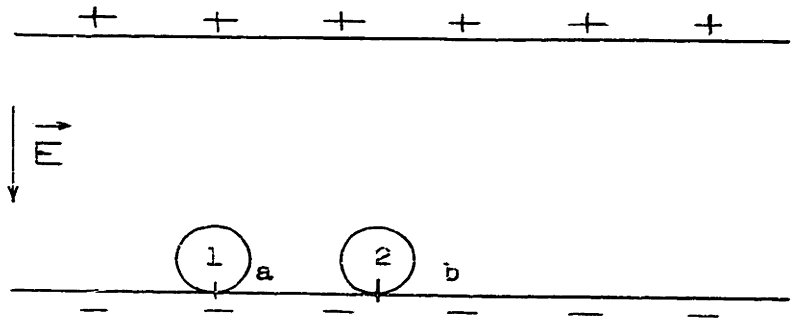

Figure 19: Charging of Particles in a Plane Condenser

If there is no electrical contact at a or b, the two particles will be polarized in such a way that the internal field will be nil for the conductor, and constant for the dielectric. From this simple remark we may see that a non-completely-liberated particle of chalcopyrite will behave like a quartz particle if the contacts are as shown in Figure 20.

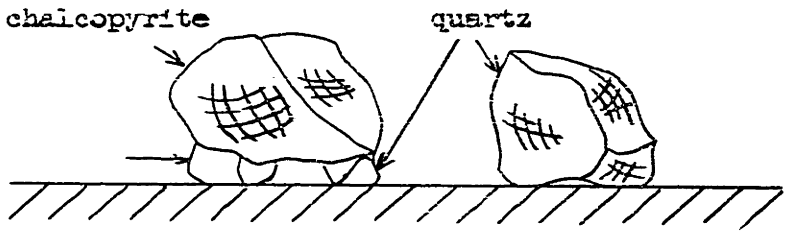

Figure 20: Anomaly of Contact Due to Non-liberation.

However, if there is an electrical contact at (a) of Figure 19, the surface of the conductor will become an equipotential surface. This is not the case for the dielectric however. The situation for both types will be that shown in Figure 21.

No net charge is generated on (2) but a net negative charge is induced by conduction on the surface of (1). If now the force due to the charge on (1) is greater than the force of gravity, particle (1) will be "lifted" but (2) will stay on the plate.

However, no mineral is either a perfect conductor like (1) or a perfect dielectric like (2). Any real mineral will require some length of time to become charged. One may assume the charging process to be equivalent to an RC circuit, as shown in Figure 22.

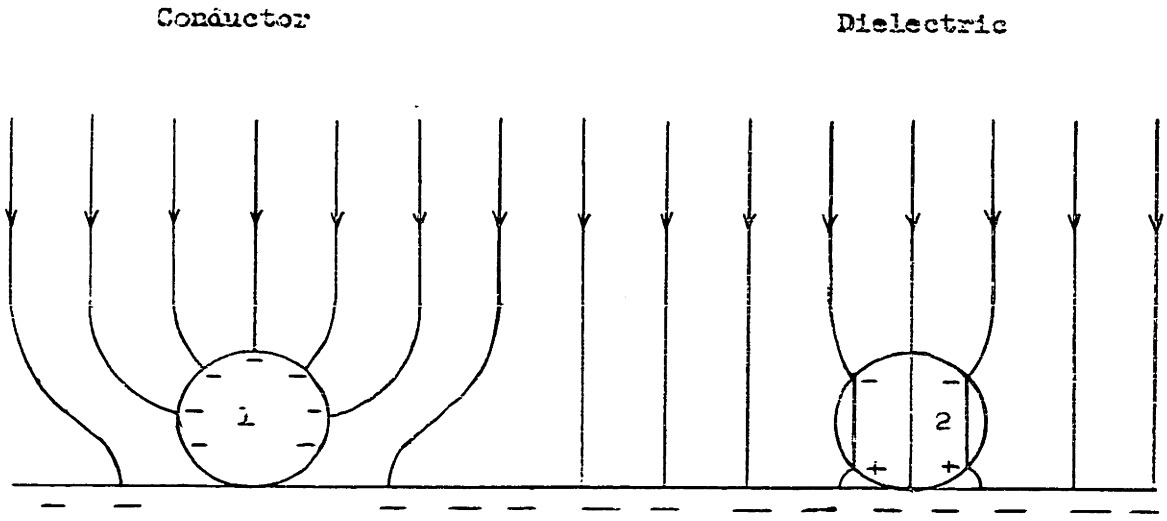

Figure 21: Modification of a Uniform Field by the Presence of Mineral Particles

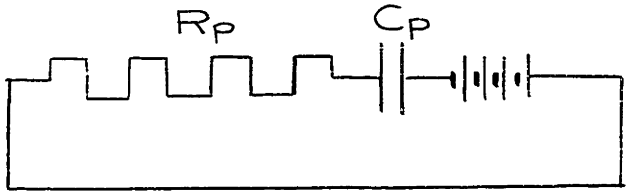

Figure 22. Electrical Circuit Equivalent to the Charging of a Mineral Particle by Contact.

The particle will have the potential of the lower plate, so that the maximum charge will be equal to $C_p V$ where C_p is the capacitance of the particle and V the voltage difference between the two plates. The resistance R_p is the equivalent total resistance of the particle.

From Figure 22 the charge Q is given by the following equation:

$$Q = Q_o + C_P V \left(1 - e^{-t/R_P C_P}\right) \quad (17)$$

Before going further in this interpretation, Q_o is the charge at time zero, which might be due to contact charging, and the resistance R_p is the result of the parallel coupling of the two named resistances (R_b and R_s) where

$$\frac{1}{R_P} = \frac{1}{R_b} + \frac{1}{R_S} \quad (18)$$

R_b is the bulk resistance and R_s the surface resistance. One may represent such a coupling as in Figure 23.

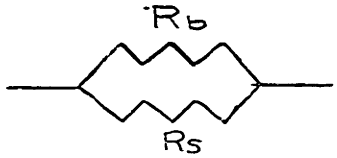

Figure 23: Equivalent Total Resistance of A Mineral Particle

From the equation 18, we see that the surface of the particle is essential in this case. The resistance of a particle, R_p, will then be a function of the state of the surface, the temperature, and the magnitude of the voltage, but not of the sign of the voltage. However, the sign of Q_o will depend on the polarity. The term, C_p, will be discussed under ion bombardment charging.

The case when a particle is lifted is expressed by the condition $F_{elec} \gg F_{gravity}$. This is represented in Figure 24.

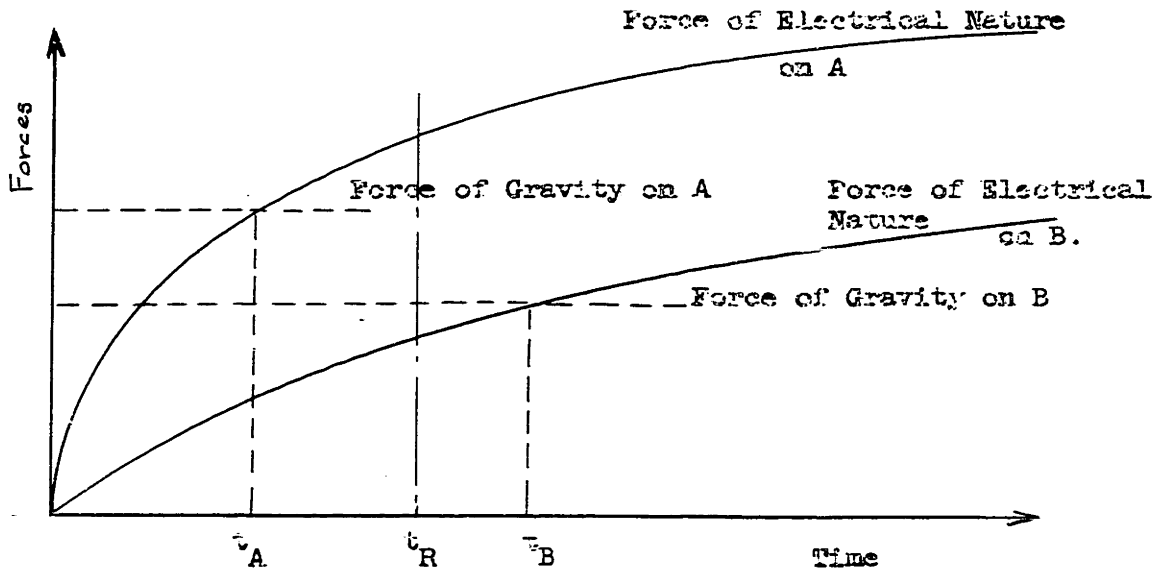

Figure 24: The lifting phenomenon, and its relation with the retention time.

At time t_A particle (A) will rise, but time t_B will be required to lift (B). However, if t_R, the retention time in the machine, is smaller than t_B, (B) will not be lifted. As was seen before, the selectivity comes from the magnitude of the charges but not from their signs.

One may add a short observation which is of major interest for setting a machine such as the Carpco separator. It has been seen that "lifting" may be performed on good conductors. When the Carpco machine is set for this purpose, we have the situation shown in Figure 25. Non-conductors follow a "normal" path, and conductors are lifted.

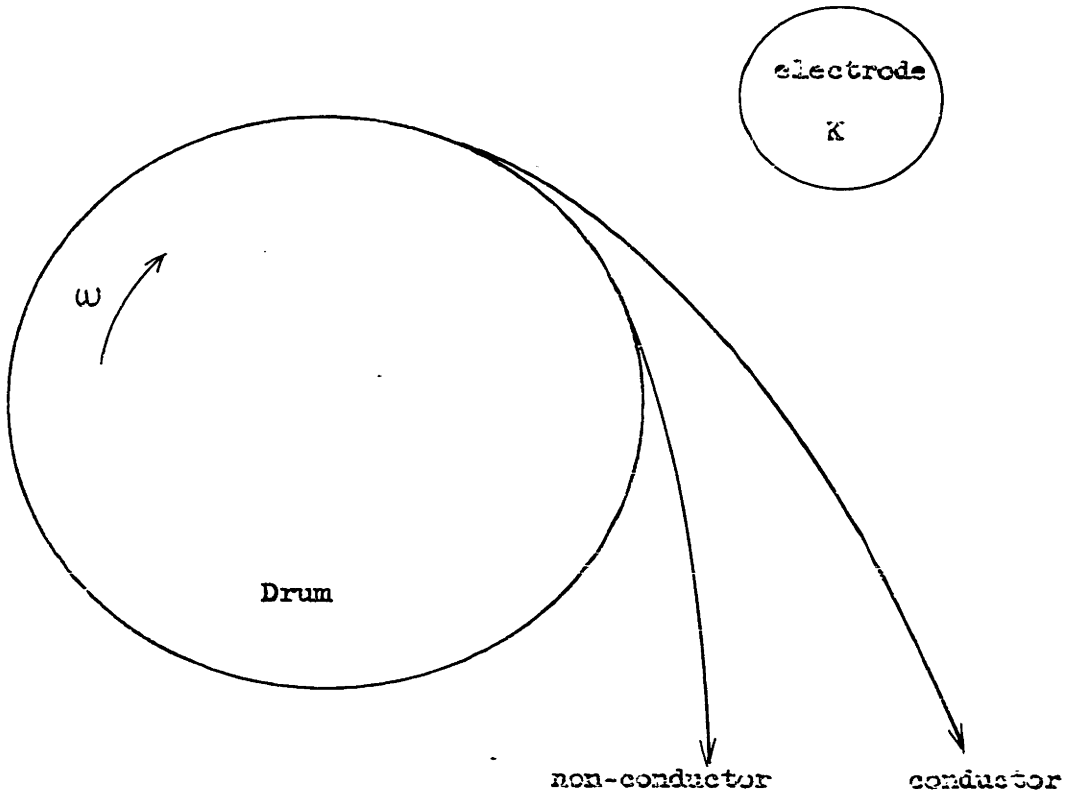

Figure 25: Paths of a non-conducting and of a conducting Particle in a Carpco Machine set for "Lifting"

However, if the electrode K is very close to the drum, conductive particles will hit the electrode become negatively charged and be lifted from the electrode, generating a rebounding motion between the drum and the electrode, thus giving rise to poor selectivity. (Figure 26).

(2) Contact Electrification Charging

It has long been known that when sulfur powder and red lead powder are mixed together, the sulfur becomes negatively charged and the red lead positively charged.[10] This phenomenon is called contact electrification. When two materials are placed in contact with each other, a double layer of charges is generated at the interface, and the charge density is given by Beach's law:

$$\sigma_c = 15 \cdot 10^{-6} (\epsilon_1 - \epsilon_2) \qquad (19)$$

σ_c being expressed in coulombs per square meter. Figure 27 represents the situation.

If we separate mechanically the two bodies, we end up with a net positive charge on (1) and a net negative charge on (2).

This phenomenon is analogous to the charging of a condenser (Figure 28), where the potential difference is the contact potential i.e., the Volta potential.

However, this picture is subject to discussion because when one of the bodies is a dielectric, it is difficult to speak of a potential. When the contact of the two bodies takes place in air the capacity of the condenser may be written as

$$C = \frac{A\epsilon_0}{\nu} \qquad (4)$$

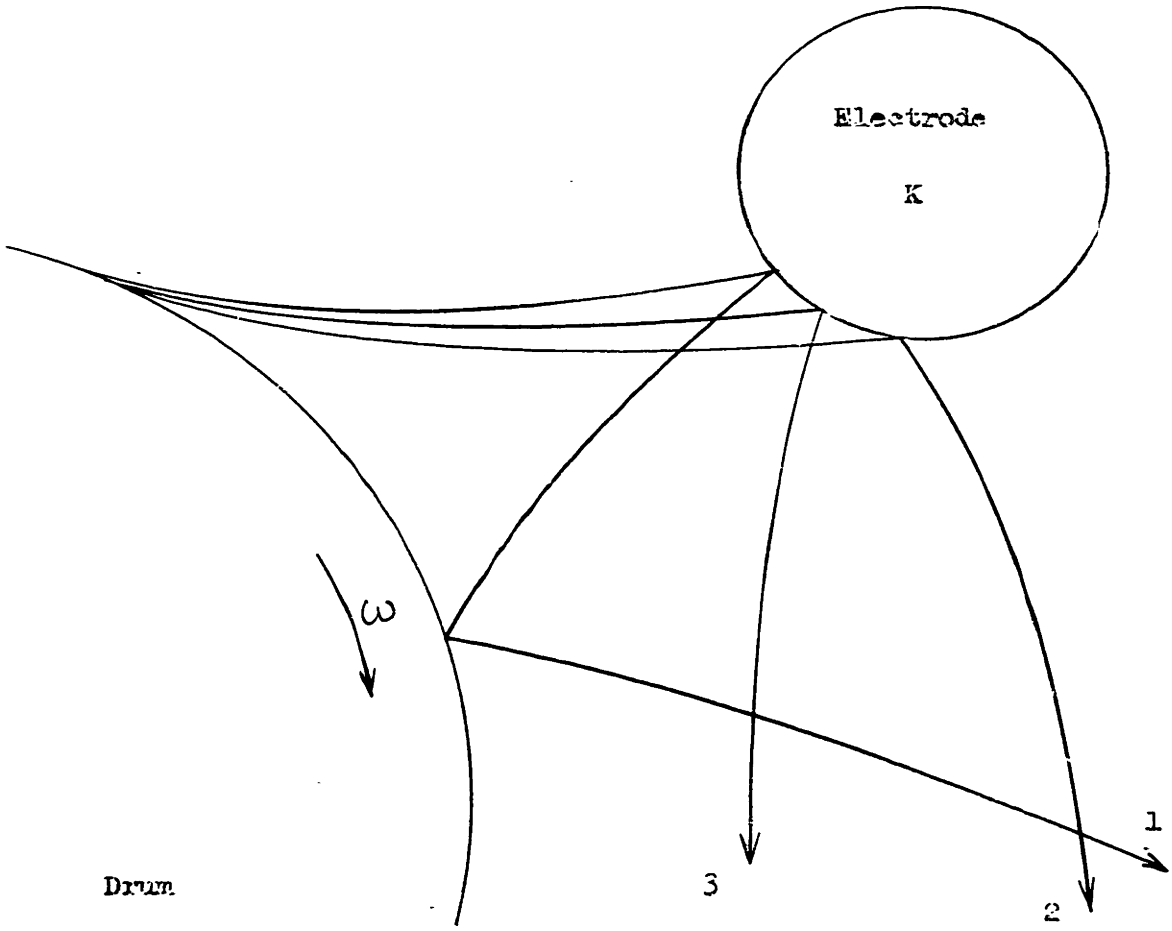

Figure 26: Rebounding motion of Conducting Particles in a Carpco Machine set for "Lifting"

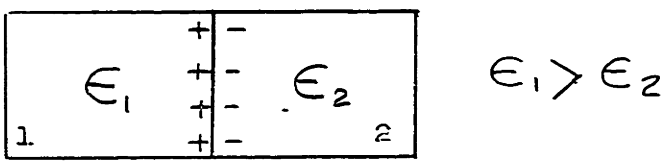

Figure 27: Electrical Double Layer Generated by Contact.

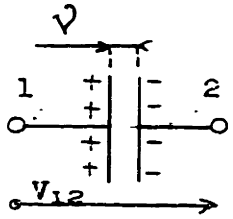

Figure 28: Plane Condenser equivalent to the Double Layer.

where A is the area of contact and ν is the clearance. If we increase ν (separation), the capacity decreases. From this previous picture, it is easily seen that:

(1) there will be a maximum charge on the bodies corresponding to the air breakdown,

(2) the charge by contact electrification should be an exponential function of time.

The maximum charge permissible is given by Gauss' law,

$$\sigma_m = \epsilon_o E_b$$

For air breakdown, $E_b = 3 \times 10^6$ volt/meter, thus giving

$$\sigma_m = 27 \times 10^{-6} \text{ coulomb/square meter.} \qquad (20)$$

In reference 11, it is shown that the contact charging of one mineral particle is an exponential function of time.

Theoretical considerations enable a more accurate analysis of the practical cases. If the machine represented in Figure 17 is now considered what can be said about the charging process? Figure 29 shows the feeding plate in greater detail. Charging here is due to mineral-plate contact and mineral-mineral contact. That is to say, contact between A or B and the copper plate, or contact between A and B.

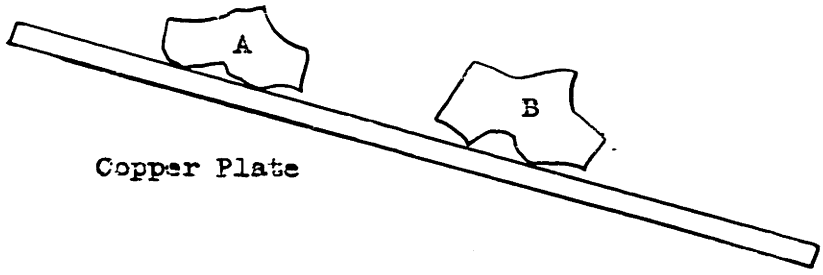

Figure 29: Charging by Metal-particle Contact.

a) Particle plate contact: It may be conceived that a particle A might roll on the copper sheet as represented by Figure 30.

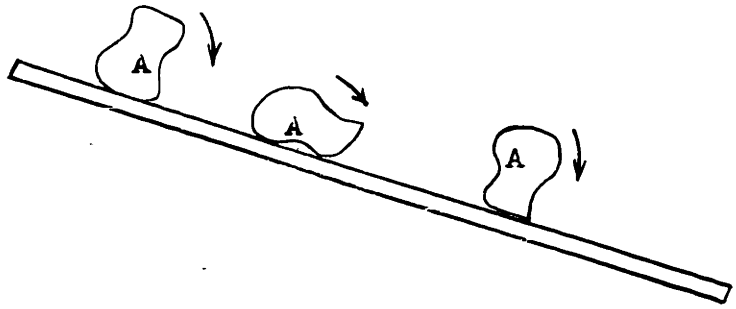

Figure 30: Rolling of a Particle on the Feeding Plate.

However, this rolling will take place in three not two dimensions. The particle will follow a zig-zag path on the plate. (Figure 31).

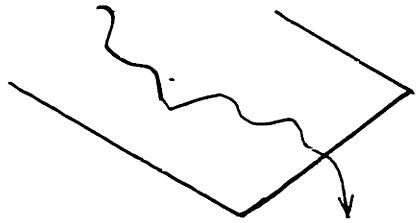

Figure 31: Path of a Particle on a Plate

In Figure 32, if we represent the areas which have been in contact with the metal; it is possible to conceive that only one small fraction has been in contact.

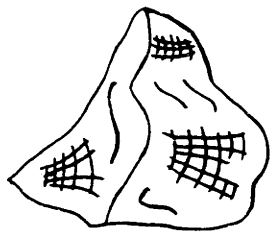

Figure 32: Illustration of the Effective Area of Contact.

If A is a conductor, charges will be distributed uniformly over the surface; but if it is a dielectric, quartz for instance, one sees easily that the charged surface is only a fraction of the total surface. The charge on the particle can then be written,

$$\varphi_c = A_{eff} (\epsilon_1 - \epsilon_2) \times 1.5\ 10^{-6} \qquad (21)$$

However, this supposes an infinite time of contact, which does not occur in practice. Then from these two arguments, small percentage of contact area and short time of contact, it is conceivable that the actual charge is something like 1 to 10% of the maximum charge expected. From a practical point of view, this might be considered unfortunate. Nevertheless, it shows again how important is the shape factor in mineral engineering. It will be seen later that for ionic bombardment charging the same kind of effect exists.

If now we consider two minerals with the same dielectric constant, the same conductivity, and the same surface area as determined by the BET method, it is possible to see that a separation can be achieved, based on the fact that if two minerals have different kinds of crystalline structure, the effective area (equation 2) will be different. In this case the selectivity will be based on the magnitude of the charges, but not on their sign.

b) Particle-Particle Contact

The same approach may be used for understanding this phenomenon. However, when the plate is covered with only one layer of particles, the phenomenon of plate-mineral contact charging is predominant; but if the layer is very thick, the phenomenon of mineral-mineral contact is predominant.

From this study it would appear that the process is very elegant. However, it is difficult to overlook the sign of the charge which will go on a given particle[12] because the two dielectric constants entering in Beach's law[19] are those of the surfaces, and can differ from those of the bulk. Since the contact potential is related to the work functions of the solids, impurities or lattice defects can reverse the predicted situation[12]. In fact mere heating to a certain temperature can make enough changes to allow satisfactory selectivity where such selectivity is lacking at room temperature.

One more observation may be added, in the case of metal-particle contact, it is very difficult to speak of work function of the metal, because the latter is covered with a film of oxide or adsorbed oxygen which makes all prediction conjectural.

(3) Ion Bombardment Charging

Among the processes studied in this work, this one is certainly the least selective. However, when it is combined with conductive induction as in the case of the Carpco machine, the selectivity of the compound process becomes very good and allows industrial rates of production at a reasonable cost.

Before commencing a mathematical discussion of the charging process, we may try to grasp a simple picture of the charging mechanism. In the previous study of the Corona field, it was seen that there is a current, of intensity i, between the electrodes. This current is due to a circulation of ions between the wire and the other electrode.

If a particle A is put into this field, it will become polarized (Figure 33).

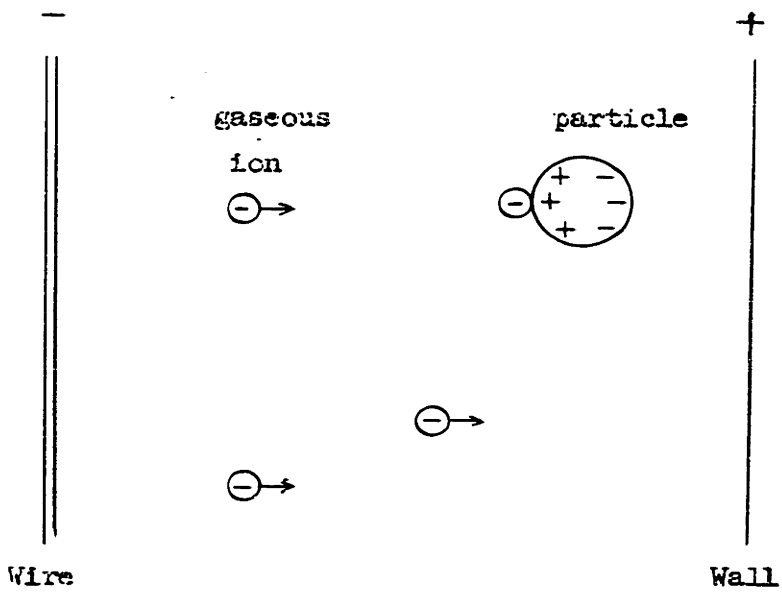

Figure 33: Picture of the Charging of a Mineral Particle in an Ionic Field

It may now be seen that a gaseous anion will tend to stick on a bound positive charge in the particle. If this simple picture is acceptable, it is obvious that after a certain time the particle A will exhibit a net negative charge. Already it is seen that whatever A is (conductor or insulator), this charge will be negative. The only selectivity, if there is any, should arise from the magnitude of the charge but not from their sign.

a) Derivation Of The Maximum Charge

A rigorous calculation of the maximum charge on a conducting sphere has been made by Pauthenier[3]. The following section is a generalization of the study made by Pauthenier. Instead of spheres the particles have been assumed to be electrically equivalent to ellipsoids of revolution, whose axes are parallel to a uniform field.

The following assumptions are made:

(1) the field is uniform,

(2) the ions are not thermally excited,

(3) the image force will be neglected in all calculations,

(4) a charged particle is considered to be equivalent to a point charge with a dipole moment equivalent to that of an ellipsoid of revolution,

(5) the method used is the study of the mechanical equilibrium of an unexcited ion in the field, modified by the presence of the particle.

(6) the axis is parallel to the field which corresponds to a stable electrical equilibrium.

When a particle falls freely in air, it presents the largest surface area to the fluid. Consequently, according to the relative position of the field gradient and the particle velocity, either oblate or prolate ellipsoids have to be considered. In the case of the following section the equivalent electrical ellipsoid would be prolate, but in the Carpco machine, they are oblate (field gradient parallel to the velocity of the particles).

b) Details Of The Calculation

Figure 34 shows the details of the several forces exerted on the ion i having a charge e.

$$\vec{F_1} = \vec{E_o}\, e$$

$$\vec{F_2} = \frac{2\vec{P}}{4\pi\epsilon_o}\, e\, \frac{1}{\rho^3(1+\nu)^3} \quad \left(\begin{array}{l}\text{due to the}\\ \text{diple moment}\end{array}\right)$$

$$\vec{F_3} = -\frac{eQ}{\rho^2(1+\nu)^2} \cdot \frac{1}{4\pi\epsilon_o} \quad \left(\begin{array}{l}\text{due to the}\\ \text{net charge}\end{array}\right)$$

where Q is the charge on the particle and $\vec{P}$ the dipole moment.

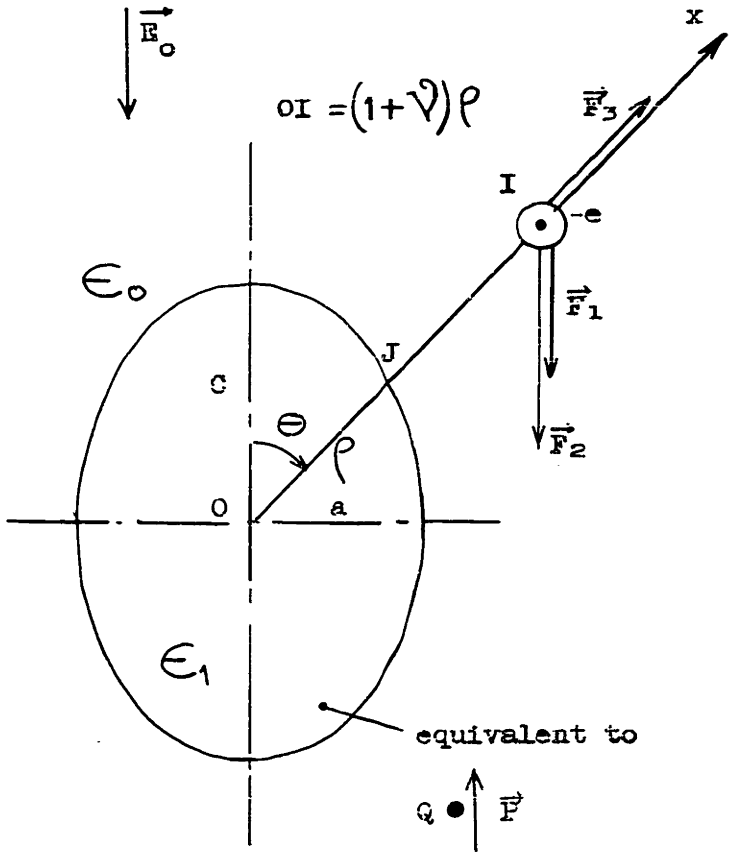

Figure 34: Diagram of the Ionic Charging.

On the axis OX the net force is then

$$\vec{F} = -\vec{E}_o e \cos\theta - \frac{2\vec{P} e \cos\theta}{4\pi\epsilon_o \rho^3 (1+\nu)^3} + \frac{eQ}{4\pi\epsilon_o} \frac{1}{\rho^2 (1+\nu)^2} \qquad (22)$$

We now have to compute $\vec{P}$.

The method used will employ the concept of the depolarization factor,(13)

$$\vec{E}_i = \vec{E}_o - \frac{N}{\epsilon_o} \vec{P}_i$$

$\vec{p_i}$ is the dipole moment per unit volume and $\vec{E_i}$ is the inside field. For several values of c/a, N is given in reference 8 and is reproduced in Figure 35

$$\vec{P_i} = (\epsilon_1 - \epsilon_0)\vec{E_i} \tag{23}$$

After substitution we get

$$\vec{P_i} = \frac{\vec{E_0}}{\frac{1}{\epsilon_1 - \epsilon_0} + \frac{N}{\epsilon_0}} \tag{24}$$

The volume of the ellipsoid is $4/3\pi a^2 c$. Then

$$\vec{P} = \frac{\epsilon_0 \vec{E_0}}{\frac{1}{K_1 - K_0} + N} \times \frac{4}{3}\pi a^2 c \tag{25}$$

Equation (22) then becomes

$$\vec{F} = -\vec{E_0} e \cos\theta \left[1 + \frac{2}{3}\frac{a^2 c}{\frac{1}{K_1 - K_0} + N} \cdot \frac{1}{\rho^3 (1+\gamma)^3}\right] + \frac{eQ}{\rho^2 (1+\gamma)^2} \tag{26}$$

The more charge we put, the larger will become the repulsive zone, and θ will tend towards zero (Figure 36). ρ tends thus toward c, and γ is very small compared to unity. Then at the maximum charge, we may write

$$0 = -\vec{E_0} e \left[1 + \frac{2}{3}\frac{a^2 c}{\frac{1}{K_1 - K_0} + N} \cdot \frac{1}{c^2}\right] + \frac{e Q_m}{c^2} \tag{27}$$

From Equation (27) we derive that

$$Q_m = 4\pi \epsilon_0 a^2 \left[\frac{c^2}{a^2} + \frac{2}{3}\frac{1}{\frac{1}{K_1 - K_0} + N}\right]\vec{E_0} \tag{28}$$

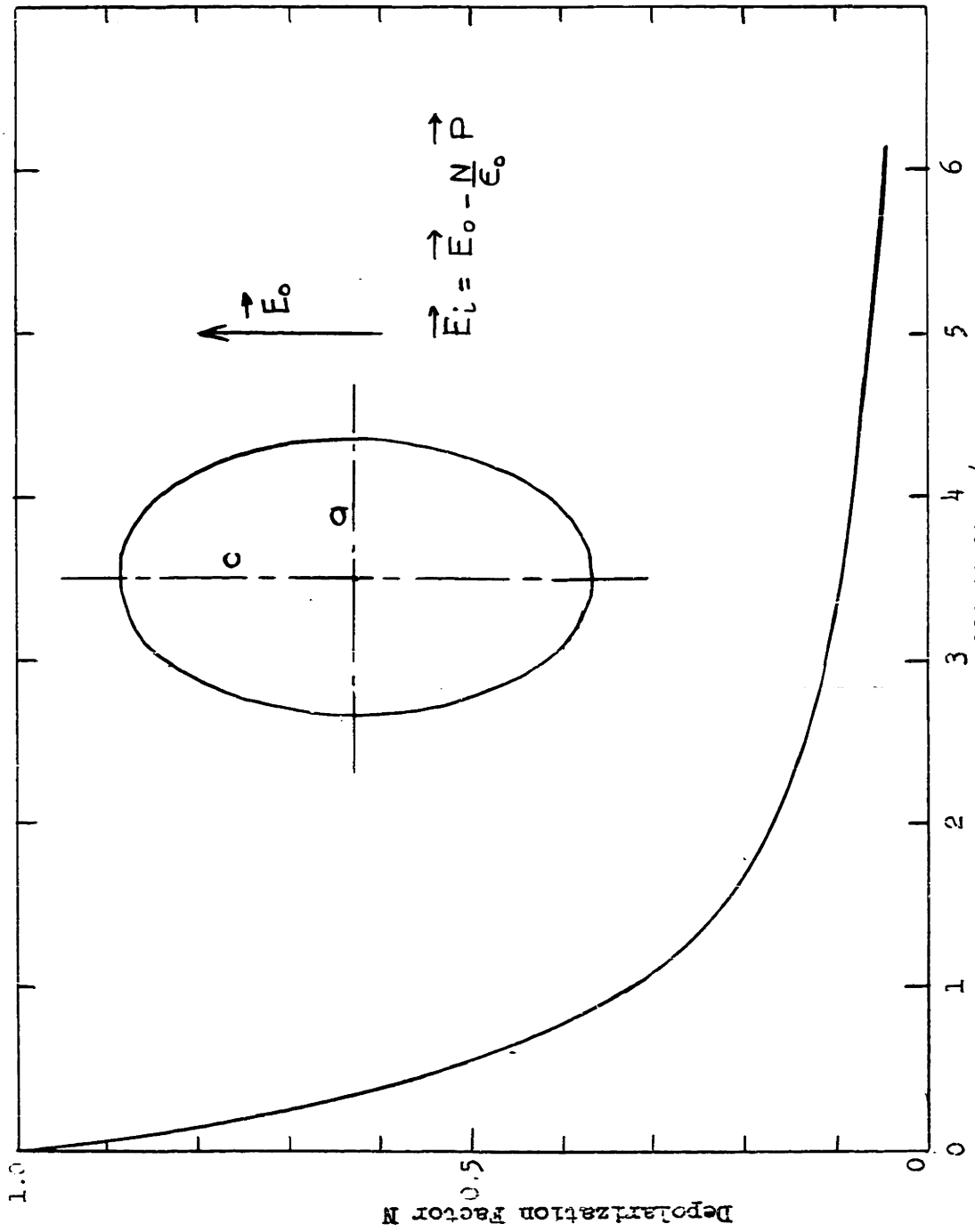

Figure 35: Variation of the Depolarization Factor N with the Ellipticity c/a

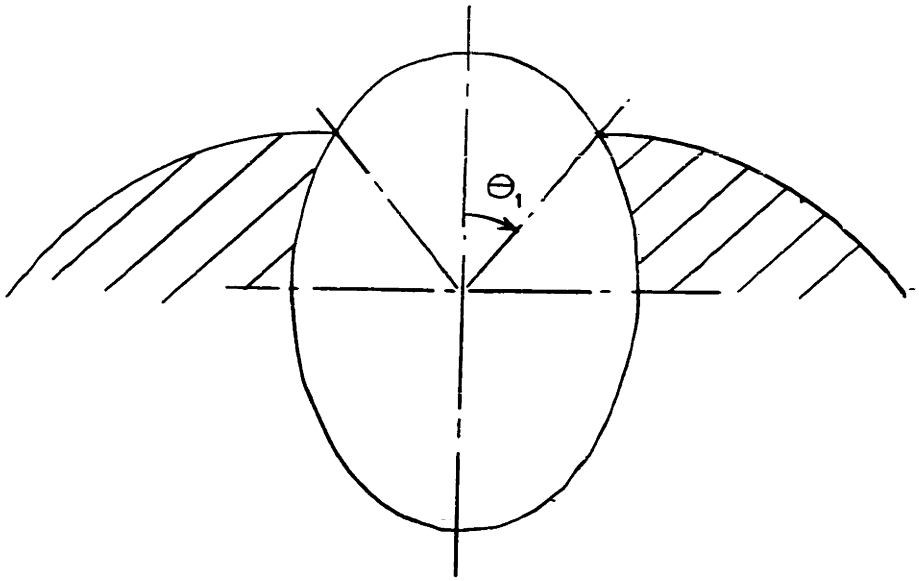

Figure 36: Schematization of the Repulsive Zone Due to the Net Charge Q on a Particle

which shortly can be written

$$Q_m = 4\pi\epsilon_0 a^2 k\left(\frac{c}{a}, K_1\right) \vec{E_0} \qquad (29)$$

The tables (2 and 3) give the values of k for different values of c/a and K_1. These results are presented in Figure 37.

c) Conclusions

Such results merit additional comments. First of all it is obvious that such a charging is not selective, and it may be that the machine represented in Figure 38 will not be a separator at all.

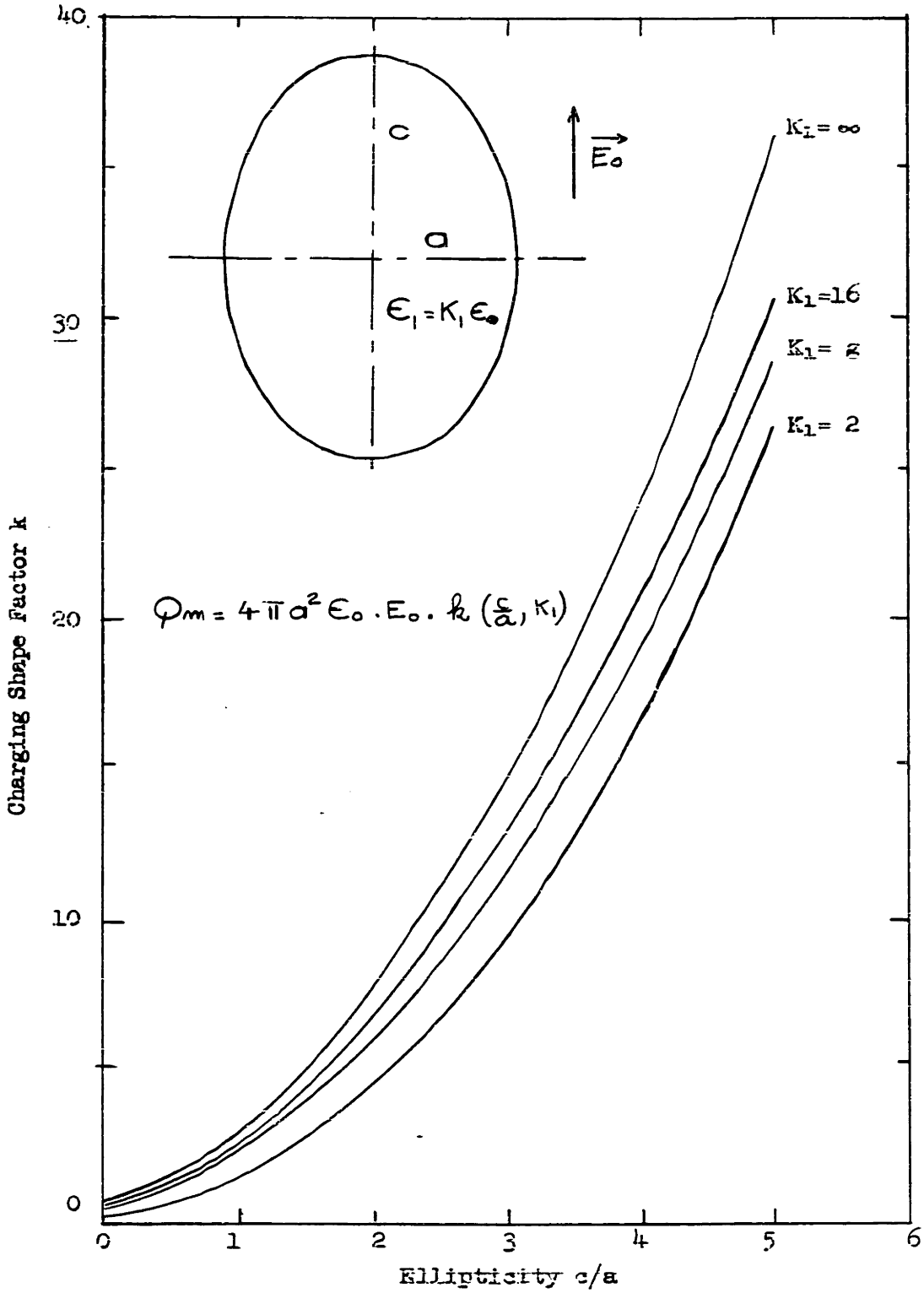

Figure 37: Variations of the Charging Shape Factor k with the ellipticity c/a for various dielectric constants K_1.

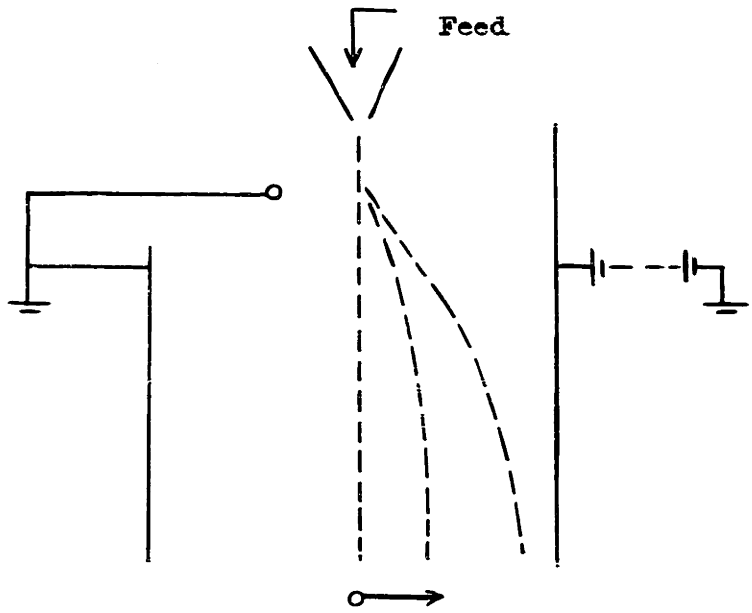

Figure 38: Electrical Classifier

By a simple study, we may show that the length of impact, L, is about proportional to $\frac{k}{\omega^3 a^5}$, assuming the values of c/a are identical for all the particles. This process is not one of separation but rather one of classification where the classification function may be written as

$$\frac{k}{\omega^3 a^5} = f(L)$$

From Figure 37 it is seen that whatever the dielectric constant be, k does not vary greatly and the approximate statement can be made that the separating function should be

$$\omega^3 a^5 = f'(L)$$

In this case, this presents no selectivity as far as the electrical properties are concerned.

On the other hand we have seen previously that the maximum charge density on a particle was expressed by $\sigma_m = \epsilon_o E_b$. As a rough approximation, one may say that $\epsilon_o E_o k\left(\frac{c}{a}, K_1\right)$ is of the same order of magnitude as the acquired charge density from ion bombardment. Then $\epsilon_o E_o k$ should be smaller than $\epsilon_o E_b$, yielding

$$k\left(\frac{c}{a}, K_1\right) \leqslant \frac{E_b}{E_o} \qquad (30)$$

Usually, $\frac{E_b}{E_o}$ varies between 2 and 5, and so it may be said that k must be less than 5 for any case. This limits the extent of the possibility of making separations based on the difference of the c/a ratios. This is one more reason why this particular process is non-selective.

VII. Compound Charging - Study of the Carpco Machine

(a) Generalities

The previous pages have shown that one may imagine any kind of electrical concentration machine based on one of the fundamental charging processes. However, it is obvious that in most machines one might imagine these processes would be combined with greater or lesser success. By its very application, the Carpco machine has shown that in some cases a good selectivity may be obtained industrially. This chapter will study the theory of the machine.

Figure 2 showed the approximate field map between the drum and the electrode K. The following Figure (Figure 39) represents all the features of the machine and the symbols which will be used in discussing the kinetics of the charging of particles.

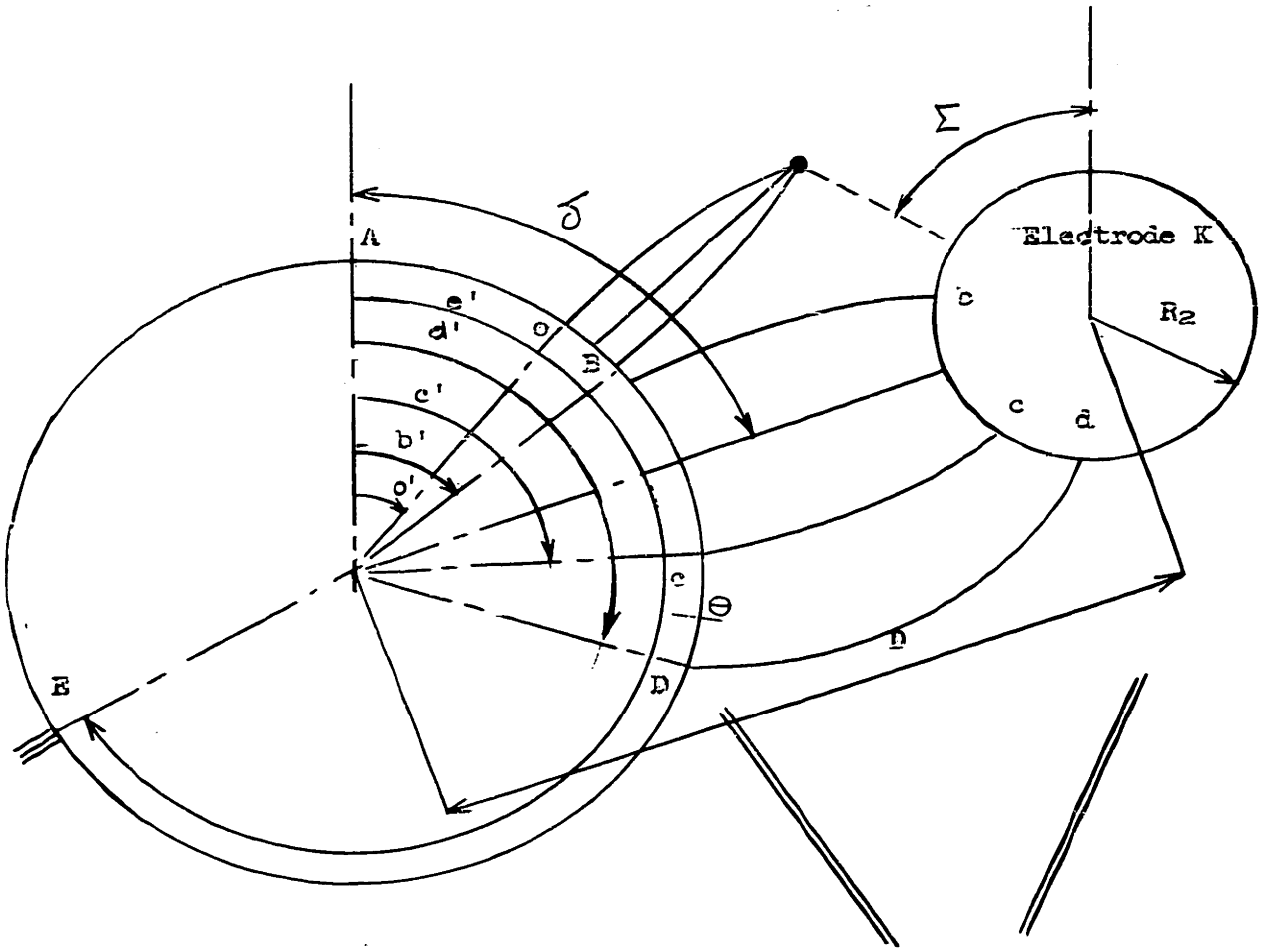

Figure 39: Variables on the Carpco Machine.

The symbols have the following meanings:

o' = feeding angle

b'- o' = ionic feed angle

c'- b' = static field angle

d'- c' = complementary static field angle

e'- d' = zero field angle

Θ = escaping angle of a given particle

Σ = characteristic ionic field angle

δ = characteristic static field angle

D = characteristic static field distance

Before analyzing the mathematical aspect of the charging, it seems useful to have a simple picture of the mechanisms involved when a particle travels from A to E.

Figures 40 and 41 show on straight lines the complete picture of the behaviors of a conducting particle, e.g., galena, and of a non-conducting particle, e.g., quartz.

Figures 40 and 41 show also that evolution of charge on a particle (conductor or not) during its travel from A to E. One may immediately see that the two main features of this evolution are the steady state charge existing between O and B, and the decay from B combined with inductive conduction. On the other hand, it has been stated in several articles that it is possible to "pin" conductors. This is true only when the steady state charge is very negative, so that the decay combined with conductive induction, does not allow a charge reversal. However, if we allow a longer residence time between B and E, the conductor will be lifted. (Figure 42).

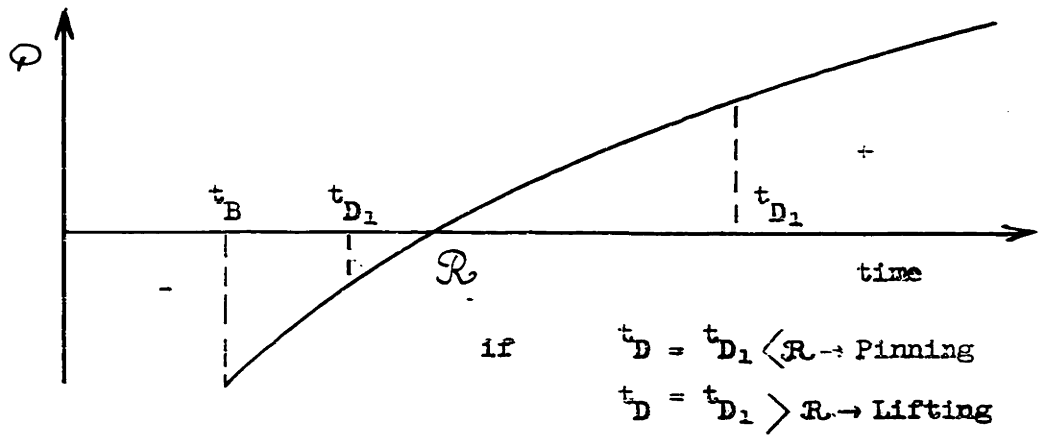

Figure 42: Interpretation of Lifting and Pinning

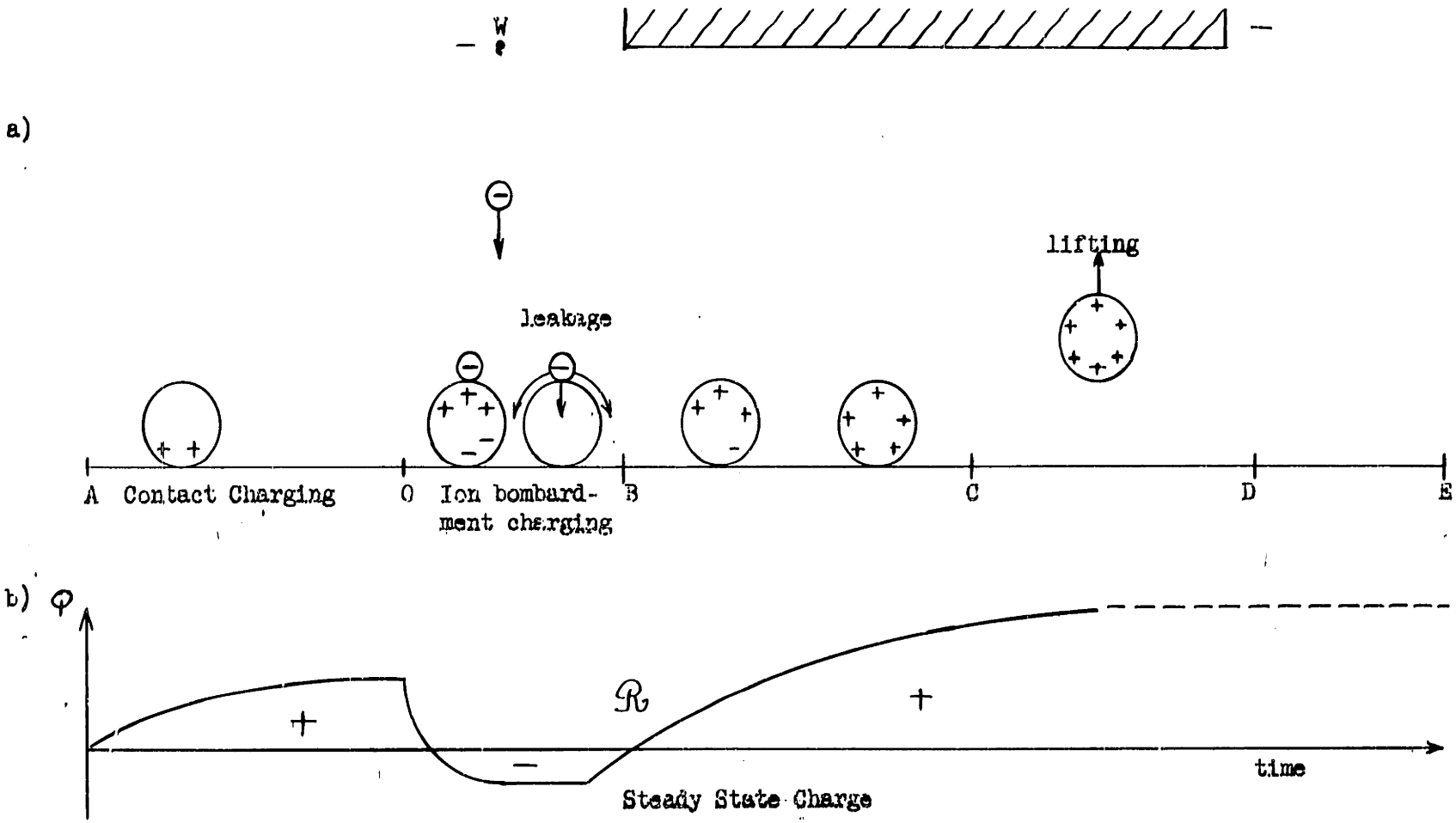

Figure 40: Behaviour of a Conducting Particle in the Carpco Machine

a) Picture of the Behaviour along the Drum

b) Evolution of Charge with Time.

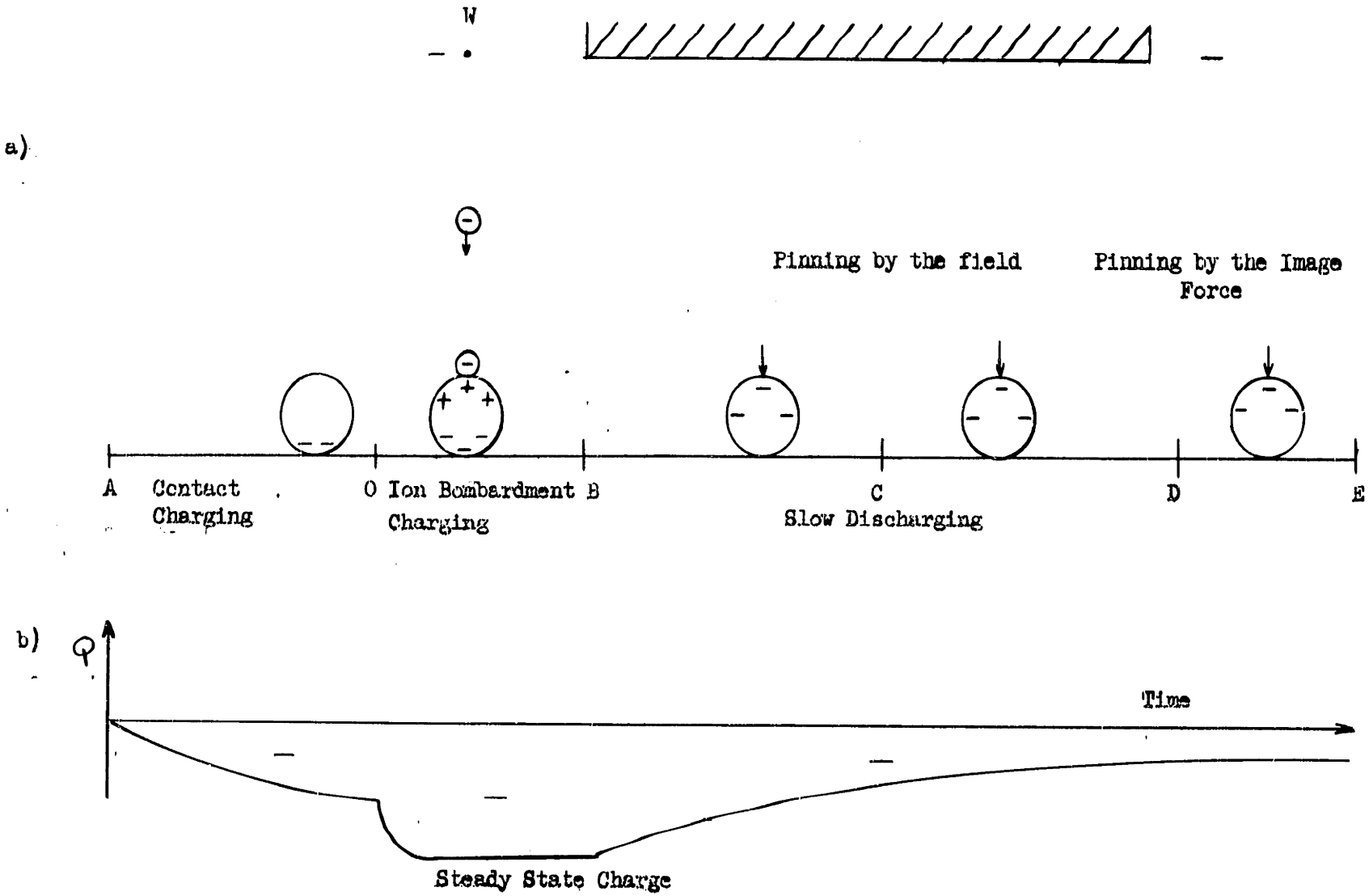

Figure 41: Behaviour of a non-conducting Particle in the Carpco Machine
a) Picture of the behaviour along the drum.
b) Evolution of charge with time.

Though this observation may seem trivial, it is of importance in practice for the industrial cleaning operation of conducting minerals.

(b) Study Of The Steady State Charge

We may speak of a steady state charge because we have ions moving simultaneously: (1) towards the surface of the particle (charging), and (2) leakage of charges due to the conductivity of the particle (discharging).

It is obvious that for a conductor the steady state charge will be very different from the previously computed maximum charge, while for a non-conductor, the difference will be small (Figures 43 & 44).

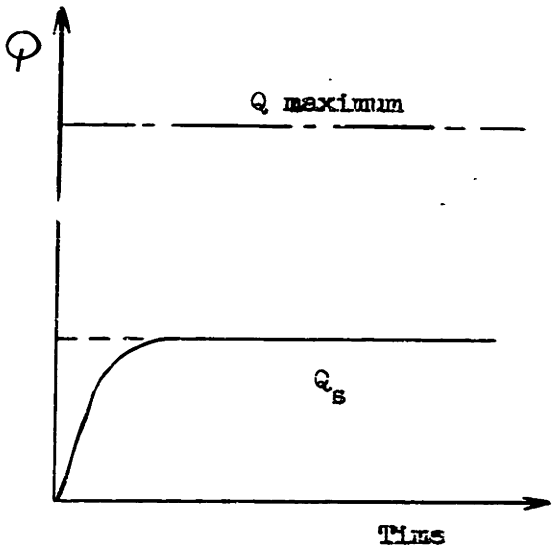

Figure 43: Achievement of the Steady State Charge on a "Conductive" Particle

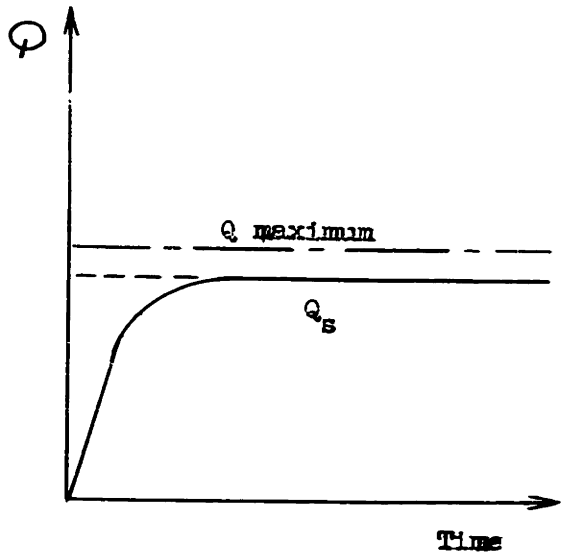

Figure 44: Achievement of the Steady State Charge on a Non-Conductive Particle

These represent two ideal cases; obviously, all real cases will be intermediate between these two.

(1) Charging By Ions

It has been seen (Equation 29) that the maximum charge on a particle is given by

$$Q_m = 4\pi \epsilon_0 a^2 k \vec{E_0} \qquad (29)$$

k being a limited function of c/a and K_1. For the allowable values of k, one may say that the considered ellipsoid is equivalent to a sphere of radius a, on which the charge density is approximately : $\epsilon_0 k \vec{E_0}$

The treatment of the charging process may be simplified by writing

$$\cos \theta_1 = \frac{Q}{4\pi \epsilon_0 E_0 a^2 k} = \varphi_0 \qquad (31)$$

Refer to Figure 45; $d\varphi^+ = Q_m d\varphi_0$ and θ_1 is the angle of the repulsive zone in this simplified model (see Figure 36).

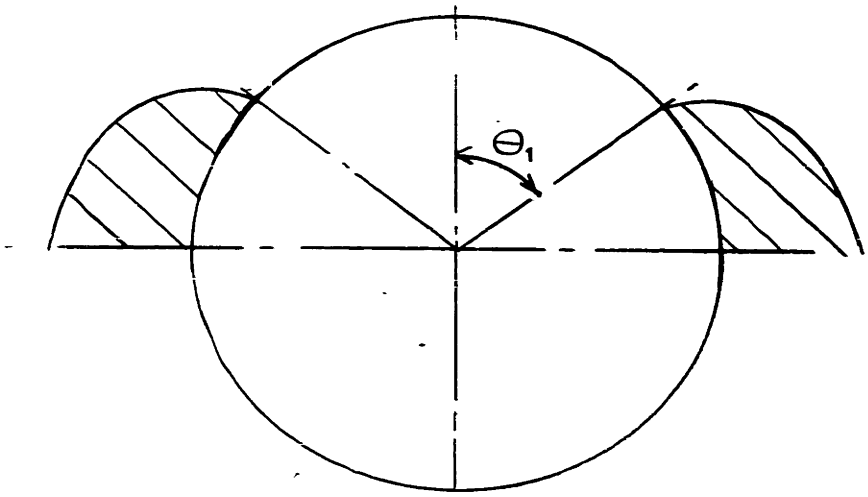

Figure 45: Simplification of the Charging Process

Then the force flux, considering the equilibrium of an ion on the sphere of radius a, can be written as

$$\phi = -e.2\pi a^2 \int_0^{\theta_1} \left(\frac{4\pi\epsilon_0 a^2 k \cos\theta}{4\pi\epsilon_0 a^2} - \frac{\varphi}{4\pi\epsilon_0 a^2} \right) \sin\theta \, d\theta \quad (32)$$

By simplification,

$$\phi = e \cdot 2\pi a^2 k E_0 \int_0^{\theta_1} (\varphi - \varphi_0) \, d\varphi$$

On integration,

$$\phi = e \cdot 2\pi a^2 k E_0 \left| \frac{(\varphi - \varphi_0)^2}{2} \right|_0^{\theta_1}$$

or $$\phi = - e k a^2 \pi E_0 (1 - \varphi_0)^2$$

Since $d\varphi^+ = q_v k' \frac{\phi}{e} dt$ if we consider the field studied in Figure 5, $d\varphi^+ = q_v k' k a^2 \pi E_0 (1 - \varphi_0)^2 dt$

We remember that $i = E_0 k' q_v \cdot 2\pi R$ (Figure 46)

then

$$d\varphi^+ = \frac{i k}{2\pi R} \pi a^2 (1 - \varphi_0)^2 dt \quad (33)$$

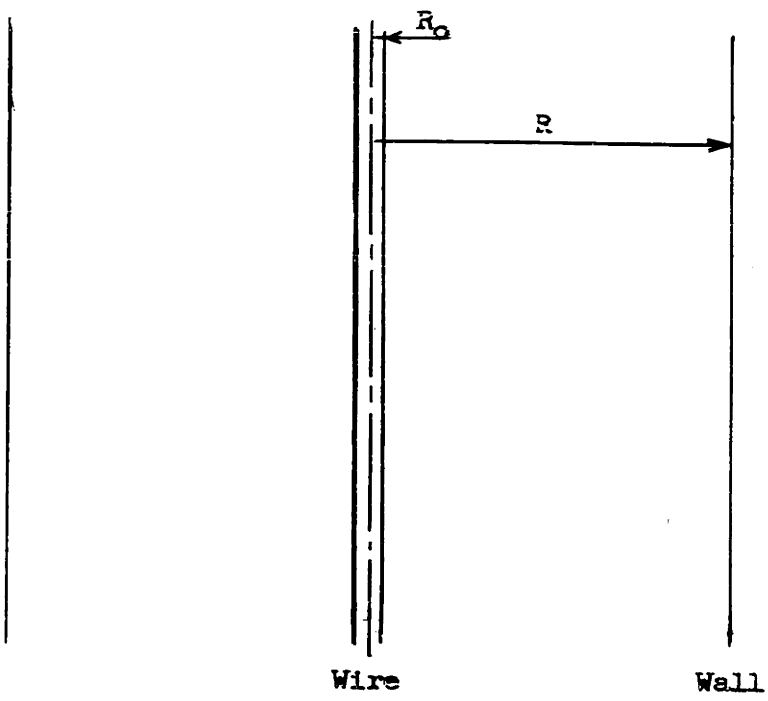

Figure 46: Corona Field

$\frac{i}{2\pi R}$ may be called i' (amper/cm^2) because the equation was derived for a unit height.

$d\varphi^+$ is then equal to $\quad i' k a^2 \pi \left(1 - \varphi_o\right)^2 dt$

giving then

$$\frac{d\varphi^+}{dt} = \pi a^2 k i' \left(1 - \frac{\varphi}{4\pi \epsilon_o a^2 E_o}\right)^2 \qquad (34)$$

(2) Discharging By Leakage

The expression for the discharge rate is merely

$$\frac{dQ}{dt} = \frac{Q}{R_P C_P} \tag{35}$$

where R_p is the particle resistance which was mentioned previously. The term C_p merits a special study.

Determination of C_p

If the ellipsoid of Figure 47 is considered, its capacity at an infinite distance is equal to (14)

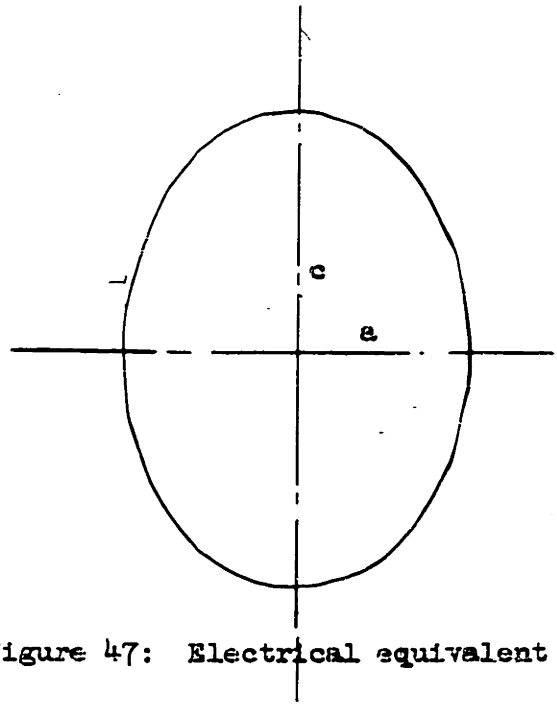

When $a > c$

$$C' = \frac{4\pi\epsilon_0\sqrt{a^2-c^2}}{\cos^{-1} c/a} \tag{36}$$

When $a < c$

$$C' = \frac{8\pi\epsilon_0\sqrt{c^2-a^2}}{\text{Log}\,\frac{c+\sqrt{c^2-a^2}}{c-\sqrt{c^2-a^2}}} \tag{37}$$

When $a = c$

$$C'' = 4\pi a \epsilon_0 \tag{38}$$

Figure 47: Electrical equivalent ellipsoid

One may write $c' = c''f(\frac{c}{a})$ where $f(c/a)$ is a function of (c/a). Tables 4 and 5 show the computation of $f(c/a)$ for several values of c/a.

Figure 48 represents the variation of f(c/a) with respect to c/a. However, since the ellipsoid is very near the drum, its capacity c' must be corrected. The image method is used for this purpose. The same assumptions will be made here as for charging. The equivalent ellipsoid has the same capacity as the sphere of radius a, modified by the factor f(c/a). In reference 1, Von Schnitzler has derived and checked this correction. Figure 49 is taken from reference 1 where m is the correction due to the proximity of the drum.

Then

$$C_p = m C' = m f \, 4\pi a \epsilon_0 \tag{39}$$

m is a function of the ratio of the clearance b between the particle and the drum to the length (Figure 50): m = f(b/c) (40)

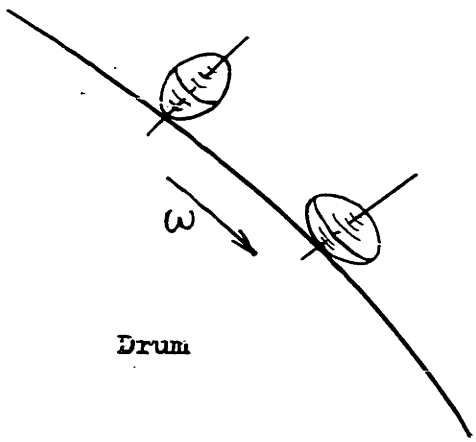

Figure 50: Oblate and Prolate Ellipsoids on the Drum.

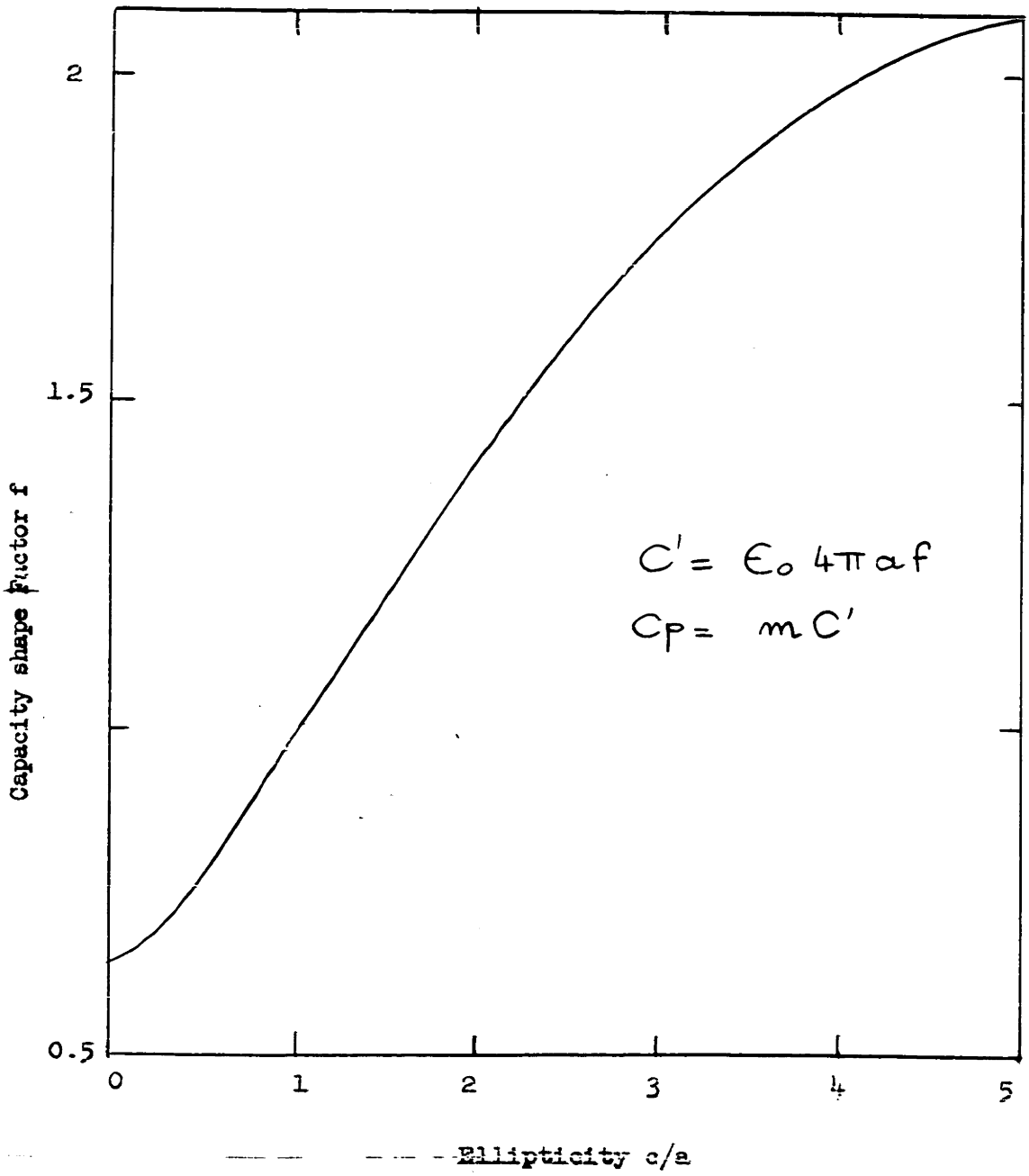

Figure 48: Variation of the Capacity Shape Factor with the Ellipticity c/a

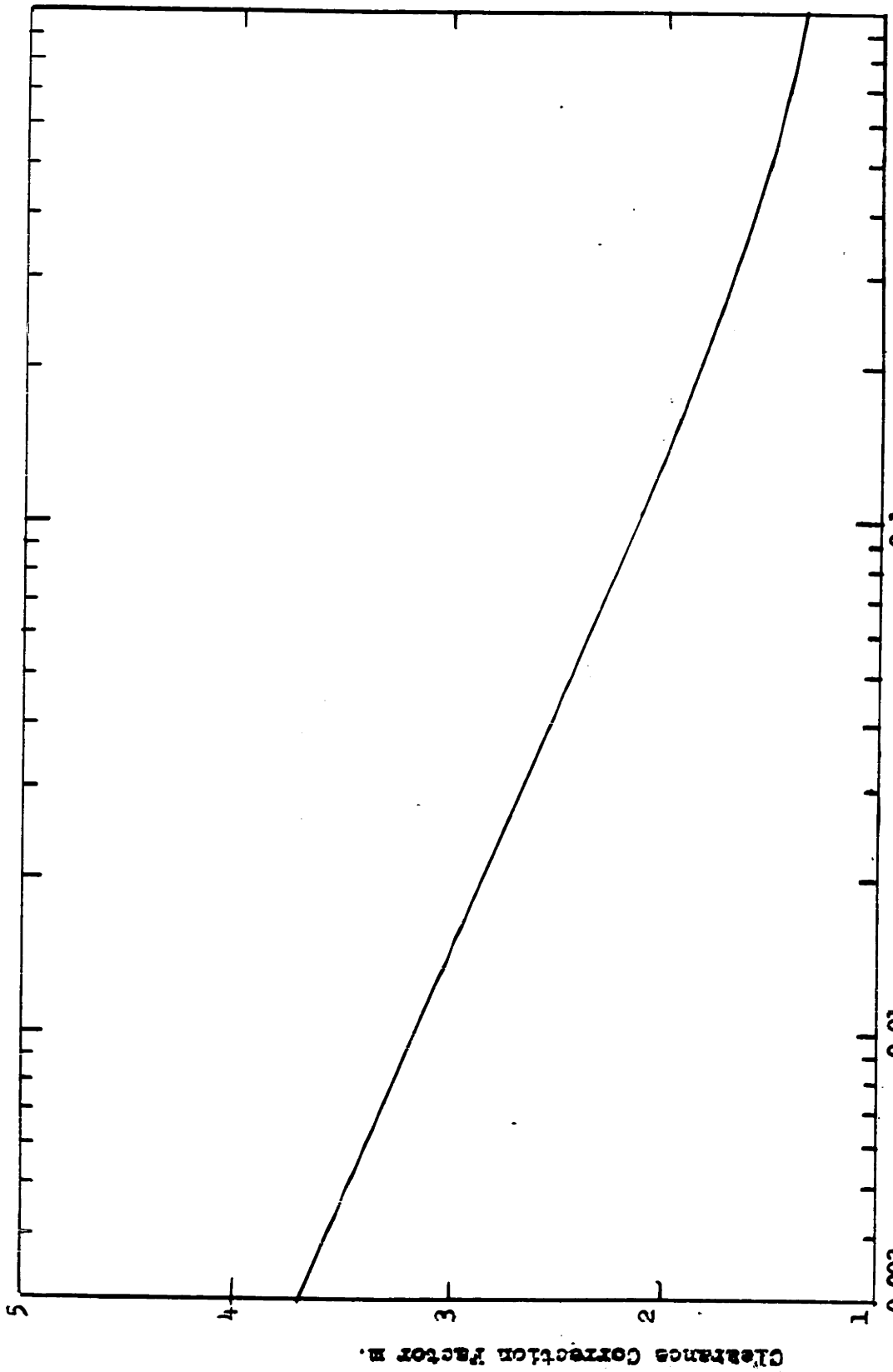

Figure 49: Variation of the Clearance Correction factor m for the capacity of a particle with the Clearance Ratio b/c

We have seen previously that the possible ratios c/a are limited. Therefore, whatever the ratio, neither b/c nor b/a makes much difference in determining the value of m.

To apply equation 40, it may be useful to avoid a possible contradiction. The considered particles are in contact with the drum; however, the equivalent ellipsoid is not, due to the angles of the particles. Then the distance b might sometimes become equal to a or c, according to the shape of the particle considered (Figure 51).

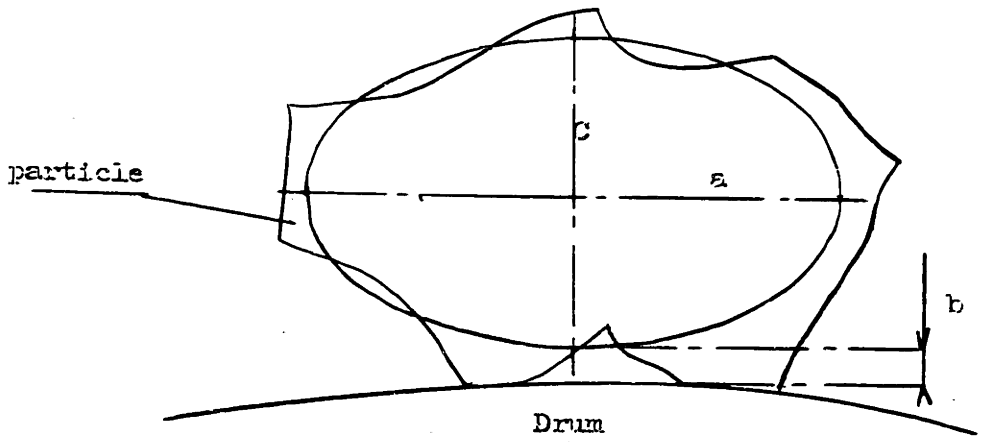

Figure 51: Position of the Electrical Equivalent Ellipsoid with respect to the Drum

(3) Value Of The Steady State Charge

The concept of a steady state charge implies the condition

$$i' \pi a^2 k \left(1 - \frac{Q_s}{Q_m}\right)^2 = \frac{Q_s}{R_p C_p} \qquad (41)$$

If one assumes

$$\varphi_s = T_f \varphi_m$$

it follows that

$$(1-T_f)^2 = \frac{\varphi_s}{R_p C_p \pi a^2 k i'} \cdot \frac{4\epsilon_o E_o}{4\epsilon_o E_o},$$

$$(1-T_f)^2 = T_f \frac{E_o}{R_p i'} \cdot \frac{4\epsilon_o}{4\pi a \epsilon_o m f},$$

$$(1-T_f)^2 = T_f \left(\frac{E_o}{i'}\right) \cdot \frac{1}{\pi a m f R_p} \qquad (42)$$

If we let (E_o/i') equal $2\mathcal{F}$ which is a field characteristic and $\frac{1}{\pi m a f R_p}$ equal $1/\mathcal{P}$ which is a particle characteristic, we obtain the equation

$$(1-T_f)^2 = 2 T_f \frac{\mathcal{F}}{\mathcal{P}},$$

$$0 = T_f^2 - 2\left(1+\frac{\mathcal{F}}{\mathcal{P}}\right) T_f + 1.$$

These roots are

$$T_f = 1 + \frac{\mathcal{F}}{\mathcal{P}} \pm \sqrt{\left(1+\frac{\mathcal{F}}{\mathcal{P}}\right)^2 - 1}$$

From physical considerations, the positive sign to the square root has no meaning; the only possible answer is that

$$T_f = 1 + \frac{\mathcal{F}}{\mathcal{P}} - \sqrt{\left(1+\frac{\mathcal{F}}{\mathcal{P}}\right)^2 - 1} \qquad (43)$$

When $\frac{\mathcal{F}}{\mathcal{P}}$ is very small, T_f tends toward 1(non-conducting particle)
When $\frac{\mathcal{F}}{\mathcal{P}}$ is very large, T_f tends toward 0(conductive particle).

Before further analysis, an evaluation of the order of magnitude of $\frac{\mathcal{F}}{\mathcal{P}}$ is necessary.

1) $\mathcal{F} = \frac{E_o}{i'}$

where: $E_o = 10^6$ volt/m

$i' = 1\ \mu A/m^2$

Therefore: $\mathcal{F} = \frac{10^6}{10^{-5}} = 10^{12}\ \Omega m$

2) $\mathcal{P} = \pi a\, m\, f\, R_p$

where: $a \sim 10^{-3}$ meter

$m \sim 2$

$f \sim 1.5$

Therefore: $\mathcal{P} = 10^{-2} R_p\ \Omega_m$

Hence, $\frac{\mathcal{F}}{\mathcal{P}}$ is of the order of $\frac{10^{14}}{R_p}$

If $\frac{\mathcal{F}}{\mathcal{P}}$ is equal to 1(T_f 0.3), R_p is equal to 10^{14} ohms. Fraas calls conventionally any particle of resistance greater than 10^{13} ohms an insulator.(15) The theoretical considerations are in agreement with those from practical experiments.

(c) Rate of Charging: Charging Time Constant

If we postulate:

$$\varphi = T\varphi_m \quad (0<T<T_f)$$

the net rate of charging is

$$\frac{d\varphi}{dt} = \frac{d\varphi^+}{dt} - \frac{d\varphi^-}{dt} = \varphi_m \frac{dT}{dt}.$$

From Equation 41 we have

$$i'\pi a^2 k(1-T)^2 - \frac{\varphi}{R_p C_p} = \varphi_m \frac{dT}{dt},$$

which gives by successive substitutions

$$(1-T)^2 - 2\frac{\mathcal{F}}{\mathcal{P}} T = 8\epsilon_0 \mathcal{F} \frac{dT}{dt},$$

We then write

$$\int_0^{\mathcal{C}_i} \frac{dt}{8\epsilon_0 \mathcal{F}} = \int_0^{T_i} \frac{dT}{(1-T)^2 - 2\frac{\mathcal{F}}{\mathcal{P}} T}, \qquad (44)$$

assuming

$$1 + \frac{\mathcal{F}}{\mathcal{P}} = M \quad \text{and} \quad \left(1+\frac{\mathcal{F}}{\mathcal{P}}\right)^2 - 1 = B^2;$$

this becomes

$$\int_0^{\mathcal{C}_i} \frac{dt}{8\epsilon_0 \mathcal{F}} = \int_0^{T_i} \frac{dT}{(M-T)^2 - B^2}$$

Now let X = M - T, giving dX = -dT; then

$$\int_0^{\mathscr{C}_i} \frac{dt}{8\epsilon_0 \mathcal{F}} = \int_0^{T_i} -\frac{dx}{x^2 - B^2} = \int_0^{T_i} -\frac{1}{B^2} \frac{dx}{\frac{x^2}{B^2} - 1}$$

If we let y = x/B, we have

$$\int_0^{\mathscr{C}_i} \frac{dt}{8\epsilon_0 \mathcal{F}} = -\frac{1}{B} \int_0^{T_i} \frac{dy}{y^2 - 1}$$

Since $y = \frac{x}{B} = \frac{M - T}{B}$, y is always greater than unity because

$T < T_f$ and $T_f = M - B$ Therefore,

$$\frac{M - T}{B} > \frac{M - M + B}{B} = 1$$

This integral, whose radius of convergence is one, may be written:

$$\int_0^{\mathscr{C}_i} \frac{dt}{8\epsilon_0 \mathcal{F}} = -\frac{1}{B} \int_{\frac{M}{B}}^{\frac{M-T_i}{B}} \frac{dy}{y^2 - 1} ,$$

yielding after integration

$$\frac{\mathscr{C}_i}{8\epsilon_0 \mathcal{F}} = -\frac{1}{2B} \left| \operatorname{Log} \frac{y-1}{y+1} \right|_{\frac{M}{B}}^{\frac{M-T_i}{B}} ;$$

$$\frac{\mathscr{C}_i}{8\epsilon_0 \mathcal{F}} = \frac{1}{2B} \left| \operatorname{Log} \frac{y+1}{y-1} \right|_{\frac{M}{B}}^{\frac{M-T_i}{B}} ;$$

$$\frac{\mathscr{E}_i}{8\epsilon_0 \mathcal{F}} = \frac{1}{2B} \operatorname{Log}\left[\frac{\frac{M-T_i}{B}+1}{\frac{M-T_i}{B}-1} \cdot \frac{\frac{M}{B}-1}{\frac{M}{B}+1}\right],$$

$$\frac{\mathscr{E}_i}{8\epsilon_0 \mathcal{F}} = \frac{1}{2B} \operatorname{Log}\left[\frac{M-T_i+B}{M-T_i-B} \cdot \frac{M-B}{M+B}\right].$$

If we let $$T_i = \mathcal{G}\, T_f = \mathcal{G}\,(M-B),$$

we arrive at the equation:

$$\frac{\mathscr{E}_i}{8\epsilon_0 \mathcal{F}} = \frac{1}{2B} \operatorname{Log} \frac{(1-\mathcal{G})M+(1+\mathcal{G})B \cdot (M-B)}{(M-B)\ (1-\mathcal{G})(M+B)}; \qquad (45)$$

$$\mathscr{E}_i = \frac{4\epsilon_0 \mathcal{F}}{\sqrt{\left(1+\frac{\mathcal{F}}{\mathcal{P}}\right)^2-1}} \operatorname{Log} \frac{(1-\mathcal{G})\left(1+\frac{\mathcal{F}}{\mathcal{P}}\right)+(1+\mathcal{G})\sqrt{\left(1+\frac{\mathcal{F}}{\mathcal{P}}\right)^2-1}}{(1-\mathcal{G})\left[1+\frac{\mathcal{F}}{\mathcal{P}}+\sqrt{\left(1+\frac{\mathcal{F}}{\mathcal{P}}\right)^2-1}\right]} \qquad (46)$$

which may be written

$$\mathscr{E}_i = U \operatorname{Log} W \qquad (47)$$

letting U and W equal the respective terms above.

Let us now examine the values of $\mathscr{E}_i$ for different types of particle.

(1) Conducting particle

$$T_f = 0; \quad M \cong B$$

Then

$$W = \frac{(1-\varphi) + (1+\varphi)}{(1-\varphi)2} = \frac{1}{1-\varphi}$$

φ is indeterminate; however, since we deal with conducting particles, its value may be taken as zero, (because of the continuing leak,), thus giving $w = 1$ and $\sigma_i = 0$

(2) Non-conducting particle

$T_f = 1$; $M = B + 1$, but B is very small and M is practically 1; we have then

$$W = \frac{(1-\varphi) + (1+\varphi)B}{(1-\varphi)(1+B)} \simeq \frac{1-\varphi}{1-\varphi}$$

$W \cong 1$, and consequently σ_i is virtually nil.

Even though this analysis seems complicated, the results are very simple and rather obvious. These results are important because since we know that the achievement of the steady state is practically instantaneous, we are not concerned with the speed of the drum, as far as the charging time is concerned. Whatever the speed of the drum may be, a steady state charge will be achieved, and the selectivity of the process (in the Carpco machine) will arise from the discharging in the static field.

(d) Discharging of Non-Conductors and Reversed Charging of Conductors In The Static Field Zone

Equation (17) written previously govern this case:

$$\varphi = \varphi_m T_f - 4\pi a \epsilon_0 m_f . V\left(1 - e^{-\frac{t}{4\pi\epsilon_0 a m_f R_p}}\right) \quad (48)$$

and the time constant is

$$\mathcal{C}_c = 4\pi\epsilon_0 a m f R_p$$

For a conductor, this time constant is small; but, for a non-conductor it is large, giving thus the features illustrated in Figures 52 and 53.

The important time is in fact the time of reversal, $\mathcal{R}$

From Equation (48) at time $\mathcal{R}$,

$$Q_m T_f = 4\pi a \epsilon_0 m f V \left(1 - e^{-\frac{\mathcal{R}}{\mathcal{C}_c}}\right), \qquad (49)$$

$$\frac{Q_m T_f}{4\pi a \epsilon_0 m f V} = 1 - e^{-\frac{\mathcal{R}}{\mathcal{C}_c}},$$

$$\frac{T_f 4\pi a^2 \epsilon_0 k E_0}{4\pi a \epsilon_0 m f V} = 1 - e^{\frac{\mathcal{R}}{\mathcal{C}_c}} = \frac{a k E_0 T_f}{m f V},$$

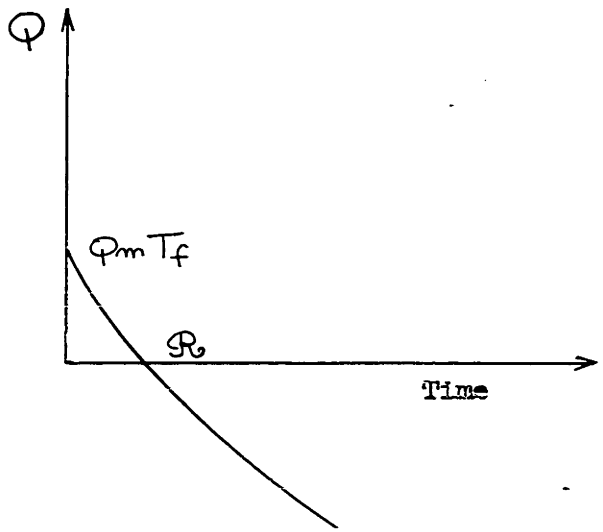

Figure 52: Evolution of the Charge on a "Conductor" in the Static Field Zone

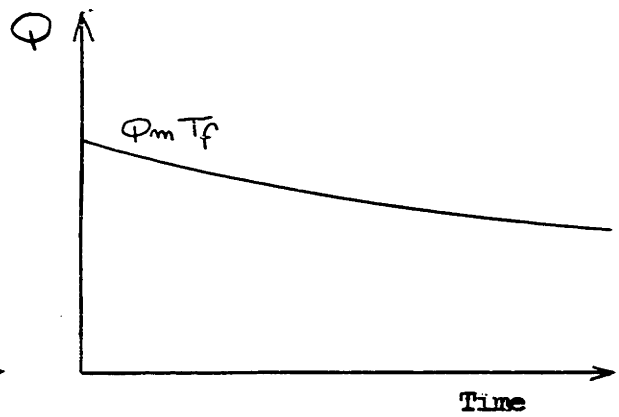

Figure 53: Evolution of the Charge on a Non-Conductor in the Static Field Zone

If we consider the field BbdD (Figure 39) to be uniform, we may write

$$E_s = \frac{V}{D-(R_1+R_2)} \quad ;$$

then

$$\left(1-e^{-\frac{\mathcal{R}}{\mathcal{C}_c}}\right) = \frac{a\,k\,E_o\,T_f}{m_f\,E_s\left[D-(R_1+R_2)\right]}$$

$$\left(1-e^{-\frac{\mathcal{R}}{\mathcal{C}_c}}\right) = \frac{E_o}{E_s}\;\frac{k}{m_f}\;\frac{a}{D-(R_1+R_2)}\cdot T_f \qquad (50)$$

$\frac{k}{m_f}$ is a shape factor, $\frac{E_o}{E_s}$ is a machine factor. $\frac{a}{D-(R_1+R_2)}$ is not a significant factor because it does not vary greatly (a is small). We may let

$$\frac{k\,a}{m_f\left[D-(R_1+R_2)\right]} = \mathcal{P}'$$

giving

$$\left(1-e^{-\frac{\mathcal{R}}{\mathcal{C}_c}}\right) = \frac{E_o}{E_s}\;\mathcal{P}'\;T_f$$

T_f, given by Equation (27) is a function of $\frac{\mathcal{F}}{\mathcal{P}}$ only, and does not depend upon the static field characteristic.

The previous equation may be written:

$$e^{-\frac{\mathcal{R}}{\mathcal{C}_c}} = 1 - \frac{E_o}{E_s}\;\mathcal{P}'\;T_f$$

$\frac{E_o}{E_s}$ is the machine selectivity factor, always larger than unity, and

$$\frac{\mathcal{R}}{\mathcal{C}_c} = \text{Log}\;\frac{1}{1-\frac{E_o}{E_s}\cdot\mathcal{P}'\,T_f}$$

$\mathcal{T}'$ may be of the order of 10^{-2} then we may write

$$\frac{\mathcal{R}}{\mathcal{C}_c} = \text{Log}\ \frac{1}{1 - 10^{-2} T_f \cdot E_o/E_s}$$

If $T_f = 0$ (good conductor), then $\frac{\mathcal{R}}{\mathcal{C}_c} = 0$, which is obvious.

If $T_f = 1$ (non-conductor), then $\frac{\mathcal{R}}{\mathcal{C}_c} = \text{Log } n$; $n > 1$ giving $\frac{\mathcal{R}}{\mathcal{C}_c} = M'$; $M' > 0$.

This study has shown that the main variables for reversal of charge are the ratio $\frac{E_o}{E_s}$ and the retention time T_r which should be greater than $\mathcal{R}$ as to permit the reversal charging of conducting particles and thus their lifting.

If we return to Figure 39, distance D and angle Σ fix the ratio $\frac{E_o}{E_s}$, while angle δ fixes the retention time in the static field.

This observation is of prime importance for the practical operation of the machine, because it is the key to an understanding of the two terms which will be used later: lifting setting and pinning setting.

VIII. Equilibrium Of A Particle: Escaping Angle Θ_o

Figure 54 shows the configuration of the forces.

The equilibrium is given by the equation:

$$m_p \omega^2 R_1 + m_p g \cos\left(180° - \Theta\right)\Big) + F_{el} = 0$$

$$m_p \left(\omega^2 R_1 - g \cos\Theta\right) + F_{el} = 0 \qquad (51)$$

Computation of the force of electrical nature F_{el}:

At B, any particle has a charge $Q_s = T_f Q_M$.

From b' to Θ, the charge is given by Equation (48):

$$Q = Q_m T_f - 4\pi a \epsilon_o m f V \left(1 - e^{-\frac{t}{\mathcal{C}_c}}\right) ;$$

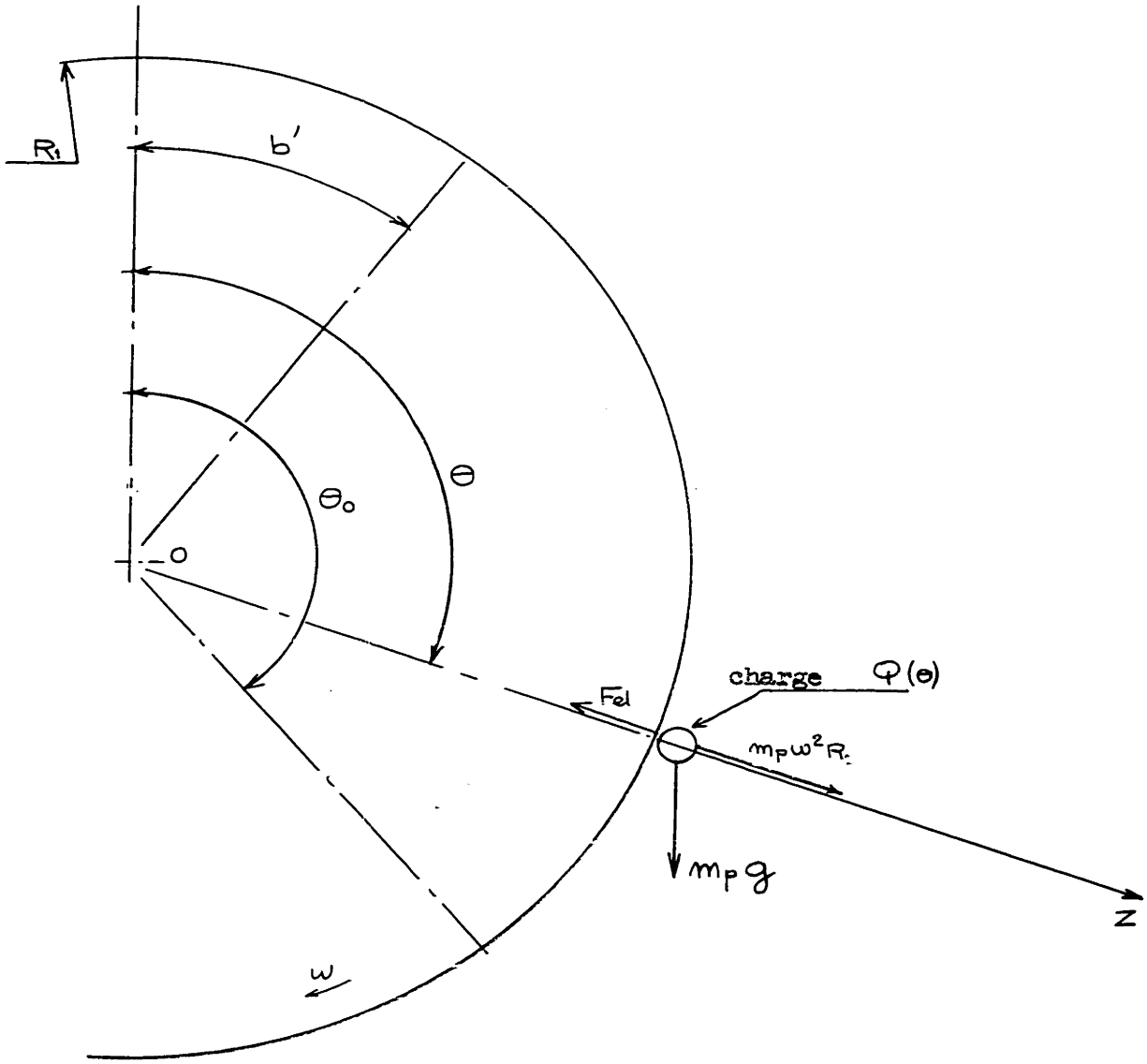

Figure 54: Equilibrium of a Charged Particle on the Drum of a Carpco Machine.

but $$t = \frac{\theta - b'}{w} ,$$

then

$$\varphi_\theta = \varphi_m T_f - 4\pi a \epsilon_0 m f V \left(1 - e^{-\frac{\theta - b'}{w \tau_c}}\right) \quad (52)$$

The net force of electrical nature is given by

$$Fel_\theta = -\left(E_s \varphi_\theta + \varphi_1 \varphi_\theta^2\right)$$

In zone BD, we may assume that $E_s Q_\theta$ is predominant, and then neglect the image force $\varphi_1 \varphi_\theta^2$ (Equation 16)

Equation (51) becomes

$$0 = m_p \left(w^2 R_1 - g \cos\theta\right) - E_s \left[\varphi_m T_f - 4\pi a \epsilon_0 m f V \left(1 - e^{\frac{b' - \theta}{w \tau_c}}\right)\right] \quad (53)$$

Such an equation is very difficult to solve in a general fashion so as to find θ analytically. However a qualitative discussion will give the key to the rules of thumb used for cleaning the tailing and the concentrate of the rougher split.

Equation (53) can be written

$$0 = \left(m_p w^2 R_1 - E_s \varphi_m T_f\right) - \left(m_p g \cos\theta - E_s \underbrace{4\pi a \epsilon_0 m f V \left[1 - e^{\frac{b' - \theta}{w \tau_c}}\right]}_{\varphi_x}\right), \quad (54)$$

(a) when $Q_x = 0$ (perfect non-conductor).

Equation 54 becomes $(M_p W^2 R_1 - E_s Q_m T_f) - M_p g \cos\theta = 0$

One sees by this equation that if the speed is low, the non-conducting

particles will adhere for a complete revolution unless they are swept from the roll.

A logical method of cleaning the tailings (non-conductors) is therefore to turn fast. It has been seen that the speed of charging by ion-bombardment is so great that a steady state charge will certainly be reached.

(b) When $T_f = 0$, (good conductor), Equation (54) becomes

$$m_p \omega^2 R_1 - m_p g \cos\theta + E_s Q_x = 0$$

If $Q_x = 0$, $\cos\theta = \frac{\omega^2 R_1}{g}$, which must be a number smaller than 1. But since this number is positive, $\theta_0 < 90°$ (Figure 55).

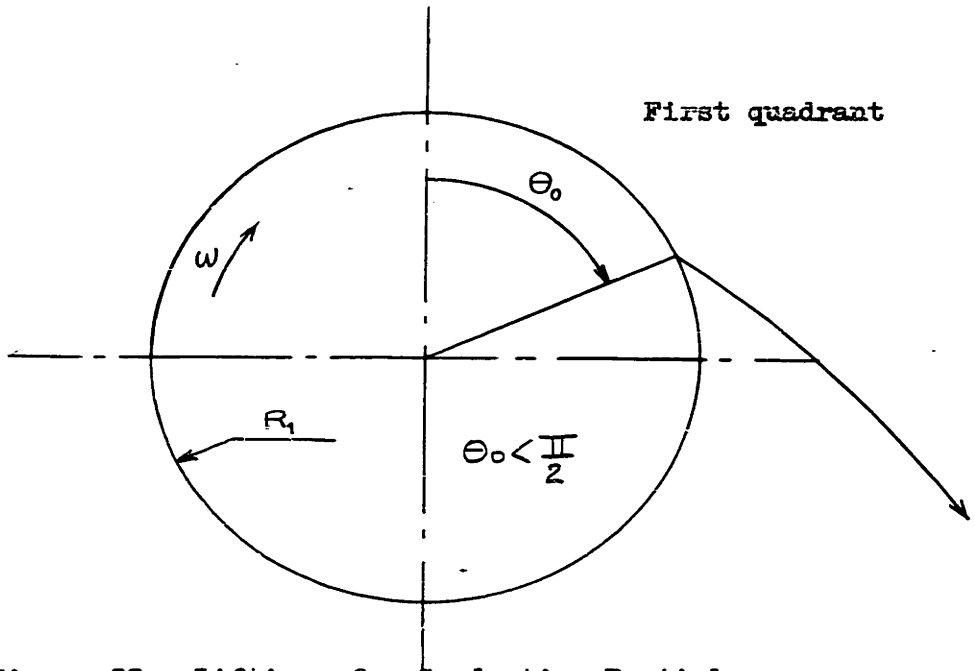

Figure 55: Lifting of a Conducting Particle

This leads to the conclusion that the actual Θ_o will be smaller than the value of Θ_o computed when Q_x is assumed to be zero. The further path of the conductive particle is due to the escaping velocity and also to the charge Q_x. In order to lift a conductive particle, the retention time in the static field should be long, and the angle δ (Figure 39) such that it allows the zone BC to be wholly in the first quadrant (this conclusion is fundamental for cleaning a concentrate).

B. TECHNICAL ASPECTS OF ELECTRICAL CONCENTRATION PROCESSES
(Example of the electrical concentration of a manganese ore)

I. Introduction

When presented with a mixture of several minerals to separate, it is useful in practice to have some empirical rules to serve as a guide in the choice of the method. The main rules are as follows:

(1) If the ground ore consists of a mixture of very conductive minerals (sulfides, arsenides) with non-conductive minerals (silicates), the Carpco machine is well suited.

(2) If the ground ore consists of a mixture of non-conductive minerals any machine using the contact-potential charging process (particle-particle contact) can give best selectivity.

(3) If the ground ore consists of a mixture of very conductive minerals, the only machine which can perform a separation is one using the inductive-conduction charging process. For example, the Carpco machine can be used with a special setting (lifting setting).

These are rules and not laws; however, they can be derived qualitatively from the previous theoretical study.

With these rules, one must remember that the determining factor is the resistance of the particle, which depends greatly on the state of the surface. For instance, pure sphalerite obtained by flotation will be covered with copper (activation), and therefore will be very conductive; porous minerals if not dry will show the same anomaly. This behavior can be used to enhance the versatility of the process. A demonstration of

this versatility on the Carpco machine can be made with a mixture of pure quartz, pure pyrite, and pure sphalerite. In the first step, the pyrite is taken out as a conductor; then in a second step, the quartz and sphalerite are soaked in a copper sulfate solution, then washed and dried, and then the sphalerite is taken out as a conductor.

The same kind of versatility can be observed for other charging processes, e.g., particle-particle contact charging under heating. Theoretically, there is no difficulty; in practice, however, the right treatment for a given case must be determined by experimentation.

II. Operation Of The Carpco Machine

Attention will now be given to the Carpco machine, which is of special interest because of its widespread industrial application. Figure 56 reproduces in a simpler way the previous Figure 39.

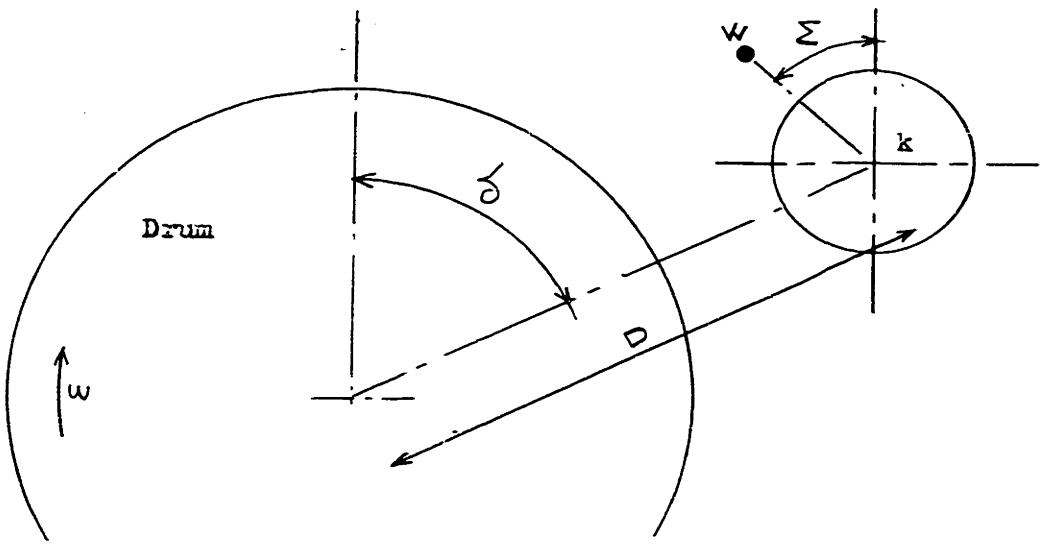

Figure 56: Carpco Machine Variables

The Carpco machine is built in such a way that δ , D, Σ , ω are adjustable.

It has been seen that for non-conductive particles, ion bombardment charging was of greatest importance. Since the non-conductors are "pinned" on the drum, the setting of the machine variables is called the "pinning setting." For a conductive mineral, the critical reversing time, $\mathcal{R}$, which is directly related to the resistance R_p, is of major importance. The setting of the machine so as to "lift" the conductors from the drum is called the "lifting setting."

(1) Typical Flowsheet

A typical flowsheet of an industrial operation is given below. (Figure 57 - Reference 16).

The symbols listed below are applicable to this figure and are completely independent of the symbols previously used.

Legend

H = New feed

A = H + Recirculating loads

P = % Non-conductor in rougher circuit

R = % Recirculating load in rougher circuit

T = % Conductor in rougher circuit

P_p = % Non-conductor in non-conductor cleaner circuit

r_p = % Recirculating load in non-conductor cleaner circuit

t_p = % Conductor in non-conductor cleaner circuit

P_t = % Non-conductor in conductor cleaner circuit

r_t = % Recirculating load in conductor cleaner circuit

t_t = % Conductor in conductor cleaner circuit

ω_r = angular velocity of the rougher drum

ω_p = angular velocity of the non-conductor cleaner drum

ω_t = angular velocity of the conductor cleaner drum

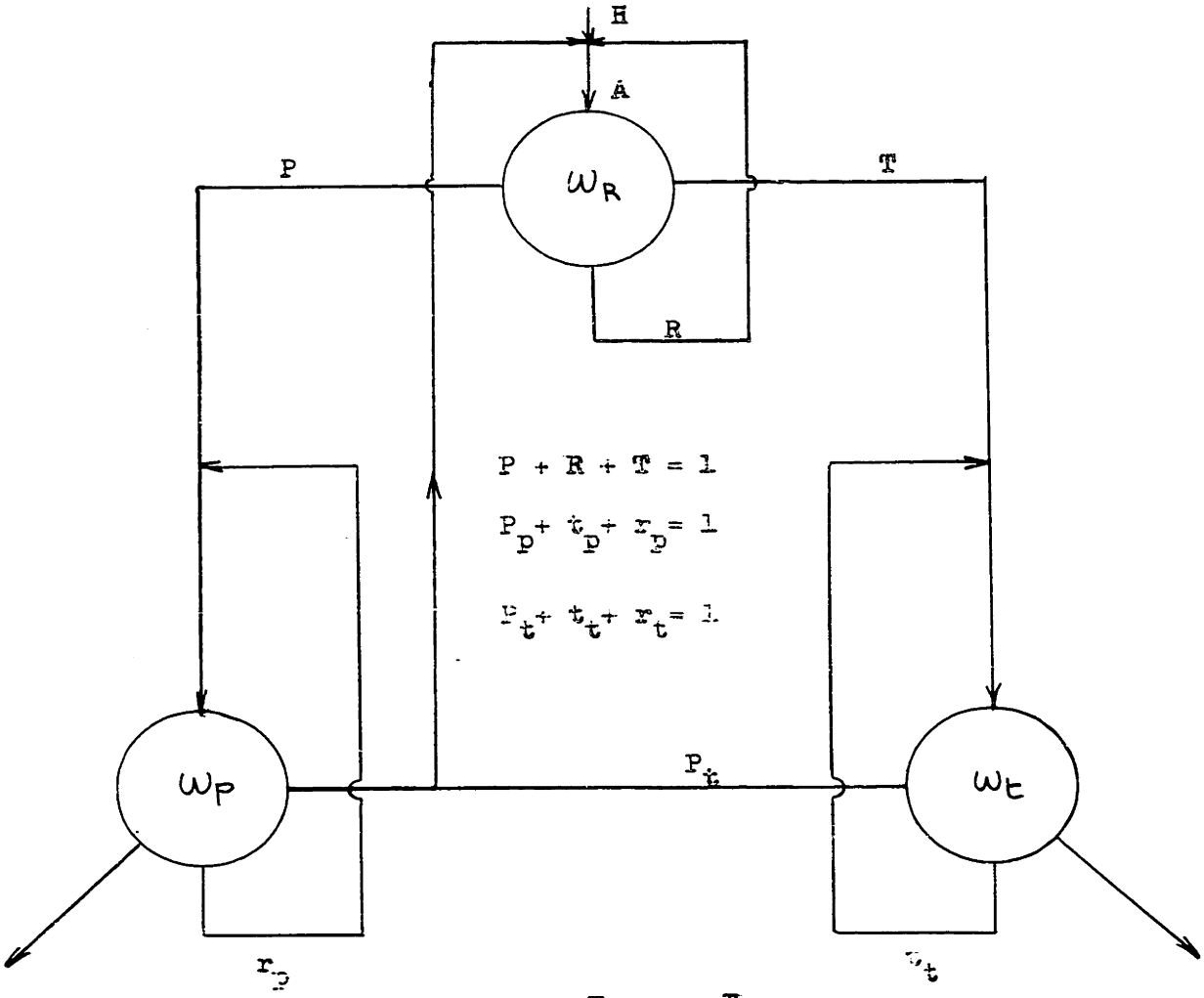

$$H = \left(1 - R - \frac{P_{tp}}{1-r_p} - \frac{T_{pt}}{1-r_t}\right)A$$

Figure 57: Typical flowsheet of an Industrial Electrical Concentration Process

From this flowsheet, it is evident that there are three different kinds of settings:

(1) a "rougher" setting

(2) a conductor cleaner setting

(3) a non-conductor cleaner setting

We know from our theoretical study that the "conductor cleaner setting" is obviously a lifting setting, whereas the "non-conductor cleaner setting" is obviously a pinning setting. As for the rougher setting, we cannot immediately tell, because it depends upon the nature of the mixture. Figure 58 shows what kind of settings are generally used.

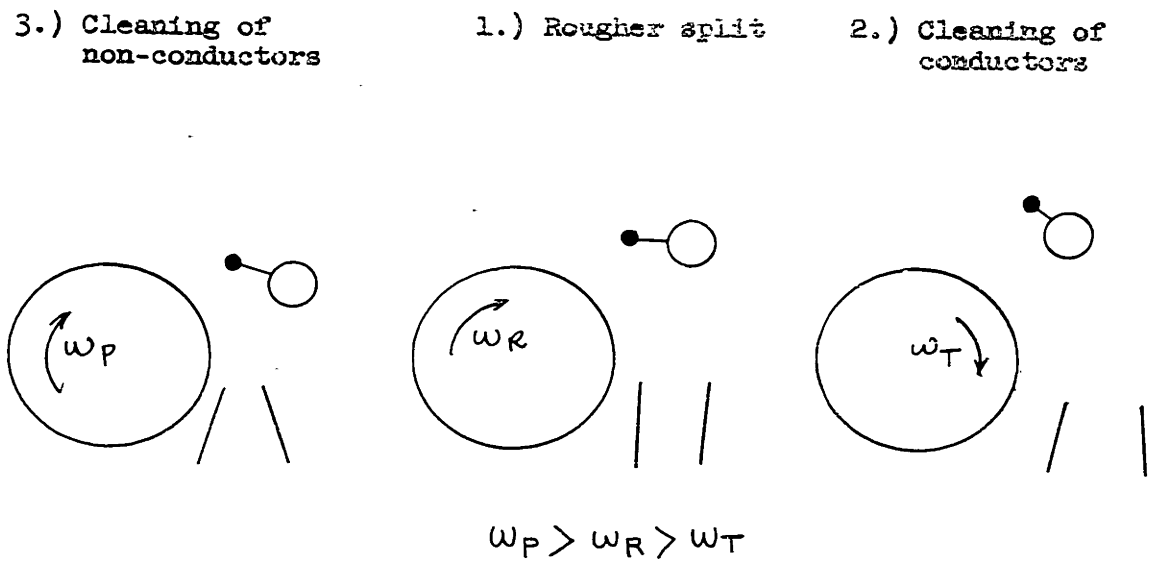

Figure 58: Schematization of the different settings used in a General Case.

Figure 58 needs no more consideration since all the features can be easily qualitatively derived from the theoretical considerations.

2) How do lifting and pinning settings differ?

The preceding chapter has shown that there are roughly two ways to operate the separator, by pinning the non-conductors and by lifting the conductors, respectively. Although there is not an absolutely sharp practical distinction between two ways of operating, this distinction remains useful.

Tests were run on a manganese ore to show the effects of the two settings. The ore was crushed in laboratory rolls, split at 48 mesh on a vibratory screen, deslimed and separated according to the following flow sheet, (Figure 59) in which manganese assays are given.

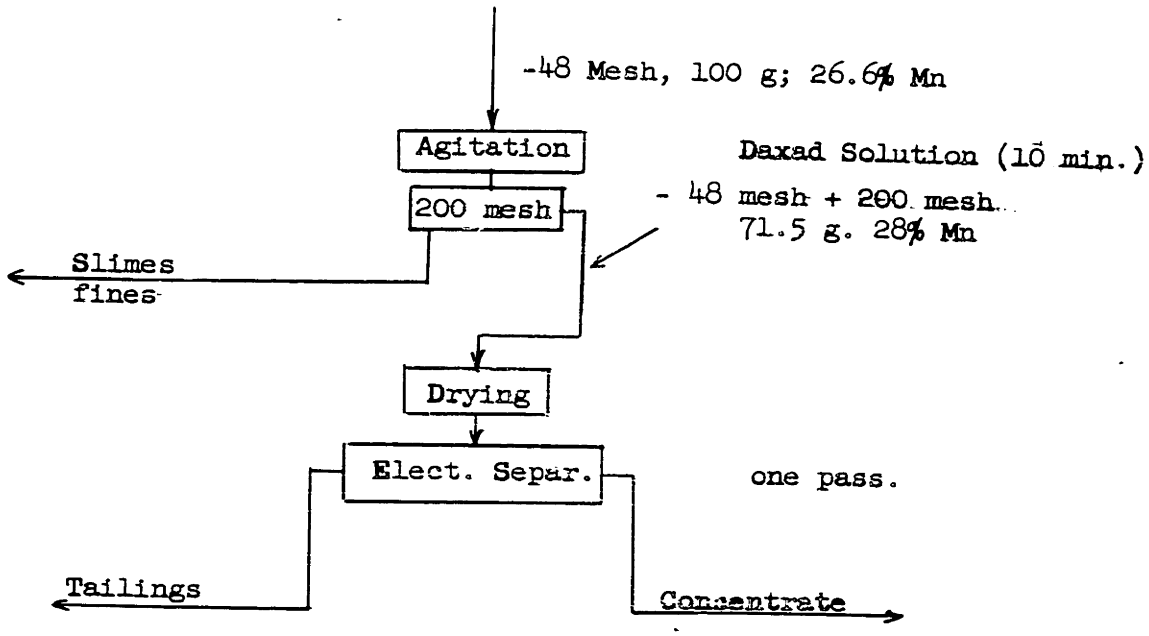

Figure 59: Processing of the Manganese Ore.

Before electrical concentration the recovery of manganese was 78.1%.

Results are summarized in Table 6; the lifting setting is called L and the pinning setting is called P. Figure 60 shows the relation between manganese recovery and grade of concentrate (during electrical separation for different pinning and lifting settings).

In Figure 60, it is seen that lifting settings give better results than the pinning settings, Curve A which joins the "L" points being to the right of Curve B which joins the best "P points."

One can explain these results by the fact that gangue particles do not have a very high resistivity: when we operate in "pinning conditions" we have not as much selectivity as when we operate in "lifting conditions For a particle to lift, it first has to be discharged, then again charged. For a particle to pin, it has to get charged but once. In the case of lifting, the selectivity is due to the reversal of charge, whereas in the case of pinning, the selectivity is due only to the magnitude of the primary charge. (Q_s)

From a practical standpoint the distinction between lifting setting and pinning setting remains qualitative. However these results have shown that the terms do have actual meanings, analogous to those used in the theoretical discussion.

To see if such a process could be applied to this ore, a bench-scale pilot plant test was performed.

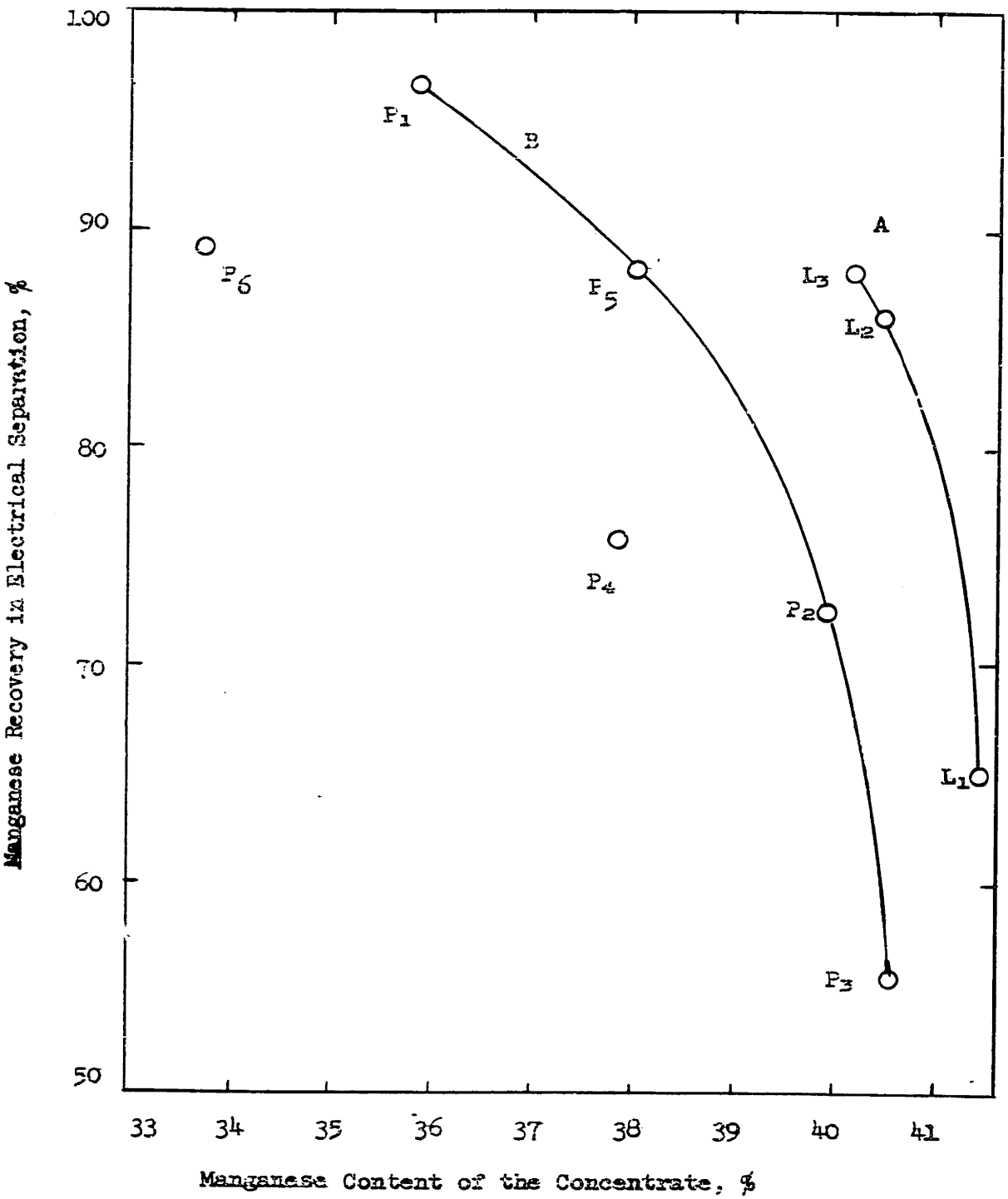

Figure 60: Results from "lifting" and "pinning" of a Manganese Ore

3) Bench-Scale Pilot Plant

a) Preparation of the ore

The minus 48 mesh fraction, prepared before, was given the treatment shown in the following flowsheet. (Figure 61)

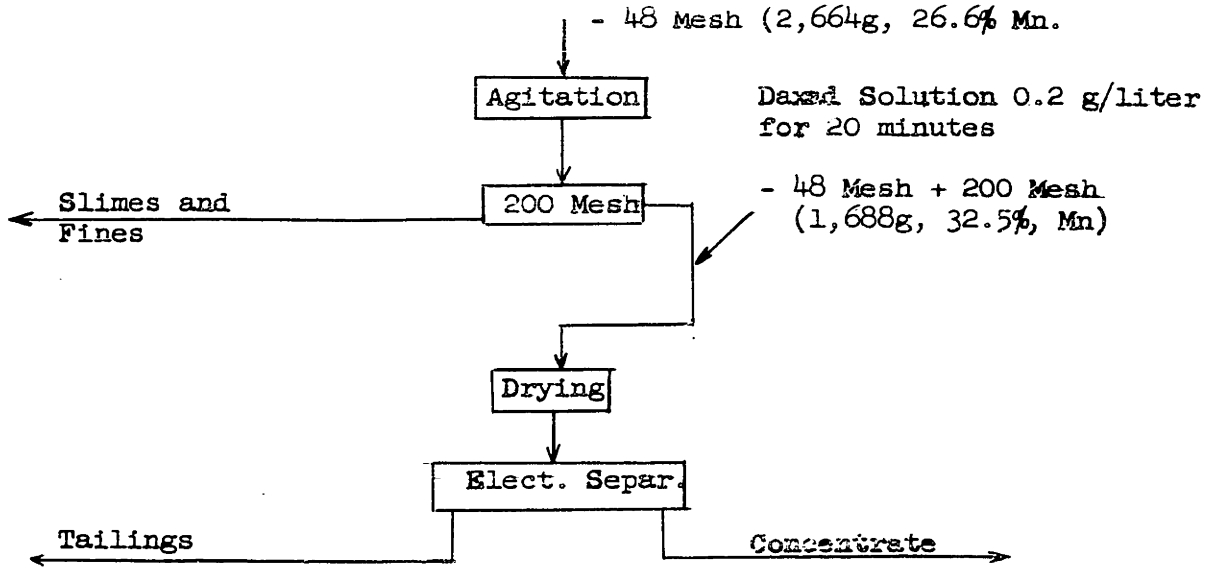

Figure 61: Flowsheet of the Process of the Manganese Ore (Bench Scale Pilot Plant Test)

The recovery of manganese before the electrical concentration was 77.5%, comparable to the recovery obtained in the previous test, which was 78.1%. However, the grade of the minus 48 plus 200 mesh fraction was slightly higher.

b) Electrical Concentration:

The results of this test are recorded in Appendix I (test 2.61 abc).

The flow sheet of the electrical concentration process is given with notations and figures in Figure 62.

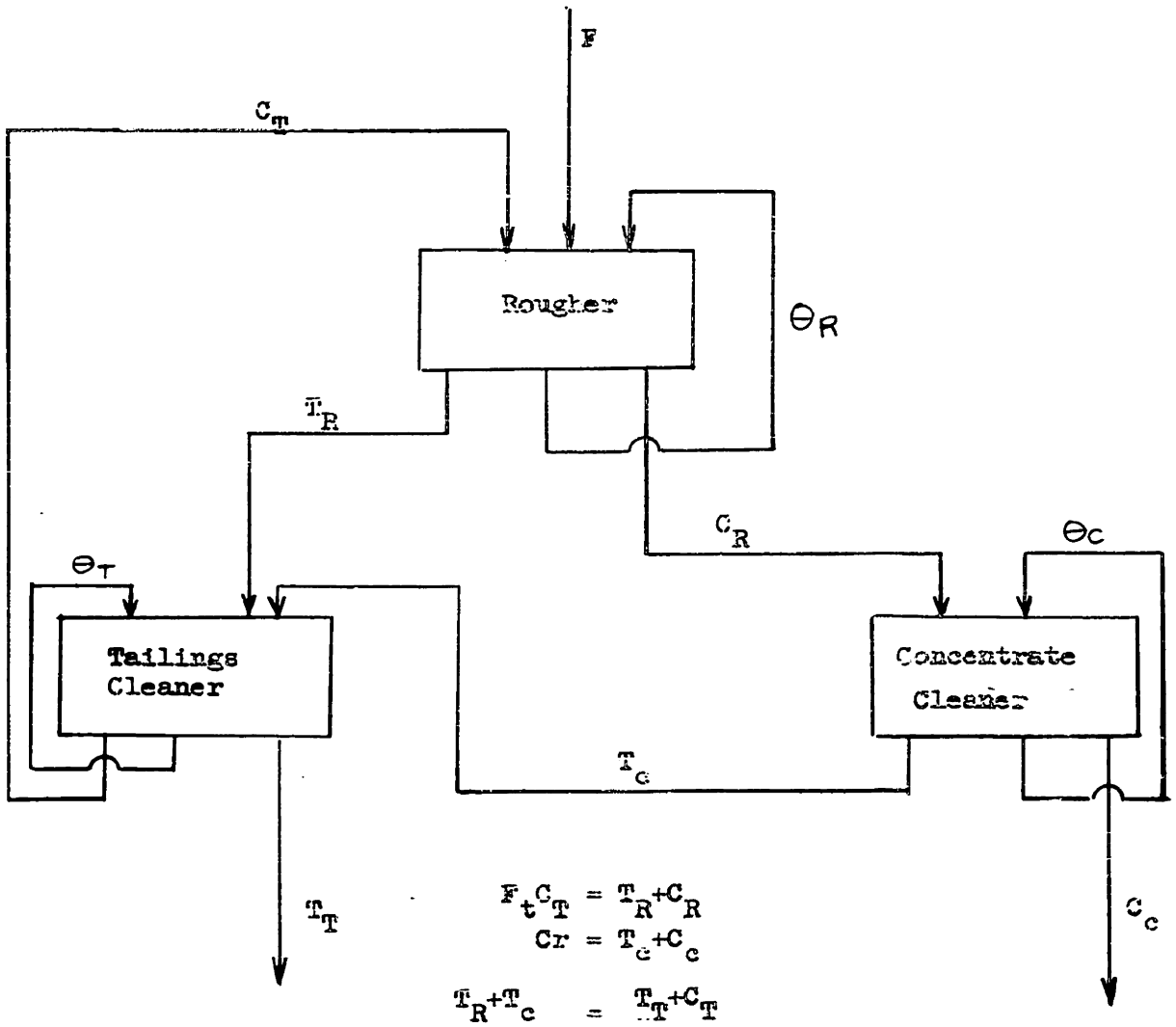

Figure 62: Pilot Plant Test

$$C_R/T_R = 26.8/22.8 = 1.18$$

$$C_c/T_c = 36.1/6.15 = 5.87$$

$$C_T/T_T = 37.5/41.8 = 0.895$$

For a 1500 g feed, final concentrate weights 912 g and final tailings weight 558g, showing a handling loss of 30g on 1500 g, or 2%; neglecting this loss, concentrate represents 62.05% of the feed by weight and tailings represent 37.95%. These numbers lead to the following values for the unknowns stated in Figure 62.

$$T_c = 158g$$
$$C_c = 925g$$
$$C_R = 1080g$$
$$T_R = 920g$$
$$C_T = 510g$$
$$T_T = 575g$$

The T_c value of 160g justifies the fact that it has been avoided to be recirculated through the rougher. (Flowsheet of figure 62 differs from the one on figure 57.)

c) Recovery of the process

1) Result of chemical analysis:

Product	Weight%	Assay Mn %	Assay Fe %	Assay SiO_2
Feed	100	32.5	2.8	19.3
Concentrate	62.05	41.7	2.7	11.5
Tailings	37.95	19.5	3.5	32.9

From concentrate and tailings analyses the computed feed assays are:

Mn, % : 32.2

Fe, % : 3.0

SiO_2% : 19.6

These figures are in good agreement with the chemical analysis.

2) Recovery of manganese

In the electrical separation step the manganese recovery is 79.2%. The overall recovery is then (including the washing)

$$79.2 \times 77.5 = \underline{61.5\%}$$

d) Rate Study

The rate for any roll (rougher or cleaners) will be given in kilograms of new feed per minute for a 4 inch feeder (the roll length being 6 inches.)

1) Rougher rate:

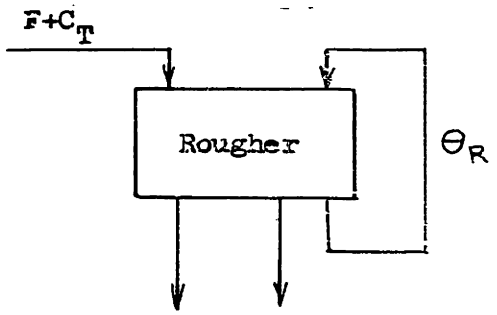

Figure 63: Rougher

The computation of the previous figures gives a rate of

2.5 kg/mn

(See Appendix II)

2) Tailings Cleaner rate:

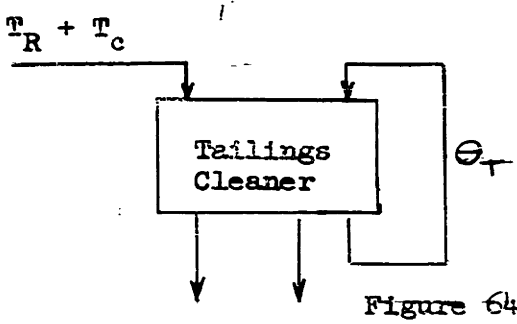

Figure 64: Tailings Cleaner

The rate is 2.63 kg/mn

(See Appendix II)

3) Concentrate cleaner rate:

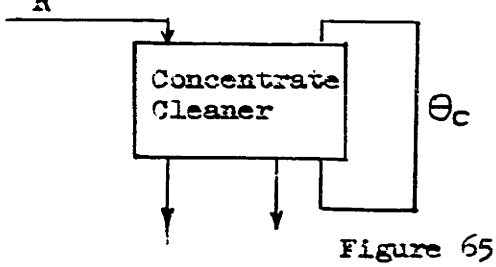

Figure 65: Concentrate Cleaner

The rate is 1.26 kg/mn

(See Appendix II)

e) Conclusions:

1.) The grade of the concentrate is 41.7% in manganese, and 11.5% in silica, the recovery of the complete process being 61.5%.

2.) From the rate studies, we notice that the rougher and the tailings cleaner operate at an industrially possible rate (over 2 kg/min of new feed for a four inch feeder), but the concentrate cleaner operates below this conventional limit. An industrial plant should have two concentrate cleaners working in parallel.

At the present level of the study it is difficult to say that we can improve the rate of the concentrate cleaning, because the setting used (lifting setting) gives, by nature, a low production rate.

III. Summary

We have seen by qualitatively applying the conclusions of our theoretical discussion how it is possible to quickly get a fairly good idea of the behavior of the ground ore in a Carpco machine. This is true even though not much emphasis has been placed on the technical part of the study of electrical concentration.

C. Experimental Study

I. Introduction

In the theoretical study, the importance of the resistance of the mineral particals has been stressed. However, the term R_p was not defined exactly. The easiest concept of resistance is that of the resistance of a wire; but in our particular case we should understand resistance as a reciprocal probability of charge leakage, having ohms for units. The total leakage probability is the sum of the bulk leakage and the surface leakage, which was represented by Equation (18).

To get an idea of the resistance R_p, some tests were performed as illustrated in Figure 66. The resistance between point A and the platinum plate was measured.

II. Tests At Room Temperature

(a) Apparatus Used

The apparatus used was as illustrated in Figure 66.

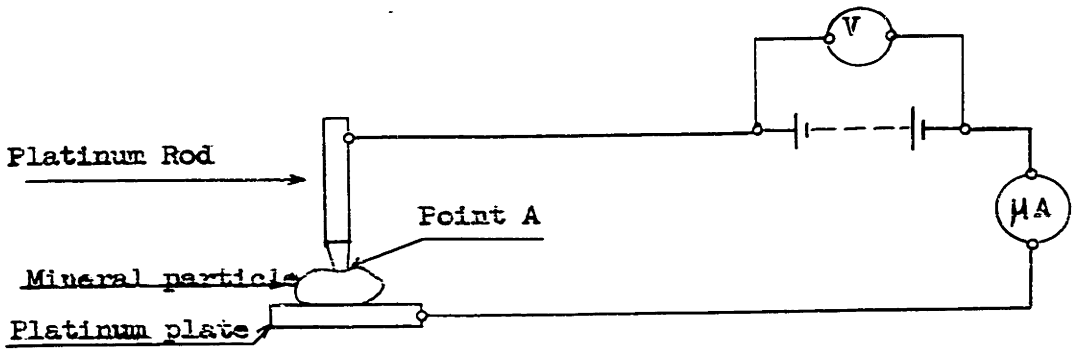

Figure 66: Apparatus used for measurements at Room Temperature. The micro-ammeter used is a DC Amplifier (General Radio 1230 A). For very low resistance a Wheatstone Bridge is used instead.

(b) Results

Several minerals were tested, namely, chrysocolla, chromite, sphene, epidote, stibnite, columbite, pentlandite+, marcasite+, and arsenopyrite+ (+ stands for the minerals whose resistance was measured with a Wheatstone bridge). All particles used in the experiment were taken from sized samples (48-65 mesh).

The results are summarized as follows:

chrysocolla-chromite	Table 7 and Figure 67
sphene-epidote	Table 8 and Figure 68
stibnite	Table 9 and Figure 69
columbite	Table 9 and Figure 70
others	Table 10

In the graphs the resistance R_p was plotted as ordinate against the voltage drop used as abscissa.

(c) Conclusions

(1) For all the minerals tested even though the size was defined only by the Tyler screens (48-65 mesh) and therefore subject to appreciable variation, the resistance does not vary too much from one particle to another.

(2) For stibnite and chrysocolla the resistance shows a great variation with changes in voltage drop.

This simple experiment has shown: (1) that the field gradient in the static field region conditioning the voltage drop across a particle is very important, (2) that the term $\mathcal{P}$ is not completely independent of

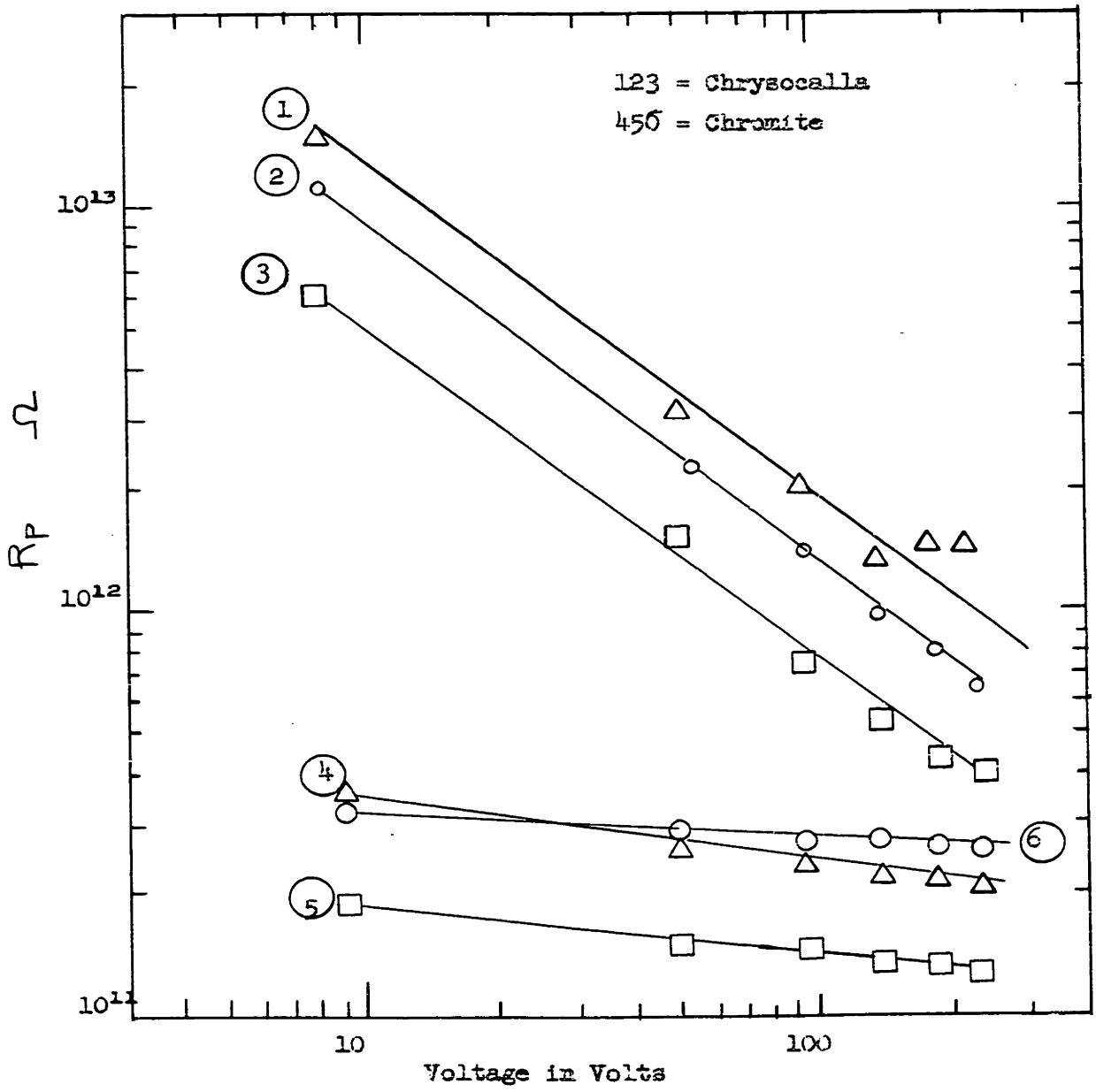

Figure 67: Variation of the Resistance of Chrysocalla and Chromite Particles with the Applied Voltage

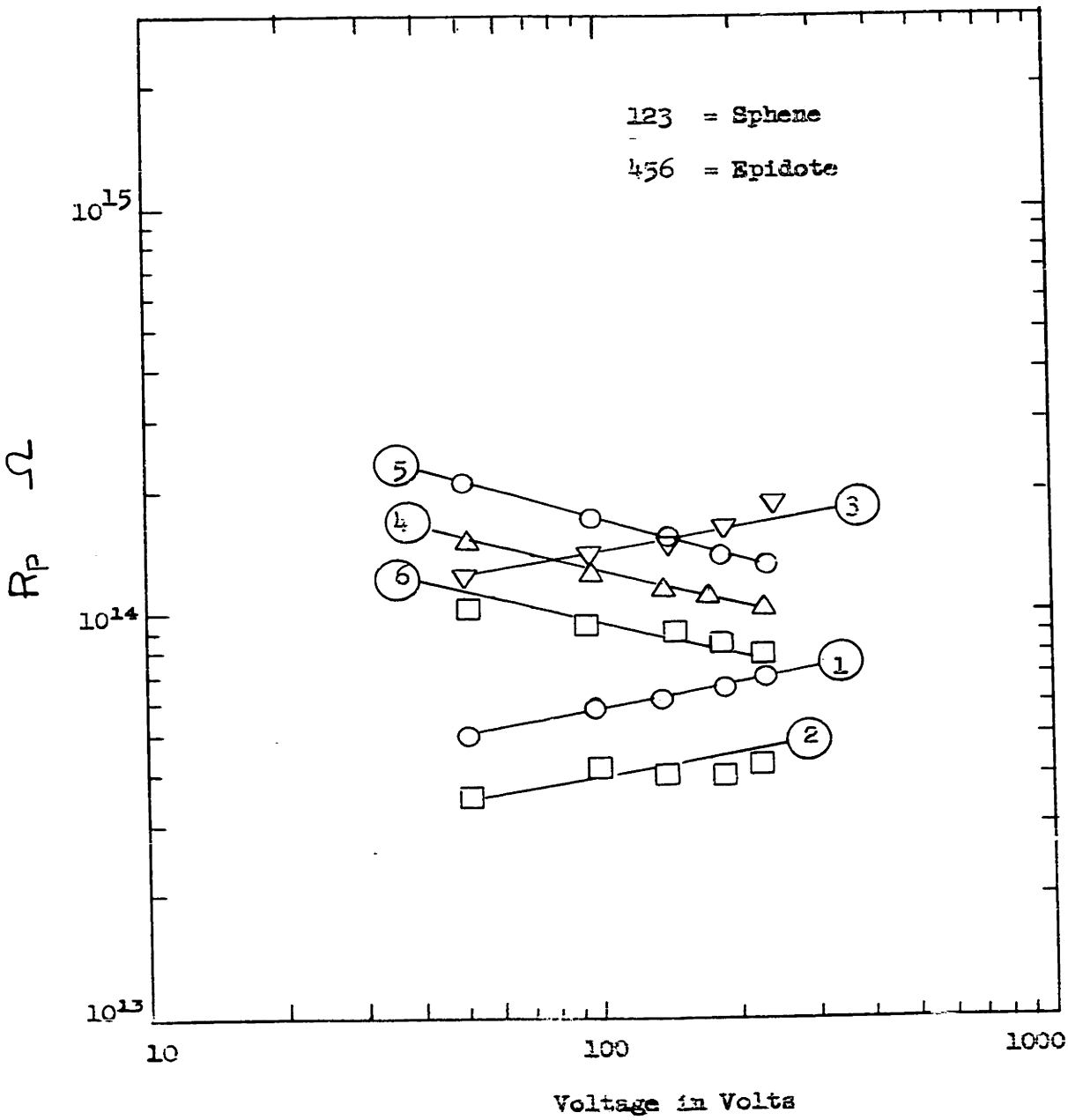

Figure 68: Variation of the Resistance of Sphene and Epidote Particles with the Applied Voltage

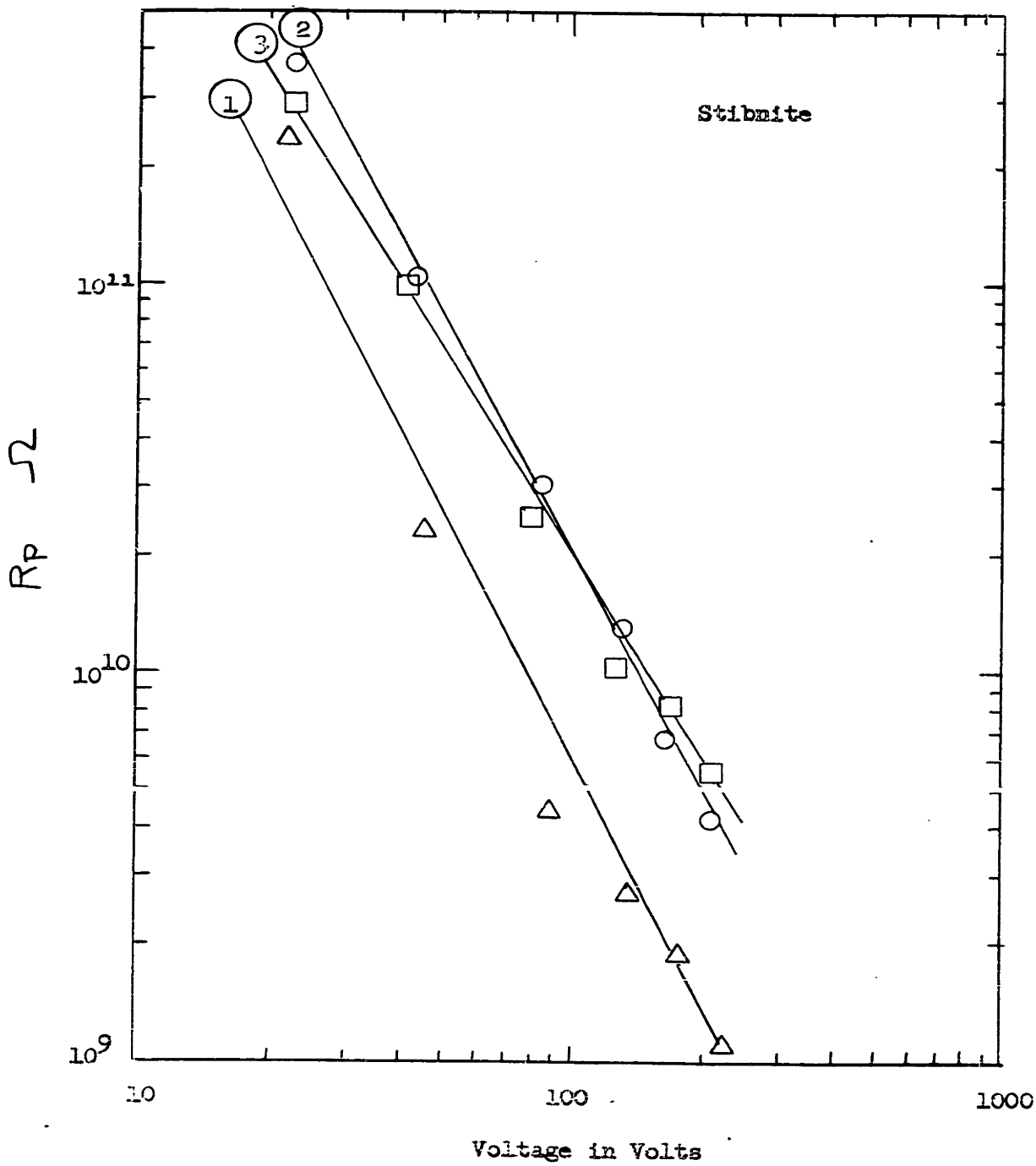

Figure 69: Variation of the Resistance of Stibnite Particles with the Applied Voltage

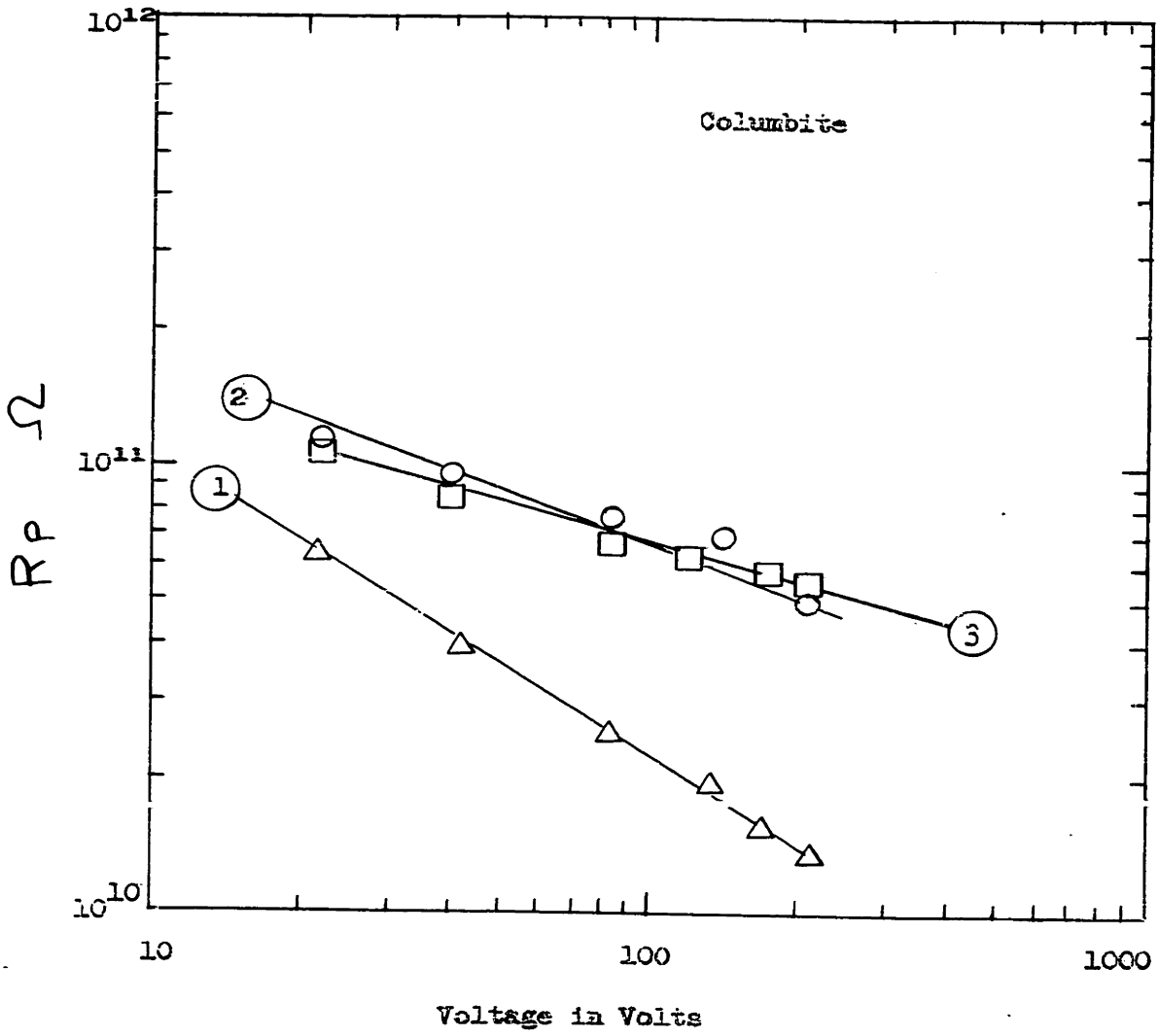

Figure 70: Variation of the Resistance of Columbite Particles with the Applied Voltage

the field. However, as seen before , the field strength will not change greatly with variation in D (Figure 4), when D is more than 14 centimeters. D is usually set greater than 14 centimeters to avoid the swinging motion of the conductors described in Figure 26.

III. Influence Of Temperature On The Resistance Of A Chromite Particle

(a) Introduction and Procedure

The resistance of chromite particles does not vary appreciably with voltage drop. This fact makes chromite a good material to use in studying the influence of temperature and resistance. A voltage drop of 86 volts was used, and particle size was 48-65 mesh.

The apparatus shown in Figure 66 was modified to the form shown in Figure 71.

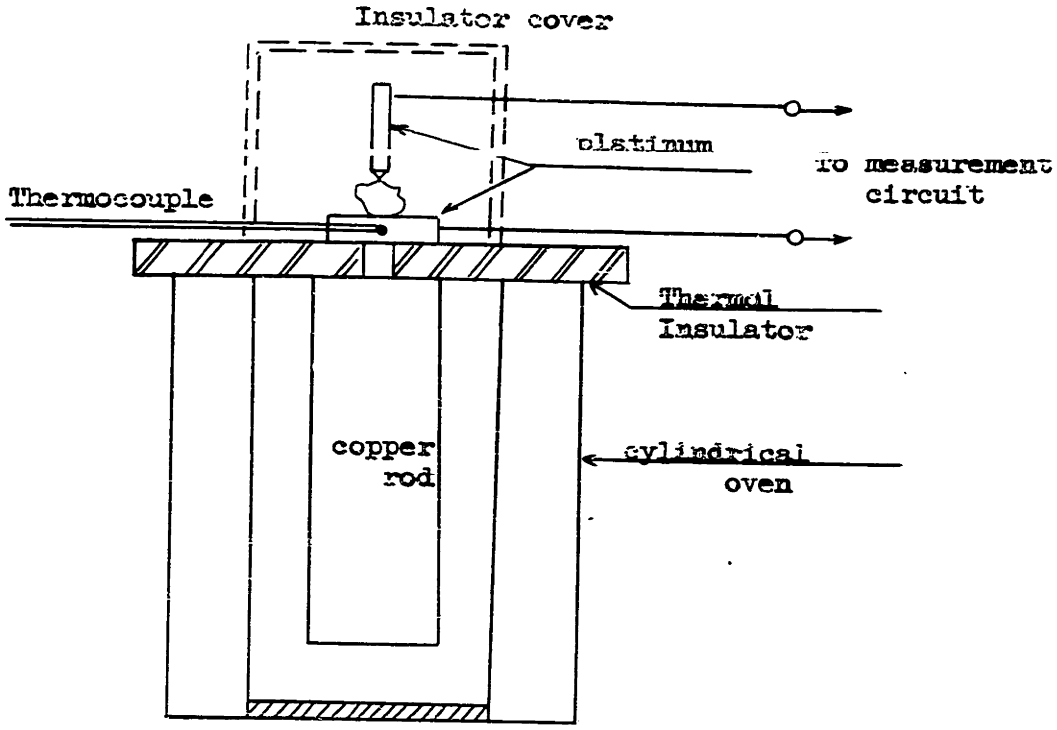

Figure 71: Modified Apparatus

(b) Results

The following test is representative of the several tests which were performed. Table 11 gives the results and Figure 72 shows the variation of resistance with the reciprocal of the absolute temperature.

(c) Conclusions

This simple experiment shows that the temperature is of major importance on R_p, and consequently on $\mathcal{P}$ and $\mathcal{P}'$. Refer to reference 15 for more information.

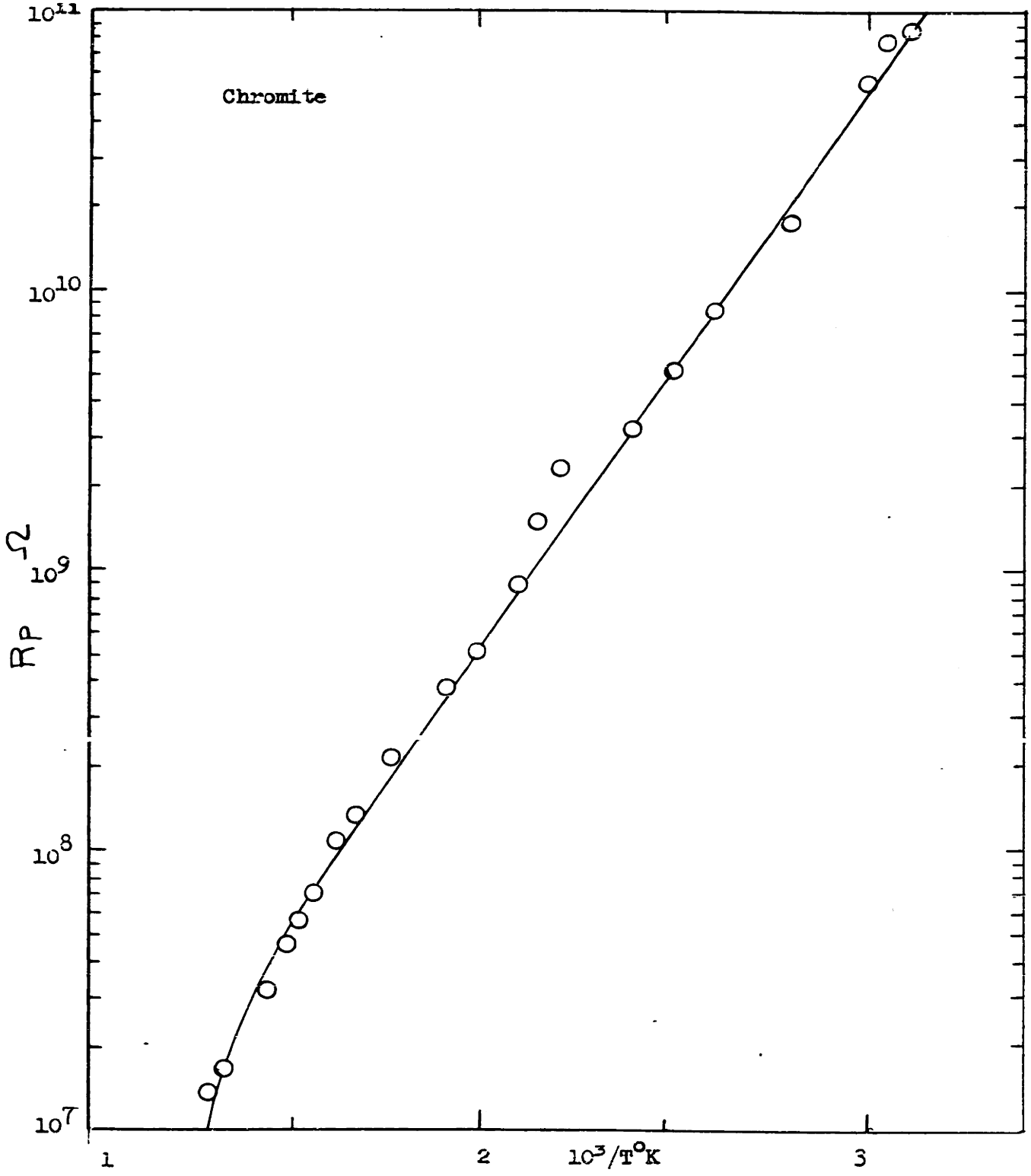

Figure 72: Dependence of the Resistance of a Chromite Particle Upon The Reciprocal of the Absolute Temperature

D. GENERAL SUMMARY

The theoretical considerations have provided a good tool for understanding how electrical concentration works. Particularly, they have shown that in the Carpco machine the important factors are the $\frac{\mathcal{F}r}{\mathcal{P}}$ ratio and the $\mathcal{P}'$ value. Study of the technique of operation of the Carpco machine has shown how useful were the qualitative rules derived from the theory. On the other hand, our experiments proved that one may manipulate the $\mathcal{P}$ and $\mathcal{P}'$ values, by changing either the field strength or the temperature.

Much work remains to be done in this field. As long as it is conducted in a general fashion, it will improve our knowledge of the process and our ability to use it with certitude. It is very important to notice that only the resistance of particles is a major factor; the dielectric constant being a minor factor in this process.

E. SUGGESTIONS FOR FURTHER WORK

The facts encountered in practice are qualitatively explained by the theory. However, it would be a great achievement to be able to compute exactly all the quantities mentioned in the theoretical discussion. For such a purpose, a special machine would be required. Figure 73 gives one among many others which could be built.

The design of such a machine would have to be such as to to provide:

(1) a known adjustable ionic field

(2) a simple static field

(3) a great variety of escaping angles.

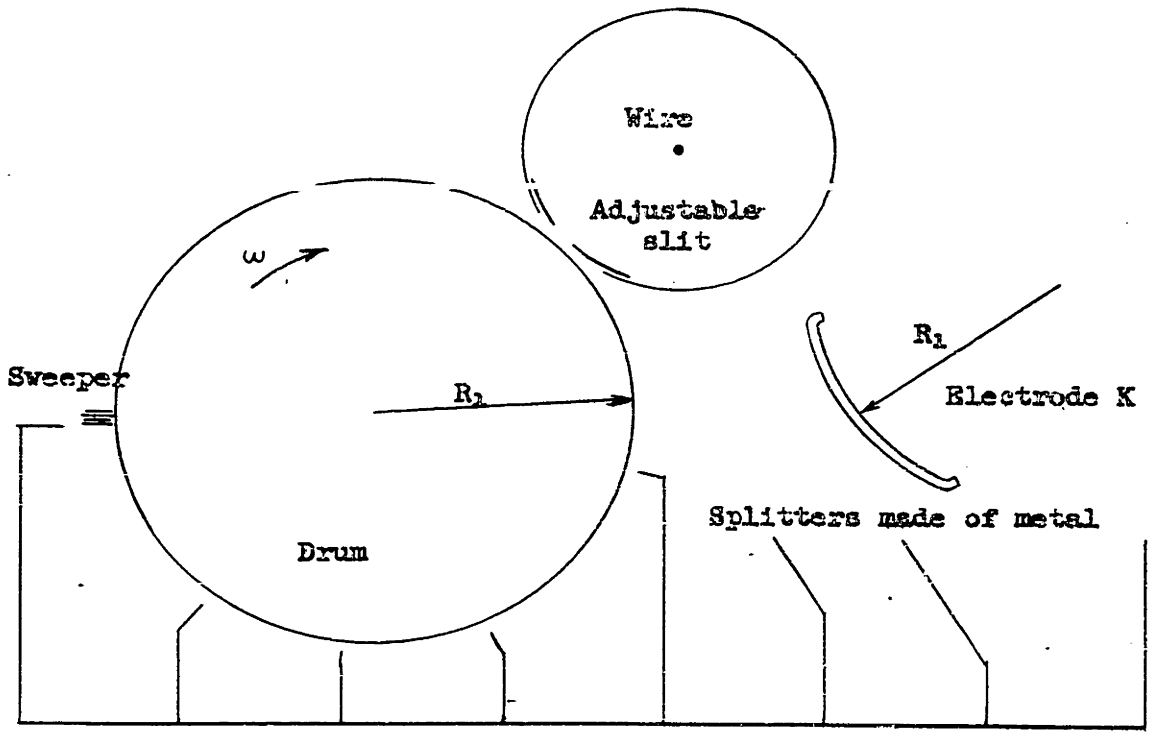

Figure 73: Proposed Electrical Concentrator

Besides the study of this new machine, some independent electrical measurements would have to be performed. However, first consideration must be given to the resistance of particles, and its dependence upon temperature, voltage and chemical treatments.

It has been seen that the shape of particles was important to a certain extent, as well as their size. Electrical sizing devices can be imagined and one (Figure 74) built at M.I.T. by two undergraduate students gave promising results.

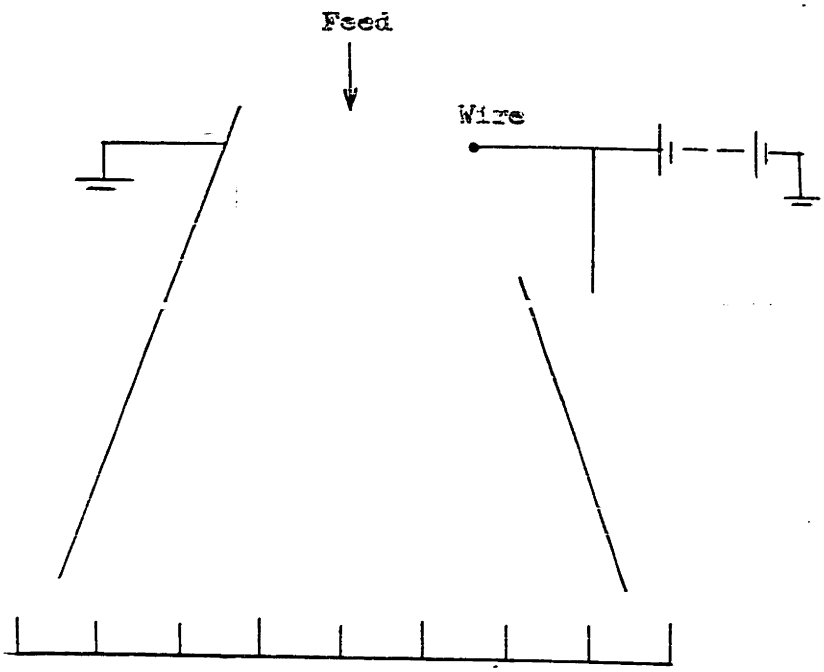

Figure 74: Electrical Classifier

BIBLIOGRAPHY

1. Schnitzler, H. "Electrostatic Separation of Coal and Other Minerals" BIOS Final Report #1035; items #21 and 30.

2. Smythe, W. R. "Static and Dynamic Electricity" McGraw-Hill Publishing Company; Page 78. (1950)

3. Pauthenier, M. M. "La théorie de la charge électrique des poussières" Revue générale de l'electricité 45 583; May 1939.

4. Gaudin, A. M. "Flotation" McGraw-Hill Publishing Co. (1957)

5. Pauling, L. E. "Nature of the Chemical Bond" Cornell University Press (1945).

6. Evans, R. C. "An Introduction to Crystal Chemistry" Cambridge University Press (1952).

7. Seitz, F. "Modern Theory of Solids" McGraw Hill Publishing Company (1940).

8. Kittel, C. "Introduction to Solid State Physics" John Wiley and Sons Inc. 2nd Edition. (1955).

9. Adam, N. K. "The Physics and Chemistry of Surfaces" Oxford University Press. 3rd Edition (1941)

10. Harnwell. G. P. "Principles of Electricity and Electromagnetism" McGraw Hill Publishing Company. 2nd Edition (1949)

11. Donald, M. B. "Electrostatic Separation of Minerals" Research Applied in Industry 11:1 19-25 January 1958.

12. Lawver, J. E. "Fundamental of Electrical Concentration of Minerals" (unpublished).

13. Von Hippel, A.R. "Dielectrics and Waves" John Wiley and Sons Inc. (1954)

14. Max, M. and Weaver, W. "The Electro-magnetic Field" Dover Publications Inc. New York.

15. Fraas, F. "Effect of Temperature on the Electrostatic Separation of Minerals." U.S. Bureau of Mines. Report of Investigations 5213 April 1956.

16. Barthelemy Roger "Private Communication". Carpco Manufacturing Inc. Jacksonville, Florida.

Table 1

Capacity Function of A Bi-cylindrical Condenser

D	D^2	$D^2-R_1^2-R_2^2$	$\frac{D^2-R_1^2-R_2^2}{2R_1R_2} = A$	$\text{Cosh}^{-1}A$	Ψ
9	81	23.5	1.25	0.7	1.41
10	100	42.5	2.25	1.45	0.69
11	121	63.5	3.37	1.88	0.53
12	144	86.5	4.6	2.21	0.45
13	169	111.5	5.9	2.46	0.405
14	186	128.5	6.6	2.57	0.39
15	225	167.5	8.9	2.88	0.346
16	256	198.5	10.5	3.05	0.33
17	289	231.5	12.3	3.2	0.31
18	314	256.5	13.6	3.3	0.303
19	361	303.5	16.1	3.45	0.29
20	400	342.5	18.2	3.6	0.278
21	440	382.5	20.5	3.71	0.27
22	484	426.5	22.7	3.85	0.26
23	529	471.5	25.0	3.92	0.255
24	576	518.5	27.5	4.05	0.246
25	625	567.5	30.0	4.1	0.243

Table 2

Values of k $(K_1, \frac{c}{a})$

c/a	$(c/a)^2$	N	K_1	$1/K_1-K_c$	$N+\frac{1}{K_1-K_o}$	$\frac{2}{3}\frac{1}{N+1/K_1-K_o}$	k
0	0	1	2	1	2	0.333	0.333
			3	0.5	1.5	0.445	0.445
			5	0.25	1.25	0.532	0.532
			9	0.125	1.125	0.592	0.592
			16	0.06	1.06	0.631	0.631
			51	0.02	1.02	0.651	0.651
			∞	0.	1.00	0.666	0.666
0.5	0.25	0.55	2	1	1.55	0.43	0.68
			3	0.5	1.05	0.635	0.883
			5	0.25	0.8	0.836	1.086
			9	0.125	0.675	0.99	1.24
			16	0.06	0.61	1.1	1.35
			51	0.02	0.57	1.18	1.43
			∞	0	0.55	1.21	1.46
1	1		2	1	1.33	0.5	1.5
			3	0.5	0.83	0.8	1.8
			5	0.25	0.58	1.15	2.15
			9	0.125	0.455	1.46	2.46
			16	0.06	0.39	1.71	2.71
			51	0.02	0.35	1.91	2.91
			∞	0	0.33	2.01	3.01

Table 3

Values of $k\left(K_1, \frac{c}{a}\right)$

c/a	$(c/a)^2$	N	K_1	$1/K_1-K_0$	$N+\frac{1}{K_1-K_0}$	$\frac{2}{3}\frac{1}{N+1/K_1-K_0}$	k
2	4	0.17	2.	1	1.17	0.57	4.5
			3	0.5	0.67	1	5
			5	0.25	0.42	1.59	5.59
			9	0.125	0.395	1.69	5.69
			16	0.06	0.23	2.9	6.9
			51	0.02	0.19	3.5	7.5
			∞	0	0.17	3.95	7.95
3	9	0.1	2	1	1.1	0.61	9.61
			3	0.5	0.6	1.11	10.11
			5	0.25	0.35	1.91	10.91
			9	0.125	0.225	2.95	11.95
			16	0.06	0.15	4.2	13.2
			51	0.02	0.12	5.55	14.55
			∞	0	0.1	6.66	15.66
4	16	0.08	2	1	1.08	0.82	16.52
			3	0.5	0.58	1.15	17.15
			5	0.25	0.33	2	18
			9	0.125	0.203	3.25	19.25
			16	0.06	0.14	4.75	20.75
			51	0.02	0.1	6.66	22.66
			∞	0	0.08	8.3	24.3

Table 3
(continued)

c/a	$(c/a)^2$	N	K_1	$1/K_1-K_0$	$N+\frac{1}{K_1-K_0}$	$\frac{2}{3}\frac{1}{N+1/K_1-K_0}$	k
5	25	0.06	2	1	1.06	0.63	25.63
			3	0.5	0.56	1.2	26.2
			5	0.25	0.31	2.15	27.15
			9	0.125	0.185	3.6	28.5
			16	0.06	0.12	5.55	30.55
			51	0.02	0.08	8.35	33.35
			∞	0	0.06	11.2	36.2

Table 4

Capacity Shape Factor of an Ellipsoid When $\frac{c}{a} < 1$

c/a	$\left(\frac{c}{a}\right)^2$	$1-\left(\frac{c}{a}\right)^2$	$1-\left(\frac{c}{a}\right)^2$	$\cos^{-1} c/a^\circ$	$\cos^{-1} c/a, r$	f
0	0	1	1	90°	1.56	0.64
0.2	0.04	0.96	0.98	$18^\circ 30'$	1.47	0.67
0.5	0.25	0.75	0.865	60°	1.05	0.82
0.8	0.64	0.36	0.6	$35^\circ 52'$	0.64	0.94
0.9	0.81	0.19	0.43	$25^\circ 50'$	0.45	0.96

Table 5

Capacity Shape Factor of an Ellipsoid When $\frac{c}{a} > 1$

c/a	$(c/a)^2$	$\frac{2}{d\sigma}$	$2\sqrt{\left(\frac{c}{a}\right)^2-1}$	$\frac{a}{c}$	$\left(\frac{a}{c}\right)^2$	$1-\left(\frac{a}{c}\right)^2$	$\sqrt{1-\left(\frac{a}{c}\right)^2}$	$\frac{1+\sqrt{\ }}{1-\sqrt{\ }}$	$\log_e \frac{1+\sqrt{\ }}{1-\sqrt{\ }}$	f
2	4	3	3.45	0.5	0.25	0.75	0.865	15	2.5	1.40
3	9	8	5.65	0.33	0.11	0.89	0.93	27.5	3.3	1.7
4	16	15	7.75	0.25	0.062	0.94	0.96	49	3.9	1.98
5	25	24	9.8	0.2	0.04	0.96	0.98	100	4.6	2.1

Table 6

Results of Pinning and Lifting of Manganese Ore

No.	Setting	Concentrate		Tailing		Manganese Recovery in Electrical Separation Step, Per Cent	Overall Manganese Recovery, Per Cent
		Weight Per Cent	Assay Mn, %	Weight Per Cent	Assay Mn, %		
1	P_1	73.9	35.9	16 1	6.2	97.2	76.1
2	P_2	50.9	40.1	49 1	16.5	72.5	56.6
3	P_3	38.1	40.6	61.9	21.7	55.1	43.2
4	L_1	46.2	41.3	53.8	18	65.8	51.4
5	L_2	61.8	40.3	38.2	9.2	87.2	68.2
6	L_3	60.6	40.1	39.4	7.7	88.9	69.5
7	P_4	55.6	38.0	44.4	16	75.1	58.9
8	P_5	68.6	37.8	31.4	10.1	89.0	69.5
9	P_6	73.6	33.8	26.4	11.9	89.0	69.5

Table 7

Resistances of Particles of Chrysocolla and Chromite

Name	Particle Number	Volts	$R_p/10^{12}$	Name	Particle Number	Volts	$R_p/10^{11}$
Chrysocolla	1	9	11	Chromite	1	9	3.15
		54	2.35			50	2.95
		96	1.45			94	2.85
		140	1			137	2.8
		182	0.8			182	2.63
		227	0.67			230	2.65
	2	9	1.5		2	9	3.6
		50	3.5			50	2.6
		95	2.			95	2.4
		140	1.33			140	2.26
		185	1.5			185	2.12
		235	1.5			235	2.06
	3	9	6		3	9	1.9
		50	1.56			50	1.5
		95	0.75			95	1.44
		140	0.54			140	1.32
		185	0.41			185	1.28
		235	0.39			235	1.22

Table 8

Resistance of Particles of Sphene and Epidote

Name	Particle number	Volts	$R_p/10^{14}$	Name	Particle number	Volts	$R_p/10^{14}$
Sphene				Epidote			
	1	50	0.5		4	51	1.46
		94	0.58			96	1.26
		139	0.6			142	1.18
		182	0.66			187	1.15
		230	0.68			235	1.06
	2	50	0.35		5	51	2.16
		96	0.44			96	1.68
		140	0.38			187	1.36
		232	0.39			235	1.3
	3	50	1.14		6	50	1
		95	1.33			96	0.92
		140	1.4			143	0.9
		185	1.68			187	0.83
		235	1.92			235	0.74

Table 9

Resistance of Particles of Stibnite and Columbite

Name	Particle Number	Volts	$R_p/10^{10}$	Name	Particle Number	Volts	$R_p/10^{10}$
Stibnite				Columbite			
	1	22	24.5		1	21.5	6.5
		45	2.38			42	4.05
		87	0.43			84	2.55
		134	0.27			135	2.05
		177	0.19			170	1.54
		225	0.11			215	1.33
	2	22	37		2	21.5	10.7
		42	10.5			40	8.5
		87	3.15			84	7.6
		134	1.34			138	6.9
		177	0.67			170	5.8
		226	0.45			215	5
	3	22	27.5		3	21.5	10.7
		42	10			42	8.6
		87	2.55			83	6.9
		134	1.28			130	6.5
		177	0.77			170	5.9
		225	0.56			215	5.7

Table 10

Resistance of Particles of Other Minerals

Name	Particle Number	Resistance in ohms (Wheatstone Bridge)
Pentlandite	1	4
	2	2.5
	3	2.5
	4	7
Marcasite	1	7,000
	2	8,000
	3	7,400
Arsenopyrite	1	44
	2	37
	3	22
	4	10

Table 11

Resistance of a Chromite Particle at Various Temperatures

$T^{o}K$	$10^{3}/T^{o}K$	R_p	$T^{o}K$	$10^{3}/T^{o}K$	R_p
300	3.3	$1.5\ 10^{11}$	655	1.53	$5.7\ 10^{7}$
322	3.1	$8.6\ 10^{10}$	670	1.5	$4.65\ 10^{7}$
327	3.05	$7.7\ 10^{10}$	685	1.46	$3.9\ 10^{7}$
332	3	$5.7\ 10^{10}$	700	1.43	$3.1\ 10^{7}$
345	2.9	$3.4\ 10^{10}$	745	1.34	$1.65\ 10^{7}$
360	2.8	$1.8\ 10^{10}$	760	1.32	$1.4\ 10^{7}$
382	2.6	$8.9\ 10^{9}$	775	1.3	$5.4\ 10^{6}$
400	2.5	$5.4\ 10^{9}$	800	1.25	$1.26\ 10^{6}$
420	2.4	$3.3\ 10^{9}$	Particle Burned Off		
435	2.2	$2.4\ 10^{9}$			
460	2.15	$1.5\ 10^{9}$			
480	2.1	$9\ 10^{8}$			
500	2	$5\ 10^{8}$			
520	1.92	$3.9\ 10^{8}$			
565	1.77	$2.15\ 10^{8}$			
600	1.67	$1.34\ 10^{8}$			
615	1.63	$1.1\ 10^{8}$			
640	1.56	$7.2\ 10^{7}$			

Appendix I

(1) Electrical Concentration of Manganese Ore

No: 2.61 b

Name of Test: Rougher Split

Feed Description

Treatment: Deslimed

Temperature:

Size Range: -48+200 Mesh

Weight: 1500 g

Time: 18s

Analysis

% Mn = 32.5

% SiO_2 = 19.3

Observations:

% Fe = 2.8

Electrode Conditions

Voltage = 36 Kv

Polarity = +

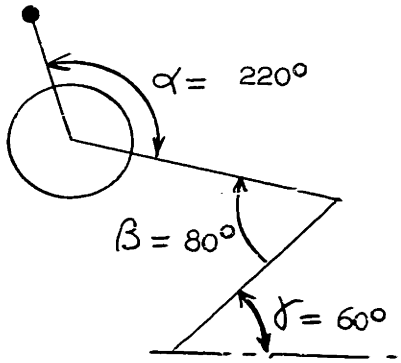

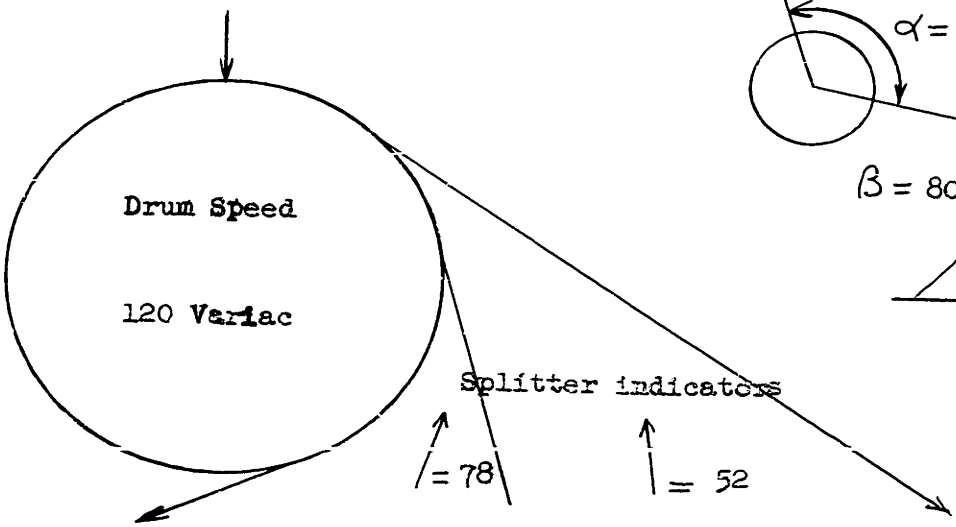

non conductors No. 1

Weight: 340 g

% Feed = 22.8%

Analysis

% =

% =

Observations

Total = 654g

Middlings No. 2

Weight: 752g

% Feed = 50.4

Analysis

% =

% =

Conductors = 438g

non Conductors=314g

Conductors No. 3

Weight: 401g

% Feed = 26.8

Analysis

% =

% =

Observations

Total = 839g

Appendix I
(2)

Electrical Concentration of Manganese Ore

No. 2.61 b
Name of the Test: Cleaning of Tailings $2.61a_1$

Feed Description		Electrode Conditions
Treatment: $2.61a_1$	Analysis	Voltage = 38 Kv
Temperature:	% =	Polarity= +
Size Range: -48 +200 Mesh	% =	
Weight: 780g	Observations:	
Time: = 20s		

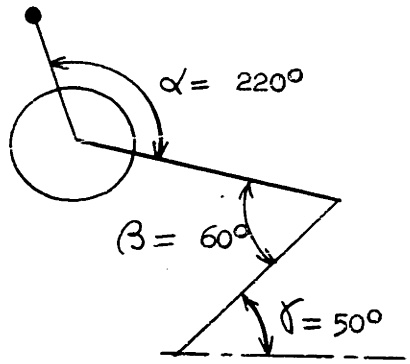

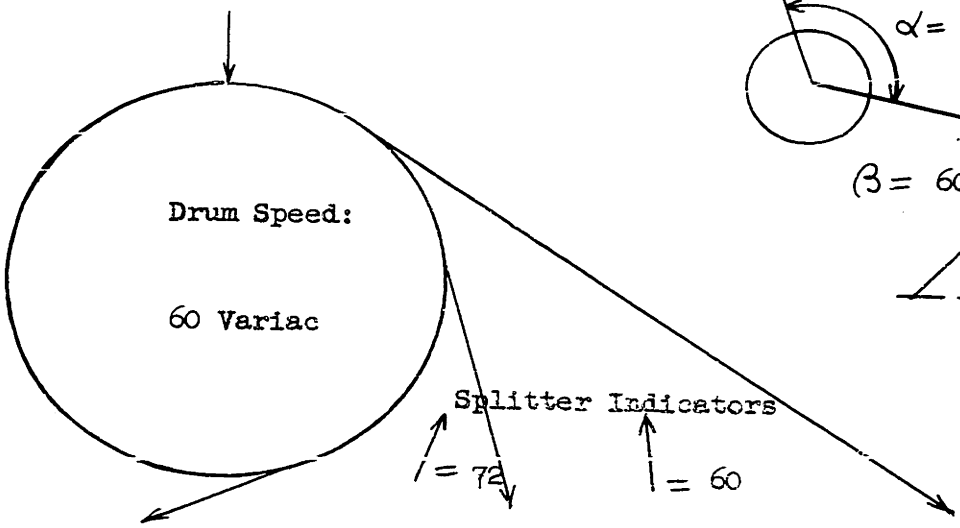

non conductors No.1	Middlings No. 2	Conductors No. 3
Weight: 324g	Weight: 160g	Weight: 290g
% Feed = 41.8	% Feed = 20.7	% Feed = 37.5
Analysis	Analysis	Analysis
% =	% =	% =
% =	% =	% =
Observations	Observations	Observations
Total 414g	non conductors = 90g	Total = 360.1g
	Conductors = 70.1g	

Appendix I
(3)

Electrical Concentration of Manganese Ore

No. 2.61 c
Name of Test: Cleaning of Concentrate $2.61a_3$

Feed Description

Treatment: $26la_3$ Analysis
Temperature: % =
Size Range: -48 + 200 Mesh % =
Weight: 839s Observations:
Time: = 35s

Electrode Conditions

Voltage = 36 Kv
Polarity = +

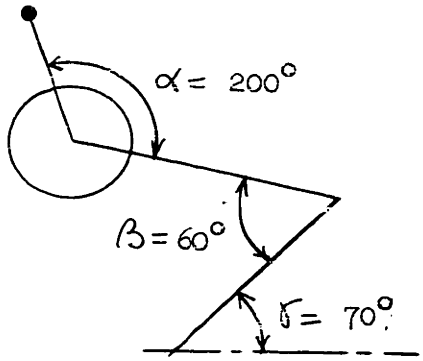

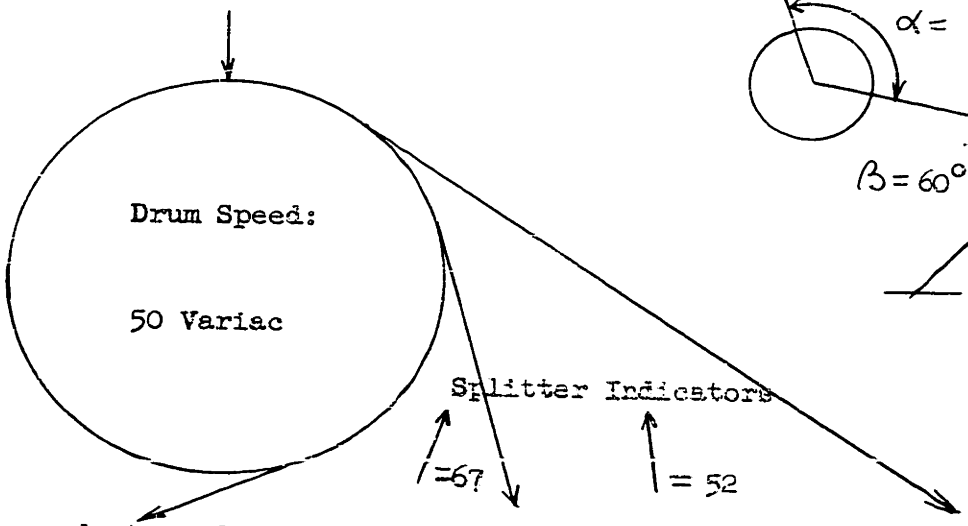

non conductors No. 1

Weight: 51g
% Feed = 6.15

Analysis

% =

Observations

Total 135g

Middlings No. 2

Weight: 480g
% Feed = 57.75

Analysis

% =

Observations

non conductors = 84g

Conductors = 396g

Conductors No. 3

Weight: 299g
% Feed = 36.1

Analysis

% =

Observations

Total 695g

APPENDIX II

1) Rate of the rougher:

$F+C_T = 1500 + 510 = 2010g$

$\Theta_R = \frac{50.4}{100} \times 2010g$

Total Circulation = 3025g

Time required: 18 seconds are needed to pass through 1500g of ore

$\text{Time} = \frac{18 \times 3025}{1500} = 36.1s.$

$\text{Rate} = 1.500 \times \frac{60}{36.1} = 2.5 \text{ kg/mn}$

2) Rate of Tailings Cleaning.

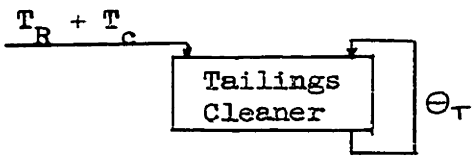

for a 1500g feed

$T_R = 920g$

$T_C = 160g$

$\Theta_T = 20.5\%$

The total circulation is 1300g. The time required to pass through 770g is 20 seconds.

$\text{Time} = \frac{20 \times 1300}{770} = 33.5s$

$\text{Rate} = 1.500 \times \frac{60}{33.5} = 2.65 \text{kg/mn}$

3) Rate of Concentrate Cleaning

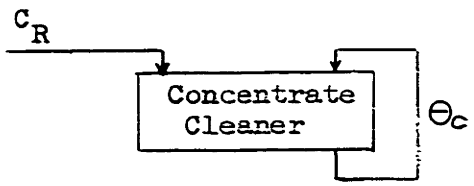

for a 1500g feed

$C_R = 1080g$

$\Theta_C = 57.5\%$

The total circulation is 1700g. 35 seconds are required to pass through 839g of feed. The time is then $\frac{35 \times 1700}{839} = 71s$

$\text{Rate} = \frac{1.500 \times 60}{} = 1.26 \text{ kg/mn}$